NOTE TO USERS

This reproduction is the best copy available.

uOttawa

L'Université canadienne
Canada's university

FACULTÉ DES ÉTUDES SUPÉRIEURES ET POSTOCTORALES

uOttawa

L'Université canadienne
Canada's university

FACULTY OF GRADUATE AND POSDOCTORAL STUDIES

Sophie Imbeault
AUTEUR DE LA THÈSE / AUTHOR OF THESIS

Ph.D. (Biochemistry)
GRADE / DEGREE

Department of Biochemistry, Microbiology and Immunology
FACULTÉ, ÉCOLE, DÉPARTEMENT / FACULTY, SCHOOL, DEPARTMENT

Connexin-Mediated Regulation of Gliogenesis
TITRE DE LA THÈSE / TITLE OF THESIS

Steffany Bennett
DIRECTEUR (DIRECTRICE) DE LA THÈSE / THESIS SUPERVISOR

CO-DIRECTEUR (CO-DIRECTRICE) DE LA THÈSE / THESIS CO-SUPERVISOR

Douglas Gray

Rashmi Kothary

Diane Lagacé

Steven Scherer (U. of Pennsylvania)

Gary W. Slater
Le Doyen de la Faculté des études supérieures et postdoctorales / Dean of the Faculty of Graduate and Postdoctoral Studies

CONNEXIN-MEDIATED REGULATION OF GLIOGENESIS

SOPHIE IMBEAULT

THESIS SUBMITTED TO THE FACULTY OF GRADUATE AND POSTDOCTORAL STUDIES IN PARTIAL FULFILLMENT OF THE REQUIREMENTS FOR THE DEGREE OF DOCTOR OF PHILOSOPHY

DEPARTMENT OF BIOCHEMISTRY, MICROBIOLOGY AND IMMUNOLOGY
FACULTY OF MEDICINE
UNIVERSITY OF OTTAWA

Your file Votre référence
ISBN: 978-0-494-69113-7
Our file Notre référence
ISBN: 978-0-494-69113-7

Abstract

Connexin (Cx) proteins are important in coordinating neural progenitor cell behaviour. Here, we show hippocampal-derived neural progenitor cells (NPCs) express a wide and novel repertoire of Cxs when cultured *in vitro*. This repertoire can be modulated by exposure to the extracellular matrix component laminin which translates into functional changes in Cx-mediated signaling within hippocampal NPCs and their progeny. Novel localization of Cx29 to NPC-derived oligodendrocyte progenitor cells (OPCs) in these cultures prompted us to investigate what role Cx29 may have in maintenance, proliferation and specification of OPCs to oligodendrocytes in the hippocampus. Using a loss-of-function approach, we show loss of Cx29 results in reduced OPC and oligodendrocyte numbers with a concomitant increase in astrocyte number. However, investigation of Cx29 *in vivo*, which also shows localization to OPCs and oligodendrocytes, reveals the role of Cx29 in oligodendrocyte specification may be overridden by the additional cues present in the microenvironment as an increase in $NG2^+$ OPC proliferation is observed. However, the effect on astrocyte proliferation is likely cell intrinsic because increased astrocyte proliferation is maintained *in vivo*. Closer examination of the hippocampal OPC population further indicates Cx32 but not Cx47 is expressed by subsets of OPCs while Cx47 is restricted to mature oligodendrocytes. Similar to the loss of Cx29, the loss of Cx32 *in vivo* results in increased proliferation of $NG2^+$ OPCs. These data can be reconciled by the novel finding that Cx29 and Cx32 likely have complementary roles in the regulation of OPC proliferation and specification and can mutually compensate for the loss of the other connexin in the OPC subpopulations of null-mutant mice. Modulation of these Cxs may thus result in new therapeutic approaches to the treatment of diseases where oligodendrocytes are primarily affected such as multiple sclerosis and where augmenting progenitor cell specification is a viable treatment option.

General Acknowledgements

I'd like to thank: my supervisor for letting me pursue research in her lab, for always being supportive, for giving us the opportunity to attend many scientific conferences/opportunities and for always having an ear to troubleshoot experiments and talk about the project; my committee members Dr. Lynn Megeney and Dr. David Park for their insightful comments over the years; our academic secretary, Carol Ann, who always has time for students; and last but not least, all the past and present members of the Bennett Lab for their help, support and camaraderie during these last 5 years. Finally to my sources of funding without whom this work would have been much more difficult to accomplish: NSERC, OGSST and the Parkinson Research Consortium.

Table of Contents

List of Abbreviations

AMPA	α-amino-3-hydroxyl-5-methyl -4-isoxazole-propionate
ANOVA	analysis of variance
Ascl1	achaete-scute homolog 1
ATP	adenosine-5'-triphosphate
bp	base pair
BrdU	5′-bromo-2-deoxyuridine
BV	blood vessel
cAMP	3'-5'-cyclic adenosine monophosphate
CGE	caudal ganglionic eminence
CL	cytoplasmic loop
CNPase	2',3'- cyclic nucleotide 3'-phosphodiesterase
CNS	central nervous system
CSPG-4	chondroitin sulphate proteoglycan 4
Cx	connexin
DCX	doublecortin
DIDS	4,4′-diisothiocyanatostilbene-2,2′-disulfonic acid
DIV	days *in vitro*
dNTPs	deoxynucleotides
ECM	extracellular matrix
EGF	epidermal growth factor
ER	endoplasmic reticulum
FBS	fetal bovine serum
FFA	flufenamic acid
FGF-2	fibroblast growth factor 2
GABA	γ–aminobutyric acid
GAPDH	glyceraldehyde 3-phosphate dehydrogenase
GFAP	glial fibrillary acidic protein
GFP	green fluorescent protein
GJIC	gap junctional intercellular communication
GRA	18α-glycyrrhetinic acid
GZA	glycyrrhizic acid
HGNC	HUGO gene nomenclature committee
HUGO	Human Genome Organisation
IL-7	interleukin-7
IP_3	inositol 1,4,5-trisphosphate
kDa	kilodalton
KO	knock-out
LGE	lateral ganglionic eminence
LSM	laser scanning microscope
LY	lucifer yellow
MAP-2	microtubule associated protein 2
Mash1	mammalian achaete-schute homolog 1
MGE	medial ganglionic eminence
mRNA	messenger ribonucleic acid
MS	multiple sclerosis
NCAM	neural cell adhesion molecule
NeuN	neuronal nuclei
NG2	neuron/glia 2
NPC	neural progenitor cell
Olig2	oligodendrocyte transcription factor 2
OPC	oligodendrocyte progenitor cell
P2YR	P2Y purinergic receptor
PBS	phosphate buffered saline
PDFGαR	platelet-derived growth factor α receptor
PDZ	post-synaptic density 95/discs large/zona-occludens-1
pHH3	phospho-histone H3
PLC	phospholipase-C
PNS	peripheral nervous system
RA	retinoic acid
RD	rhodamine B isothiocyanate-dextran
RT-PCR	reverse transcriptase polymerase chain reaction
SGZ	subgranular zone
shRNA	short hairpin ribonucleic acid
SVZ	subventricular zone
TM	transmembrane
TNFα	tumour necrosis factor α
TUNEL	terminal deoxynucleotidyl transferase-mediated dUTP nick end labeling
Ub	ubiquitinated
UTR	untranslated region
VZ	ventricular zone
WT	wild-type
ZO-1	zona occludens-1

List of Figures

List of Tables

Chapter 1: General Introduction

1.1. Preface

The importance of gap junctions and their component "hemichannels" in the regulation of progenitor* cell proliferation, specification and migration has now entered mainstream scientific thought (reviewed in (1, 2)) however the underlying mechanisms have only begun to be elucidated. It is clear the microenvironment (niche) in which progenitor cells reside plays a crucial role in maintaining and directing progenitor cell behaviour and, furthermore, likely influences expression and function of gap junction proteins. This is especially true in the brain where progenitor cells that are restricted to glial fates within their niche demonstrate the ability to generate neurons once removed and cultured *in vitro (3)*.

With these observations in mind, I sought to investigate how microenvironment-gap junction crosstalk might influence neural progenitor cell (NPC) fate, specifically how altering expression of gap junction proteins might restrict NPC specification to a glial cell lineage. I first used a simplified model of central nervous system (CNS) development to investigate which connexins (Cxs) are expressed by neural progenitor cells (NPCs) and how the extracellular matrix influences Cx expression and functionality (Chapter 2). One of the novel findings in this study was the expression of Cx29 by oligodendrocyte progenitor cells (OPCs) - prior to this thesis it was assumed Cx29 expression was restricted to mature oligodendrocytes. I then delved deeper into the localization and function of Cx29 in these progenitor cells using an *in vitro* loss-of-function approach (Chapter 3). To expand my findings *in vivo*, I also looked at the localization and role of the "oligodendrocytic" Cxs (Cx29, Cx32, and Cx47) in the progenitor cell niche of the dentate gyrus using genetic dissection: a combination of single, double and triple null-mutant mice to identify novel roles of these three proteins in NPC proliferation and specification (Chapter 4). To place the genesis of these studies in context, I will

* The term "progenitor cell" will be used to refer to stem cells and progenitor cells throughout this thesis

discuss, as part of this general introduction, the connexin protein family and the current understanding of the role of the specific connexins examined herein, the cell lineage affected by connexin loss in this thesis (oligodendrocytes and oligodendrocyte progenitor cells), and finally our current knowledge about the role of connexin proteins in development of the nervous system and the regulation of NPCs.

1.2 Connexin proteins

1.2.1 Structure, Assembly and Nomenclature

Connexins are a protein superfamily comprised of 20 members in mice and 21 members in humans (4). Cxs are found within every tissue of the body except red blood cells, spermatozoa, and skeletal muscle, although the respective progenitor cell populations giving rise to these tissues have been shown to possess gap junctions (5). Furthermore, the expression patterns of Cxs show tissue and cell-type specificity (5, 6). Defining features of Cxs are intracellular N- and C-termini, 4 transmembrane-spanning domains (TM1-TM4), one intracellular (CL) and two extracellular loops (E1 and E2) each of which contains three conserved cysteine residues that form disulfide bridges between E1 and E2 (7) (Figure 1.1a). The C-terminal tail and the CL loop exhibit the most diversity and define individual Cx family members although all members of the family are highly homologous showing ~50% amino acid homology (8).

Historically, Cxs were divided into alpha, beta, gamma and epsilon subgroups based on the length of their CL and their overall homology to each other (9, 10); gamma and epsilon Cxs are the most divergent of the groups. Although nomenclature has been a controversial issue in the field, the current registration with the Human Genome Organisation Gene Nomenclature Committee (HGNC) separates Cx genes into five groups with new gene designations for some of these Cxs, while the protein nomenclature still relies on predicted molecular weight, e.g. Cx29, introduced earlier, has a predicted molecular weight of 29 kDa. As some Cxs have different predicted weights in mice and humans, a table (Table 1.1) has been

Figure 1.1 Connexins and connexin-mediated signalling. A) Structure and salient features of a connexin protein. Note the disulfide bridges formed by the conserved cysteine residues of the two extracellular loops. TM - transmembrane domain, E - extracellular loop, CL - intracellular loop. B) Six connexins hexamerize to form a connexon or "hemichannel" that can be composed of the same Cxs in which case the connexon is homomeric or different connexins in which case the connexon is heteromeric C) Connexons present at junctional membranes between adjacent cells form an intercellular channel allowing the passage of ions and small metabolites. D) A connexon ("hemichannel") in a non-junctional membrane allows the passage of ions and small metabolites to and from the cytosol to the extracellular fluid. E) Connexons can form protein-protein interactions via the C-terminal tails of the composing connexins especially through interactions of PDZ domains. F) Adhesion domains formed by gap junction plaques allow the migration of cells, eg. of a neuroblast (green cell) along the process of a radial glial cell (purple cell).

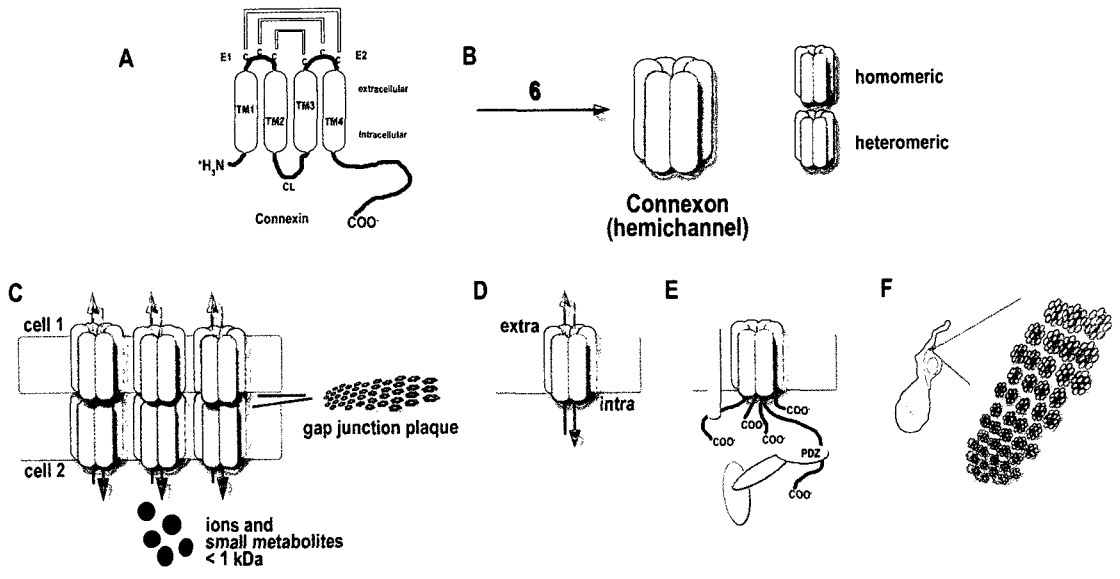
A
E1
E2
extracellular
TM1
TM2
TM3
TM4
intracellular
+H3N
CL
Connexin
COO-
B
6
Connexon
(hemichannel)
homomeric
heteromeric
C
cell 1
cell 2
gap junction plaque
ions and
small metabolites
< 1 kDa
D
extra
intra
E
COO-
PDZ
F

Figure 1.1

Table 1.1 Human and mouse connexin genes and proteins

Gene name	Human Connexin	Previous Human Gene name	Mouse Connexin	Previous Mouse Gene name
GJA1	Cx43	nc	Cx43	nc
GJA3	Cx46	nc	Cx46	nc
GJA4	Cx37	nc	Cx37	nc
GJA5	Cx40	nc	Cx40	nc
GJA6	---	---	Cx33	nc
GJA8	Cx50	nc	Cx50	nc
GJA9	Cx59	GJA10	---	---
GJA10	Cx62	---	Cx57	nc
GJB1	Cx32	nc	Cx32	nc
GJB2	Cx26	nc	Cx26	nc
GJB3	Cx31	nc	Cx31	nc
GJB4	Cx30.3	nc	Cx30.3	nc
GJB5	Cx31.1	nc	Cx31.1	nc
GJB6	Cx30	nc	Cx30	nc
GJB7	Cx25	nc	---	---
GJC1	Cx45	GJA7	Cx45	GJA7
GJC2	Cx47	GJA12	Cx47	GJA12
GJC3	Cx31.3[a]	GJE1	Cx29	GJE1
GJD2	Cx36	GJA9	Cx36	GJA9
GJD3	Cx31.9	GJC1, GJA11	Cx30.2	GJC1, GJA11
GJD4	Cx40.1	---	Cx39	---
GJE1	Cx23	---	Cx23	---

nc - no change

[a] This human ortholog of mCx29 was first entered into GenBank and thus HGNC by Sohl *et al.* (45) as hCx30.2. However work from Altevogt *et al.* (46) and Sargiannidou *et al.* (54) have shown the functional form found in human brain to be hCx31.3 and will be referred to as such here.

included to provide clarity when discussing these proteins and to highlight differences and similarities between mouse and human Cxs. It should be noted that adoption of this new gene naming system is not widespread. Therefore, to simplify matters for the reader, the molecular weight nomenclature will be used throughout this thesis to refer to both the gene and protein.

Six connexins hexamerize to form one connexon or hemichannel (Figure 1.1b). Homomeric connexons are composed of the same Cx proteins while heteromeric connexons are formed by different Cxs. Information on the site of assembly of the hemichannels is not available for all Cx family members. However, work from Musil and Goodenough (11) and from Koval *et al. (12)* indicates Cx43 and Cx46 hexamerize in the trans-Golgi while Diez *et al. (13)* have demonstrated assembly of heteromeric Cx26/Cx32 connexons in the ER/Golgi intermediate compartment. Further experiments using various Cx constructs suggest the site of oligomerization may be different for each Cx (14) and some propose this mechanism to occur in a progressive fashion beginning in the ER, moving through the ER/Golgi intermediate compartment and ending up with stable connexons in the late Golgi compartments (15). It is these stable complexes that are then transported to the cell surface (16-18) and inserted into the plasma membrane to form hemichannels in non-junctional membranes or, when aligned with compatible connexons present at the plasma membrane of adjacent cells, gap junction intercellular channels.

In vivo and cell culture studies have shown Cxs to have half-lives of a few hours (1-5h) (19-24). In order to reconcile many studies on the degradation of Cxs, two modes of degradation have been proposed as reviewed in Laird (15): plasma membrane Cxs are recycled through the lysosomal pathway, with reports Cx43 is mono-ubiquitinated (Ub) for internalization, whereas other signals, possibly poly-Ub, would target Cxs for ER-associated degradation via the proteasome. However, as stated in the Laird review, this reconciliatory model remains to be concretely tested for Cx43 and whether it applies globally to the Cx superfamily is unknown.

1.2.2 General function and signalling

Connexins can mediate signalling in four main ways (Figure 1.1c-f). The best known function is gap junctional intercellular communication (GJIC). This occurs when a pair of neighbouring cells each contribute one connexon to form an intercellular channel (Figure 1.1c). Docking of the connexons from adjacent cells is achieved through the interaction of the extracellular loops (25). Many channels assembled together in one area are called a gap junction plaque (Figure 1.1c). However, only certain connexon combinations yield functional intercellular channels – this is likely due to the inability of the amino acids of each connexon, especially those found in E2, to form the proper non-covalent bonds required for association with the connexon from the adjacent membrane (26, 27). Such selectivity confers a rich diversity as well as a tight regulation to Cx-mediated GJIC. Small molecules and metabolites such as Ca^{2+} (28), cAMP (29) and ATP (30) (≤ 1-1.2 kDa (31, 32)) typically pass through the channels although there have been reports of larger molecules such as shRNAs (33, 34) being transferred from one cell to another via GJIC. It is generally thought Cx channels are non-selective although different permeabilities to certain substrates have been reported (35-37).

When a connexon is inserted into a non-junctional membrane, passage of metabolites to and from the extracellular milieu is facilitated. In this case, communication is said to occur via "hemichannels", as mentioned above (Figure 1.1d). Both intercellular channels (reviewed in Sáez *et al.* (6)) and hemichannels (reviewed in Sáez *et al.* (38)) are voltage-sensitive and can be regulated by extracellular Ca^{2+} concentration and intracellular pH.

Channel-independent functions of Cxs include protein-protein interactions and the formation of adhesion domains. Certain members of the Cx family possess protein-protein interaction domains, mostly in the region of the C-terminus (Figure 1.1e). Many have been found to interact through PDZ domains with ZO-1 (39, 40) which can lead to downstream participation in gene transcription and cytoskeletal regulation (41). Perhaps, the most novel channel-independent function of Cxs identified to date is the formation of adhesion domains via the gap junction plaques

present on the cell surface. In a series of elegant experiments, Elias *et al.* (42) demonstrated the migration of neuroblasts along the processes of radial glia in the developing brain was mediated by the adhesion of Cx26 and Cx43-containing connexons expressed by adjacent cells and not by their channel function. It also appears there is no segregation of a particular Cx to either neuroblasts or radial glia but rather that expression is developmentally regulated (or perhaps regulated by components of the microenvironment such as the extracellular matrix) demonstrating the heterogeneity of expression of Cxs within and across various (neural) cell types during different developmental windows. For example, while Cx26 and Cx43 are found in the developing brain, along with other Cxs outlined below, the general consensus for mature cell types in the adult brain is that neurons contain Cx36 and Cx45; astrocytes express Cx43, Cx30, and some Cx26; while oligodendrocytes express Cx29, Cx32 and Cx47 (43) (Figure 1.2). I argue that this diversity in Cx cell-type expression and functional association plays an important role during development and in the maintenance of proper brain homeostasis, notably during postnatal neurogenesis and gliogenesis. To this end, I focussed on understanding whether altering Cx29, Cx32, and Cx47 would influence oligodendrogenesis.

1.2.3 The "oligodendrocytic" connexins: Cx29, Cx32, and Cx47

First described in an abstract by Altevogt (44) and further characterized by Sohl *et al.* (45), when this thesis research was initiated, it was well known Cx29 was expressed by oligodendrocytes and Schwann cells in both the central and peripheral nervous systems (46-48) and was the most divergent of all Cx family members (46). Null-mice for Cx29 have been generated by two groups (49, 50) with both inserting a *lacZ* reporter gene coding for β-galactosidase in place of the Cx29 gene and under control of the Cx29 promoter. Both strains show no overt phenotype with respect to myelination although the Altevogt mouse eventually develops deafness (51) while the Eiberger mouse does not (50). The former strain was used in the experiments of this thesis.

Figure 1.2. Connexins are expressed by the major cell types of the brain. Schematic diagram demonstrating known connexin protein expression, at the time of this thesis, in the major cell types of the mature brain including Type 1 nestin^{+}GFAP^{+} neural progenitor cells (NPCs), Type 2 nestin^{+}GFAP^{-} NPCs, Type 3 doublecortin (DCX)$^{+}$ neuroblasts, neurons, astrocytes, oligodendrocyte progenitor cells (OPCs) and oligodendrocytes.

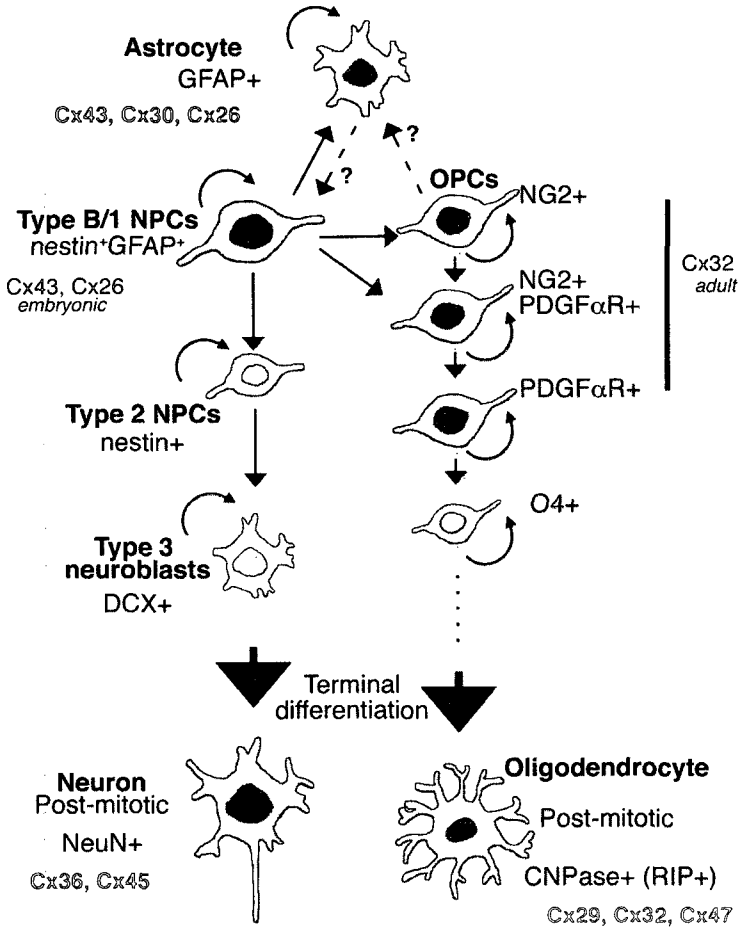
Astrocyte
GFAP+
Cx43, Cx30, Cx26
?
?
OPCs
NG2+
Type B/1 NPCs
nestin+GFAP+
Cx43, Cx26
embryonic
NG2+
PDGFαR+
Cx32
adult
PDGFαR+
Type 2 NPCs
nestin+
O4+
Type 3
neuroblasts
DCX+
Terminal
differentiation
Neuron
Post-mitotic
NeuN+
Cx36, Cx45
Oligodendrocyte
Post-mitotic
CNPase+ (RIP+)
Cx29, Cx32, Cx47

Figure 1.2

Interestingly, the function of Cx29 remains unknown. Cx29 connexons likely do not form functional intercellular channels (46, 52). Due to its localization to the adaxonal membrane of oligodendrocytes and Schwann cells, it has been frequently postulated Cx29-mediated hemichannels (i.e., single membrane channels) participate in K^+ buffering (46, 53) but this hypothesis has never been concretely tested. Indeed, hemichannel activity has also not been rigorously investigated. Certainly, dye transfer to and from the extracellular milieu from HeLa cells transfected with hCx31.3 (human Cx29) has been shown but this group was unable to record a current from these cells (54) leaving whether or not Cx29 truly forms hemichannels and what ion or metabolite normally passes through the channel undetermined. A recent study confirmed the Altevogt mouse phenotype demonstrating mutations in hCx31.3 are genetic determinants of non-syndromic deafness (55). Although this group has produced point mutants and found retention of these mutants in the ER (56) - they have not further explored why the lack of Cx29 trafficking to the plasma membrane results in hearing loss.

Following earlier ambiguities about the localization of Cx32 in the nervous system, it is now agreed the main cell types expressing Cx32 are oligodendrocytes of the CNS and Schwann cells of the peripheral nervous system (PNS). Our lab has further demonstrated expression of Cx32 in oligodendrocyte precursor cells (OPCs) of the adult dentate gyrus, specifically in OPCs expressing the neuron/glia antigen 2 (NG2) (57) chondroitin sulphate proteoglycan and in platelet-derived growth factor receptor alpha$^+$ (PDGFαR) cells (58). Unlike Cx29, Cx32 forms both intercellular channels and hemichannels. In oligodendrocytes, Cx32 is found on the soma and in the paranodal region. It has been shown to form 'reflexive' gap junctions within compact myelin, which is believed to provide a shunt for ions to be removed from the adaxonal space. It is apposed to Cx30 containing channels on astrocytes and mediates, in part, astrocyte-oligodendrocyte (A:O) GJIC (49, 59). Mutations of Cx32 in humans lead to a peripheral neuropathy, X-linked Charcot-Marie-Tooth Disease, which has been replicated in Cx32 null-mutant mice (60, 61).

Cx47 was first identified by Teubner *et al.* (62) in 2001. Northern blot analysis revealed a peak in transcript at P14, which coincides with peak myelination (62). Cx47 is localized to oligodendrocyte soma and proximal processes. Again, two groups have generated null-mutant mice. Odermatt *et al.* (63) inserted a GFP reporter in place of the Cx47 gene inserted in-frame after the seventh codon of the Cx47 gene and removing some of the 3'UTR. Menichella *et al.* (64) used a neo-cassette insert to remove most of the 5'UTR, the N-terminus and the four transmembrane domain sequences leaving only a small portion of the C-terminus intact however no mRNA or protein was observed in knock-out (KO) spinal cord. While the Menichella mouse shows no overt phenotype and no defects in myelin using semithin sections, the Odermatt mouse develops vacuolized myelin in the CNS of some but not all Cx47$^{-/-}$ mice examined. In animals with no vacuoles, there is no difference in the state of the myelin when compared to wild-type controls. When crossed with Cx32 KO, both Cx47$^{-/-}$ null-mouse lines produce double KOs which develop tremor, tonic seizures, and sporadic convulsions that generally lead to death during the 6th postnatal week. In addition to thin myelin sheath and presence of vacuoles, Menichella observed macrophages containing myelin debris and apoptotic oligodendrocytes. Odermatt *et al.* also show myelination was developmentally delayed in Cx47$^{-/-}$ mice versus WT. Although the demyelination phenotype is mild in Cx47 -/- mice, point mutations of Cx47 in humans result in a rather devastating leukodystrophy, Pelizaeus-Merzbacher-like disease (PMLD)(65). Reasons for these drastic differences may be linked to ER retention of certain point mutants combined with a more pronounced effect of loss of Cx47/Cx43 A:O GJIC in humans than in mice (66). In the single and double KOs, PNS myelin was unaffected which is consistent with Cx47 not being expressed by Schwann cells of the PNS.

Together, these three Cxs form the oligodendrocyte component of the glial syncytium (Figure 1.3). A recent review from Rash (53) nicely highlights the role of the glial syncytium in K^+ buffering and clearance in the brain. Propagation of action potentials along axons causes local increases in K^+ that are cleared through the action of the syncytium. As suggested above, it is proposed Cx29 might be involved

Figure 1.3. The glial syncytium plays a major role in K^+ buffering. Schematic diagram of how the glial syncytium uptakes and buffers K^+. Following neuronal activity, K^+ is taken up by oligodendrocytes (OL) which transfers the K^+ to astrocytes (A) via gap junctional intercellular communication mediated mainly by Cx47:Cx43 and Cx32:Cx30 channels. K+ then flows through the astrocytic network to be extruded into the blood stream or cerebral spinal fluid via astrocytic endfeet. BV - blood vessel, ECM - extracellular matrix.

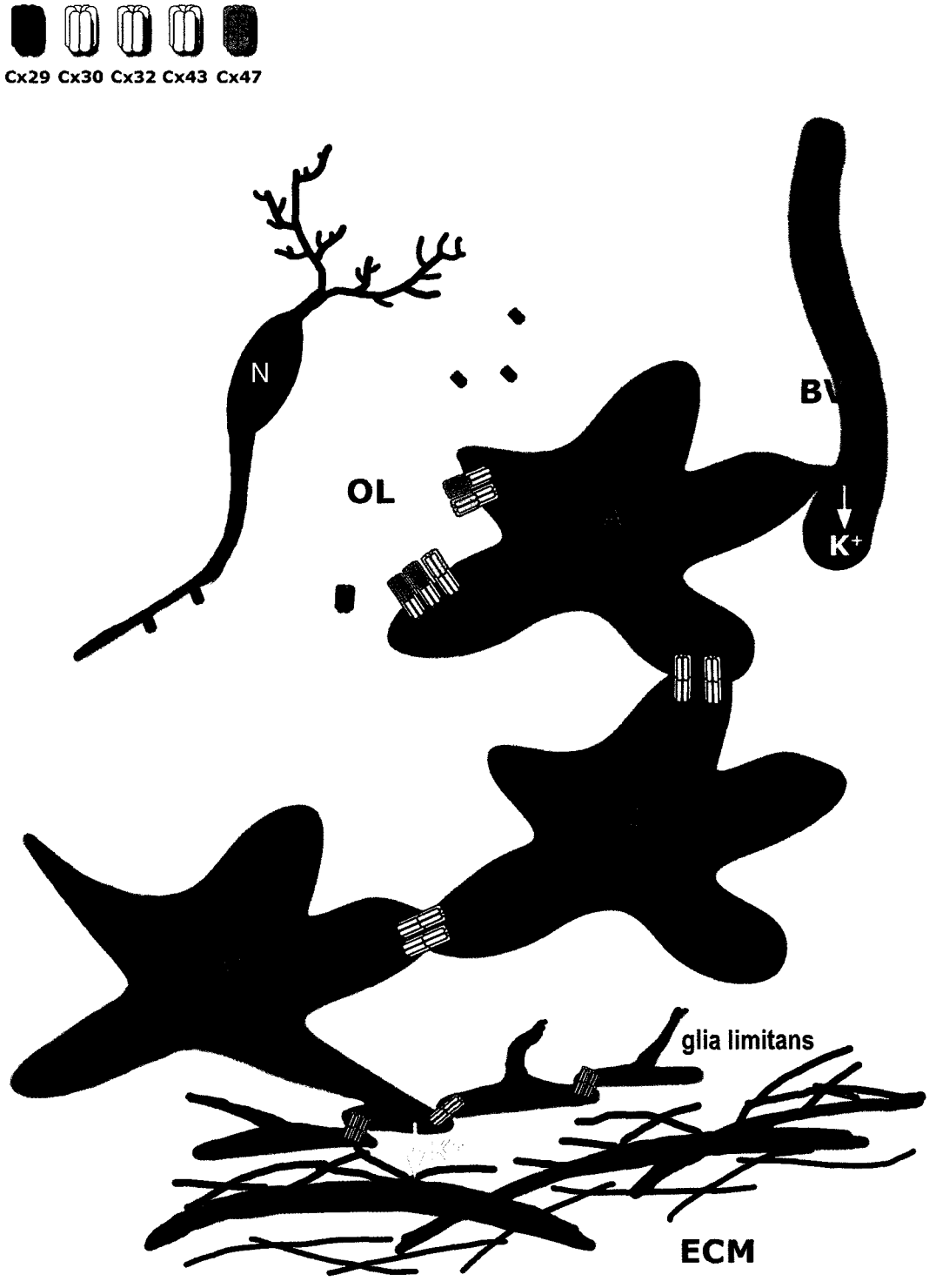

Figure 1.3

in the initial K^+ uptake from the adaxonal space, although, again, this hypothesis has yet to be empirically tested. Once inside the oligodendrocyte, K^+ flows through reflexive gap junctions formed of Cx32 to the outer myelin wrap and finally to the soma where the majority of Cx47 and Cx32 gap junctions are found. Cx47 forms intercellular channels with Cx43 on astrocytes and is the main mediator of A:O GJIC (48, 49, 59, 67). K^+ would thus flow from the oligodendrocyte to the astrocyte via GJIC. Astrocytes are highly coupled to each other by gap junctions, this would permit the distribution of K^+ throughout the astrocyte system and eventual release of K^+ (and accompanying osmotic water) from astrocytic endfeet into blood vessels or into the cerebral spinal fluid. Interestingly, Cx30/Cx43 double-null mutant mice, where Cx30 is constitutively deleted and Cx43 selectively deleted from astrocytes, show a similar albeit milder demyelinating phenotype as Cx32/47 double-null mutant mice (68) thus stressing the importance of proper functioning of the glial syncytium in maintaining oligodendrocyte number.

1.3 Oligodendrocytes

1.3.1 Origins of oligodendrocytes

In general, neurogenesis, the birth of neurons, occurs early in the embryonic stage while gliogenesis, the birth of astrocytes and oligodendrocytes, occurs in the late embryonic/early postnatal period (69). However, OPCs are born early in development in the embryonic forebrain and mainly express the marker PDGFαR, a receptor tyrosine kinase. Originating in the medial ganglionic eminence (MGE) at embryonic day 12.5 (E12.5), these OPCs migrate radially and dorsally to populate all areas of the cerebrum and activate at later developmental time frames to generate oligodendrocytes (70, 71). Cells bearing the OPC marker NG2 (also known as CSPG-4) appear a few days after the first PDGFαR$^+$ cells. It seems most PDGFαR$^+$ cells during this embryonic stage co-express NG2 although a few scattered cells do not. At E18, these initial OPCs are supplemented by OPCs from the lateral and/or caudal ganglionic eminences (LGE and CGE, respectively) whereas a third wave of cortical-derived OPCs contributes to oligodendrocyte production postnatally (72).

At the end of the embryonic stage, all PDGFαR$^+$ cells express NG2 except for the PDGFαR$^+$ Type B cells (stem cells) along the SVZ (73). Interestingly, an OPC intrinsic* differentiation mechanism seems to exist whereby OPCs in culture will initiate a specification program after a certain amount of cell divisions and days *in vitro* (DIV) (74-76). This program is, however, readily overridden by extrinsic cues including co-culture with neurons (77). Interestingly, the initial OPCs from the MGE are almost completely eliminated in the forebrain postnatally (72). Upon deletion of the OPC populations from the MGE or LGE/CGE, the OPCs born at different developmental stages expand their territories to compensate for the missing populations, suggesting functional equality of these OPC subtypes, despite morphological and biochemical differences in the final OL population (78-80). This expansion occurs because OPCs seemingly compete for space - with a limiting amount of growth factor available the OPCs will migrate toward remaining sources of growth factor. However, they stop migrating upon encountering other OPCs likely due to contact inhibition (72, 81). Furthermore, interaction of OPCs with the extracellular matrix component laminin can augment the effects of growth factor signalling because of reciprocal synergism between integrin- (laminin receptors) and growth factor-mediated signalling pathways (82). This synergy therefore promotes the survival and specification of OPCs that have migrated to their proper targets and highlights the importance of extracellular matrix components in proper brain development, a focus of this thesis.

1.3.2 Postnatal oligodendrogenesis

In the adult, the Type B GFAP$^+$/nestin$^+$/PDGFαR$^+$ stem cells which line the SVZ, generate oligodendrocytes, neurons (83) and non-myelinating NG2$^+$ cells (84). A small proportion of Type B cells express Olig2, a transcription factor required for NG2 cell specification (85) also expressed by both OPCs and oligodendrocytes (86).

---

* The term "intrinsic" will be used to denote the complement of proteins, transcriptions factors, epigenetic changes, etc. found within a progenitor cell that affect its proliferation and specification as nicely demonstrated in a review by Suh *et al.* (87)

However, in Olig2 fate mapping studies in the adult, cells expressing the target reporter gene were found to be NG2 cells, oligodendrocytes or grey matter astrocytes but not neurons, although only cortical regions were examined (88). No link was made specifically to the Type B cells of the SVZ making it difficult to establish the origin of these Olig2$^+$ cells. In a separate study, NG2$^+$ OPCs were found to yield a small population of grey matter astrocytes (89). This highlights the continuing debates over whether OPCs are, in fact, multipotential (i.e., can produce not only oligodendrocytes but also other glia and, even more controversially neurons (90, 91)) *in vivo* and whether different OPC populations exist (i.e., those born embryonically, those generated from multipotential Type B neural stem cells in adult tissue and those generated by self-renewal of existing NG2$^+$ cells in adults). NG2$^+$ cells are mainly thought to be OPCs and indeed continue to give rise to new oligodendrocytes throughout the lifespan of the animal. OPCs are therefore the major cycling cell population in the adult brain (92) (Figure 1.4a). A subpopulation of NG2 glia do not divide in uninjured brain and likely "monitor" neuronal activity given that some NG2 glia possess AMPA receptors and are responsive to glutamate (93, 94) thus making them sensitive to neuronal activity. This hypothesis is further supported by the finding that NG2 glia can also be responsive to GABA (via the $GABA_A$ receptor) which leads to activation of sodium channels followed by changes in intracellular calcium levels and stimulation of migration (95).

Using Olig2 and NG2 reporter mice where marker genes are placed under the control of these respective promoters, it has been found the rate of adult generation of oligodendrocytes is higher in white matter than in grey matter (88, 96). Often, OPCs express both PDGFαR and NG2 with reports that 75% of NG2$^+$ cells are also PDGFαR$^+$ (97) in the adult. These data yet again demonstrate heterogeneity in the OPC population with functional impact having yet to be investigated. Furthermore, morphological and electrophysiological differences between grey and white matter NG2$^+$ cells have been observed. Grey matter NG2$^+$ cells show activity resembling immature action potentials following depolarization (98). Subpopulations of white matter NG2 cells have been shown to generate action potentials while the other

Figure 1.4. The process of oligodendrogenesis. A) Embryonic origins of oligodendrocytes and progeny of oligodendrocyte progenitor cells with indicated cell-type specific protein markers and transcription factors. B) Oligodendrogenesis which occurs *in vitro* in hippocampal-derived neural progenitor cells cultures derived from single nestin^{+}GFAP^{+} putative stem cells.

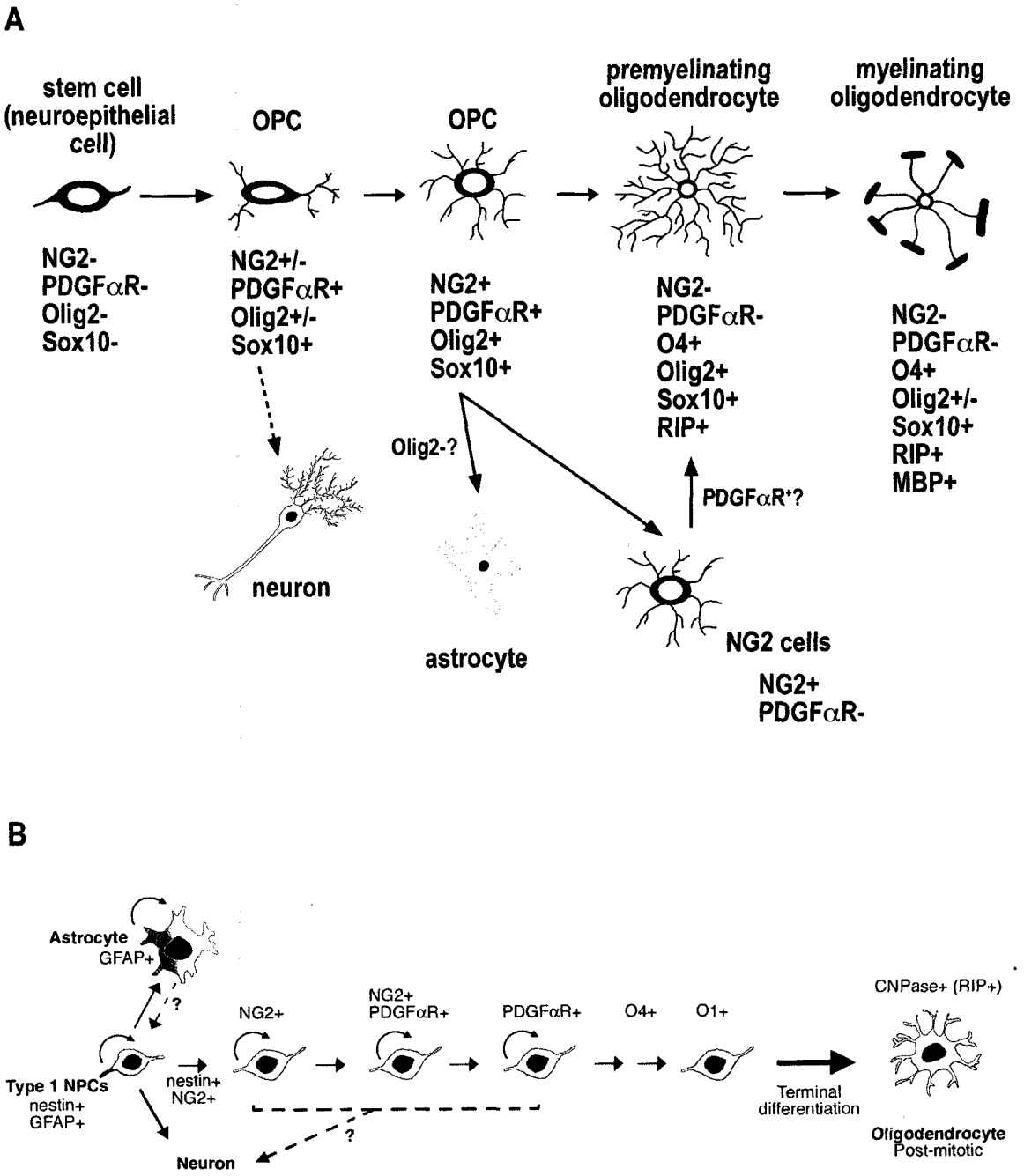
A
stem cell (neuroepithelial cell)
OPC
OPC
premyelinating oligodendrocyte
myelinating oligodendrocyte
NG2-
PDGFαR-
Olig2-
Sox10-
NG2+/-
PDGFαR+
Olig2+/-
Sox10+
NG2+
PDGFαR+
Olig2+
Sox10+
NG2-
PDGFαR-
O4+
Olig2+
Sox10+
RIP+
NG2-
PDGFαR-
O4+
Olig2+/-
Sox10+
RIP+
MBP+
Olig2-?
PDGFαR+?
neuron
astrocyte
NG2 cells
NG2+
PDGFαR-
B
Astrocyte
GFAP+
?
NG2+
NG2+
PDGFαR+
PDGFαR+
O4+
O1+
CNPase+ (RIP+)
Type 1 NPCs
nestin+
GFAP+
nestin+
NG2+
Terminal differentiation
Oligodendrocyte
Post-mitotic
?
Neuron

Figure 1.4

white matter population is non-excitable (99, 100). In the hippocampus, the focus of this study, $NG2^+$ cells show heterogeneity based upon their electrophysiological properties (101) and response to growth factors (102). Again, this functional heterogeneity has yet to be reconciled with lineage heterogeneity. However, generally, the use of reporter mice clearly demonstrates all oligodendrocytes are derived from cells having expressed NG2 at one time or another over the course of embryonic or postnatal development.

1.3.3 Dysfunction and death of oligodendrocytes: psychiatric and demyelinating disorders

While many in the neurosciences first concentrated on the role of neurons in the brain, followed by a focus on astrocytes, less attention has been given to the role of non-myelinating and myelinating oligodendrocytes eventhough defects in these cells underlie multiple neurodegenerative diseases. Multiple sclerosis (MS) is a prime example of a devastating demyelinating disorder. Demyelination of axons eventually leads to the degeneration of axons and results in both motor and behavioural deficits, some linked to cognition. Hippocampal oligodendrocyte loss, a grey matter pathology, for example, is thought to be responsible for some of the cognitive deficits seen in MS patients (103, 104). Remyelination does occur in MS but eventually fails resulting in exacerbation of axonal loss. Remyelination failure is thought to be due to three possible factors: eventual deficiency in OPC availability (105, 106), failure of OPC recruitment to the lesion site (especially observed in older animals), and/or failure of OPCs to specify to oligodendrocytes (107). Thus, two therapeutic approaches seem plausible - augmenting endogenous progenitor pools and promoting their specification to mature oligodendrocytes. Recently, Jessberger *et al.* (108) demonstrated multipotential NPCs from the subgranular zone (SGZ) of the dentate gyrus of the hippocampus, which normally become granule neurons, can be reprogrammed by overexpression of Ascl1 (Mash1) to become oligodendrocytes, providing further support for such strategies. Moreover, postmortem studies have shown abnormalities in white matter tracts of schizophrenia patients further linking defects in oligodendrocyte homeostasis to

psychiatric disorders (109, 110). Many oligodendrocyte genes have been determined as risk factors for development of schizophrenia - in fact, almost half of the risk alleles lie within genes determining oligodendrocyte function, survival and specification (111). Resulting changes in transcript are often found without accompanying deficits in neuronal genes demonstrating a primary role of oligodendrocyte dysfunction in disease manifestation.

Taken together, these studies highlight the importance of understanding the intrinsic and extrinsic (niche) factors regulating OPC proliferation and specification as well as oligodendrocyte survival. This understanding is certainly required to identify possible new avenues of therapy for both demyelinating and cognitive disorders.

1.4 Role of connexins in neurodevelopment

1.4.1 Embryonic neurodevelopment

Multiple Cxs begin to be expressed during the embryonic phase of neural development. Cx26 and Cx43 are known to be expressed by radial glia and NPCs found within the ventricular zone (VZ) of the developing brain (112-114). Seminal studies by LoTurco and Kriegstein have shown VZ progenitors to be coupled by gap junctions (114, 115). It is hypothesized this coupling helps synchronize entry (or exit) into (out of) different phases of the cell cycle as coupling increases the chance a cell will enter S phase. Indeed, coupled clusters are composed of radial glial cells and cycling precursors but not migrating or post-mitotic neurons (114). A subsequent study found Cx26 and Cx43 protein expression to be regulated reciprocally over the course of the cell cycle. Cx26 levels increase during S phase until cell entry into G1 while Cx43 levels decrease during this same time suggesting coupling is mediated by different Cxs in NPCs at different cell cycle phases (113). Certainly, Fushiki *et al.* (116) have shown loss of Cx43 results in decreased coupling between cells and in mislamination of cortical neurons. They surmised this was possibly due to "disrupted interactions between migrating neurons and radial glial fibers" perhaps mediated by the above mentioned mechanism elucidated by Elias and Kriegstein

(42). Another mechanism by which this may occur could be related to Ca^{2+} wave propagation, which is linked to cell migration and proliferation with changes in intracellular Ca^{2+} known to occur in VZ cells (117). ATP release through hemichannels can stimulate purinergic receptors (P2YRs) that leads to PLC-IP_3 signalling and release of Ca^{2+} from intracellular stores (118). In fact, Cina *et al.* (119) have proposed, based on work from Scemes *et al.* (120) that expression of P2Y1R might be linked to Cx43 because diminished expression of these receptors is seen in NPCs from Cx43 null-mice and that these two proteins are part of a signalling pathway controlling neuronal migration.

Early studies also showed extensive coupling between neurons in the postnatal cortex with a majority of dye-injected neurons being coupled to upwards of 80 neurons. This coupling showed a drastic decline after the first two postnatal weeks, likely upon maturation of the chemical synapses within cortical networks (121, 122). Work by Cina *et al.* (119) has looked at cortical Cx expression at the transcript and protein level within the developing embryonic neocortex to identify Cxs responsible for functional GJIC. They found transcript and protein expression of Cx26, Cx36, Cx37, Cx43 and Cx45 at all stages examined (E14, E16, and E18) while Cx40 transcript was only expressed at low levels at E14. Cx43 and Cx45 were the most abundant, with Cx43 showing increased expression at later developmental timepoints. Cx36 and Cx26 immunoreactivity was associated with the neuronal marker (MAP-2) indicative of expression in immature neurons. Cx26 was also found associated with nestin positive fibers in the cortical plate along with Cx43, suggesting expression in undifferentiated NPCs. In adult brain, only Cx36 expression was retained. The authors thus conclude Cx36 plays a role in coupling neuroepithelial cells in the VZ during early neurogenesis followed by coupling of migrating neurons of the cortical plate during corticogenesis. As for Cx43, a wealth of evidence from this study and others (112, 113, 123-125) implicate Cx43 in cell cycle regulation of progenitors, neurogenesis and neuronal migration. In other CNS regions, Leung *et al.* (126) investigated expression of Cx26, Cx32, Cx43 and Cx45 in the developing rat midbrain floor which gives rise to dopaminergic neurons of the

substantia nigra. All four Cxs were expressed throughout embryonic and postnatal development both in neuronal and non-neuronal cells. The authors hypothesize these Cxs play a role in the coordinated migration of dopaminergic neurons from the VZ to the substantia nigra and ventral tegmental area. *In vitro,* Rozental *et al.* (127) found a similar expression pattern focusing on the immortalized hippocampal neuronal progenitor cell line MK31. In untreated neuroblasts, Cx43 and Cx45 mRNA was detected. Upon stimulation of differentiation with IL-7, additional expression of Cx26, Cx33, Cx36 and Cx40 was observed (similar results were obtained for hippocampal primary cultures kept for 14 days *in vitro* (DIV)). Cx43 mRNA levels drop, Cx40 is not detected, and Cx36 form functional intercellular channels by the time these cells exhibit neuritic extensions, having additionally been treated with TGFα.

Together, these studies point to general roles of Cxs in proliferation, specification and migration of neural cells during development. To date, focus has been placed on the study of Cxs in embryonic development because these proteins are thought to metabolically and electronically (before the establishment of chemical synapses) couple new networks of cells that will be functionally connected in the adult. Less has been done to determine the role of Cxs in metabolic and electronic coupling of progenitor cells in the neurogenic and gliogenic areas of the adult brain. The role of Cx expression in regulating postnatal progenitor cell fate, specifically in the neurogenic and gliogenic niche of the hippocampal formation, will be the focus of this thesis.

1.4.2 Adult neurogenesis and gliogenesis

In adult brain, radial glial-like cells of the SGZ are coupled through gap junctions and express Cx43 and Cx30. Removal of these connexins results in uncoupling and reduced proliferation of the radial glial-like cells which leads to a decreased numbers of granule neurons (128). Furthermore, ablation of Cx30 alone is sufficient to reduce the number of proliferating neuroblasts in this region (129). Loss of Cx32 in $NG2^+$ cells of the SGZ causes overproliferation of these $NG2^+$ cells that

are then promptly deleted via apoptosis, presumably because no new oligodendrocytes are required. Otherwise, studies investigating whether postnatal neural progenitor cells, glial progenitors or neuroblasts express connexins, the role these connexins might play in the process of neurogenesis and gliogenesis, and whether Cxs influence proliferation, specification, migration and/or integration of these cells into functional networks are few and far between.

1.5 Hypothesis and objectives

The overarching hypothesis of my work is therefore that the *repertoire of Cxs expressed by neural progenitor cells in the SGZ directs, in part, their capacity to respond to competing neurogenic and gliogenic factors found within the microenvironment.* To test this hypothesis, I first looked at which Cxs were expressed in hippocampal-derived NPCs using an *in vitro* model (Figure 1.4b). Taking advantage of this model, I next investigated whether the ECM component within this niche regulated the expression and function of Cx proteins *in vitro*. In this model, novel localization of Cx29 to OPCs led me to further explore the role of this Cx on OPC proliferation and specification. Finally, to move these *in vitro* findings *in vivo*, I used a genetic loss of function approach to investigate whether Cx29 and the other 'oligodendrocytic' Cxs (Cx32 and Cx47) regulate adult progenitor cell proliferation, specification, and cell replacement in the SGZ.

1.6 References

1. Riquelme, P.A., E. Drapeau, and F. Doetsch. 2008. Brain micro-ecologies: neural stem cell niches in the adult mammalian brain. *Philos Trans R Soc Lond B Biol Sci* 363:123-137.

2. Elias, L.A., and A.R. Kriegstein. 2008. Gap junctions: multifaceted regulators of embryonic cortical development. *Trends Neurosci* 31:243-250.

3. Lie, D.C., G. Dziewczapolski, A.R. Willhoite, B.K. Kaspar, C.W. Shults, and F.H. Gage. 2002. The adult substantia nigra contains progenitor cells with neurogenic potential. *J Neurosci* 22:6639-6649.

4. Sohl, G., and K. Willecke. 2003. An update on connexin genes and their nomenclature in mouse and man. *Cell Commun Adhes* 10:173-180.

5. Saez, J.C., V.M. Berthoud, M.C. Branes, A.D. Martinez, and E.C. Beyer. 2003. Plasma membrane channels formed by connexins: their regulation and functions. *Physiol Rev* 83:1359-1400.

6. Goodenough, D.A., J.A. Goliger, and D.L. Paul. 1996. Connexins, connexons, and intercellular communication. *Annu Rev Biochem* 65:475-502.

7. Foote, C.I., L. Zhou, X. Zhu, and B.J. Nicholson. 1998. The pattern of disulfide linkages in the extracellular loop regions of connexin 32 suggests a model for the docking interface of gap junctions. *J Cell Biol* 140:1187-1197.

8. Dahl, G., W. Nonner, and R. Werner. 1994. Attempts to define functional domains of gap junction proteins with synthetic peptides. *Biophys J* 67:1816-1822.

9. Haefliger, J.A., R. Bruzzone, N.A. Jenkins, D.J. Gilbert, N.G. Copeland, and D.L. Paul. 1992. Four novel members of the connexin family of gap junction proteins. Molecular cloning, expression, and chromosome mapping. *J Biol Chem* 267:2057-2064.

10. Sohl, G., J. Degen, B. Teubner, and K. Willecke. 1998. The murine gap junction gene connexin36 is highly expressed in mouse retina and regulated during brain development. *FEBS Lett* 428:27-31.

11. Musil, L.S., and D.A. Goodenough. 1993. Multisubunit assembly of an integral plasma membrane channel protein, gap junction connexin43, occurs after exit from the ER. *Cell* 74:1065-1077.

12. Koval, M., J.E. Harley, E. Hick, and T.H. Steinberg. 1997. Connexin46 is retained as monomers in a trans-Golgi compartment of osteoblastic cells. *J Cell Biol* 137:847-857.

13. Diez, J.A., S. Ahmad, and W.H. Evans. 1999. Assembly of heteromeric connexons in guinea-pig liver en route to the Golgi apparatus, plasma membrane and gap junctions. *Eur J Biochem* 262:142-148.

14. Das Sarma, J., F. Wang, and M. Koval. 2002. Targeted gap junction protein constructs reveal connexin-specific differences in oligomerization. *J Biol Chem* 277:20911-20918.

15. Laird, D.W. 2006. Life cycle of connexins in health and disease. *Biochem J* 394:527-543.

16. Lauf, U., B.N. Giepmans, P. Lopez, S. Braconnot, S.C. Chen, and M.M. Falk. 2002. Dynamic trafficking and delivery of connexons to the plasma membrane and accretion to gap junctions in living cells. *Proc Natl Acad Sci U S A* 99:10446-10451.

17. Thomas, T., K. Jordan, J. Simek, Q. Shao, C. Jedeszko, P. Walton, and D.W. Laird. 2005. Mechanisms of Cx43 and Cx26 transport to the plasma membrane and gap junction regeneration. *J Cell Sci* 118:4451-4462.

18. Jordan, K., J.L. Solan, M. Dominguez, M. Sia, A. Hand, P.D. Lampe, and D.W. Laird. 1999. Trafficking, assembly, and function of a connexin43-green fluorescent protein chimera in live mammalian cells. *Mol Biol Cell* 10:2033-2050.

19. Fallon, R.F., and D.A. Goodenough. 1981. Five-hour half-life of mouse liver gap-junction protein. *J Cell Biol* 90:521-526.

20. Beardslee, M.A., J.G. Laing, E.C. Beyer, and J.E. Saffitz. 1998. Rapid turnover of connexin43 in the adult rat heart. *Circ Res* 83:629-635.

21. Laing, J.G., and E.C. Beyer. 1995. The gap junction protein connexin43 is degraded via the ubiquitin proteasome pathway. *J Biol Chem* 270:26399-26403.

22. Musil, L.S., E.C. Beyer, and D.A. Goodenough. 1990. Expression of the gap junction protein connexin43 in embryonic chick lens: molecular cloning, ultrastructural localization, and post-translational phosphorylation. *J Membr Biol* 116:163-175.

23. Laird, D.W., K.L. Puranam, and J.P. Revel. 1991. Turnover and phosphorylation dynamics of connexin43 gap junction protein in cultured cardiac myocytes. *Biochem J* 273(Pt 1):67-72.

24. Lampe, P.D. 1994. Analyzing phorbol ester effects on gap junctional communication: a dramatic inhibition of assembly. *J Cell Biol* 127:1895-1905.

25. White, T.W., D.L. Paul, D.A. Goodenough, and R. Bruzzone. 1995. Functional analysis of selective interactions among rodent connexins. *Mol Biol Cell* 6:459-470.

26. White, T.W., R. Bruzzone, S. Wolfram, D.L. Paul, and D.A. Goodenough. 1994. Selective interactions among the multiple connexin proteins expressed in the vertebrate lens: the second extracellular domain is a determinant of compatibility between connexins. *J Cell Biol* 125:879-892.

27. Maeda, S., S. Nakagawa, M. Suga, E. Yamashita, A. Oshima, Y. Fujiyoshi, and T. Tsukihara. 2009. Structure of the connexin 26 gap junction channel at 3.5 A resolution. *Nature* 458:597-602.

28. Saez, J.C., J.A. Connor, D.C. Spray, and M.V. Bennett. 1989. Hepatocyte gap junctions are permeable to the second messenger, inositol 1,4,5-trisphosphate, and to calcium ions. *Proc Natl Acad Sci U S A* 86:2708-2712.

29. Bedner, P., H. Niessen, B. Odermatt, K. Willecke, and H. Harz. 2003. A method to determine the relative cAMP permeability of connexin channels. *Exp Cell Res* 291:25-35.

30. Pearson, R.A., N. Dale, E. Llaudet, and P. Mobbs. 2005. ATP released via gap junction hemichannels from the pigment epithelium regulates neural retinal progenitor proliferation. *Neuron* 46:731-744.

31. Bruzzone, R., T.W. White, and D.L. Paul. 1996. Connections with connexins: the molecular basis of direct intercellular signaling. *Eur J Biochem* 238:1-27.

32. Kumar, N.M., and N.B. Gilula. 1996. The gap junction communication channel. *Cell* 84:381-388.

33. Valiunas, V., Y.Y. Polosina, H. Miller, I.A. Potapova, L. Valiuniene, S. Doronin, R.T. Mathias, R.B. Robinson, M.R. Rosen, I.S. Cohen, and P.R. Brink. 2005. Connexin-specific cell-to-cell transfer of short interfering RNA by gap junctions. *J Physiol* 568:459-468.

34. Wolvetang, E.J., M.F. Pera, and K.S. Zuckerman. 2007. Gap junction mediated transport of shRNA between human embryonic stem cells. *Biochem Biophys Res Commun* 363:610-615.

35. Bedner, P., H. Niessen, B. Odermatt, M. Kretz, K. Willecke, and H. Harz. 2006. Selective permeability of different connexin channels to the second messenger cyclic AMP. *J Biol Chem* 281:6673-6681.

36. Goldberg, G.S., P.D. Lampe, and B.J. Nicholson. 1999. Selective transfer of endogenous metabolites through gap junctions composed of different connexins. *Nat Cell Biol* 1:457-459.

37. Ayad, W.A., D. Locke, I.V. Koreen, and A.L. Harris. 2006. Heteromeric, but not homomeric, connexin channels are selectively permeable to inositol phosphates. *J Biol Chem* 281:16727-16739.

38. Saez, J.C., M.A. Retamal, D. Basilio, F.F. Bukauskas, and M.V. Bennett. 2005. Connexin-based gap junction hemichannels: gating mechanisms. *Biochim Biophys Acta* 1711:215-224.

39. Li, X., A.V. Ionescu, B.D. Lynn, S. Lu, N. Kamasawa, M. Morita, K.G. Davidson, T. Yasumura, J.E. Rash, and J.I. Nagy. 2004. Connexin47, connexin29 and connexin32 co-expression in oligodendrocytes and Cx47 association with zonula occludens-1 (ZO-1) in mouse brain. *Neuroscience* 126:611-630.

40. Singh, D., J.L. Solan, S.M. Taffet, R. Javier, and P.D. Lampe. 2005. Connexin 43 interacts with zona occludens-1 and -2 proteins in a cell cycle stage-specific manner. *J Biol Chem* 280:30416-30421.

41. Giepmans, B.N. 2004. Gap junctions and connexin-interacting proteins. *Cardiovasc Res* 62:233-245.

42. Elias, L.A., D.D. Wang, and A.R. Kriegstein. 2007. Gap junction adhesion is necessary for radial migration in the neocortex. *Nature* 448:901-907.

43. Nagy, J.I., F.E. Dudek, and J.E. Rash. 2004. Update on connexins and gap junctions in neurons and glia in the mammalian nervous system. *Brain Res Brain Res Rev* 47:191-215.

44. Altevogt, B.M., D.L. Paul, and D.A. Goodenough. 2000. Cloning and characterization of a novel central nervous system connexin, mouse connexin29. *Mol Biol Cell* 11:abstract 1713.

45. Sohl, G., J. Eiberger, Y.T. Jung, C.A. Kozak, and K. Willecke. 2001. The mouse gap junction gene connexin29 is highly expressed in sciatic nerve and regulated during brain development. *Biol Chem* 382:973-978.

46. Altevogt, B.M., K.A. Kleopa, F.R. Postma, S.S. Scherer, and D.L. Paul. 2002. Connexin29 is uniquely distributed within myelinating glial cells of the central and peripheral nervous systems. *J Neurosci* 22:6458-6470.

47. Nagy, J.I., A.V. Ionescu, B.D. Lynn, and J.E. Rash. 2003. Connexin29 and connexin32 at oligodendrocyte and astrocyte gap junctions and in myelin of the mouse central nervous system. *J Comp Neurol* 464:356-370.

48. Kleopa, K.A., J.L. Orthmann, A. Enriquez, D.L. Paul, and S.S. Scherer. 2004. Unique distributions of the gap junction proteins connexin29, connexin32, and connexin47 in oligodendrocytes. *Glia* 47:346-357.

49. Altevogt, B.M., and D.L. Paul. 2004. Four classes of intercellular channels between glial cells in the CNS. *J Neurosci* 24:4313-4323.

50. Eiberger, J., M. Kibschull, N. Strenzke, A. Schober, H. Bussow, C. Wessig, S. Djahed, H. Reucher, D.A. Koch, J. Lautermann, T. Moser, E. Winterhager, and K. Willecke. 2006. Expression pattern and functional characterization of connexin29 in transgenic mice. *Glia* 53:601-611.

51. Tang, W., Y. Zhang, Q. Chang, S. Ahmad, I. Dahlke, H. Yi, P. Chen, D.L. Paul, and X. Lin. 2006. Connexin29 is highly expressed in cochlear Schwann cells, and it is required for the normal development and function of the auditory nerve of mice. *J Neurosci* 26:1991-1999.

52. Ahn, M., J. Lee, A. Gustafsson, A. Enriquez, E. Lancaster, J.Y. Sul, P.G. Haydon, D.L. Paul, Y. Huang, C.K. Abrams, and S.S. Scherer. 2008. Cx29 and Cx32, two connexins expressed by myelinating glia, do not interact and are functionally distinct. *J Neurosci Res* 86:992-1006.

53. Rash, J.E. 2009. Molecular disruptions of the panglial syncytium block potassium siphoning and axonal saltatory conduction: pertinence to neuromyelitis optica and other demyelinating diseases of the central nervous system. *Neuroscience*

54. Sargiannidou, I., M. Ahn, A.D. Enriquez, A. Peinado, R. Reynolds, C. Abrams, S.S. Scherer, and K.A. Kleopa. 2008. Human oligodendrocytes express Cx31.3: function and interactions with Cx32 mutants. *Neurobiol Dis* 30:221-233.

55. Wang, W.H., J.J. Yang, Y.C. Lin, J.T. Yang, C.H. Chan, and S.Y. Li. Identification of novel variants in the Cx29 gene of nonsyndromic hearing loss patients using buccal cells and restriction fragment length polymorphism method. *Audiol Neurootol* 15:81-87.

56. Hong, H.M., J.J. Yang, C.C. Su, J.Y. Chang, T.C. Li, and S.Y. Li. A novel mutation in the connexin 29 gene may contribute to nonsyndromic hearing loss. *Hum Genet* 127:191-199.

57. Wilson, S.S., E.E. Baetge, and W.B. Stallcup. 1981. Antisera specific for cell lines with mixed neuronal and glial properties. *Dev Biol* 83:146-153.

58. Melanson-Drapeau, L., S. Beyko, S. Dave, A.L. Hebb, D.J. Franks, C. Sellitto, D.L. Paul, and S.A. Bennett. 2003. Oligodendrocyte progenitor enrichment in the connexin32 null-mutant mouse. *J Neurosci* 23:1759-1768.

59. Nagy, J.I., A.V. Ionescu, B.D. Lynn, and J.E. Rash. 2003. Coupling of astrocyte connexins Cx26, Cx30, Cx43 to oligodendrocyte Cx29, Cx32, Cx47: Implications from normal and connexin32 knockout mice. *Glia* 44:205-218.

60. Nelles, E., C. Butzler, D. Jung, A. Temme, H.D. Gabriel, U. Dahl, O. Traub, F. Stumpel, K. Jungermann, J. Zielasek, K.V. Toyka, R. Dermietzel, and K. Willecke. 1996. Defective propagation of signals generated by sympathetic nerve stimulation in the liver of connexin32-deficient mice. *Proc Natl Acad Sci U S A* 93:9565-9570.

61. Scherer, S.S., Y.T. Xu, E. Nelles, K. Fischbeck, K. Willecke, and L.J. Bone. 1998. Connexin32-null mice develop demyelinating peripheral neuropathy. *Glia* 24:8-20.

62. Teubner, B., B. Odermatt, M. Guldenagel, G. Sohl, J. Degen, F. Bukauskas, J. Kronengold, V.K. Verselis, Y.T. Jung, C.A. Kozak, K. Schilling, and K. Willecke. 2001. Functional expression of the new gap junction gene connexin47 transcribed in mouse brain and spinal cord neurons. *J Neurosci* 21:1117-1126.

63. Odermatt, B., K. Wellershaus, A. Wallraff, G. Seifert, J. Degen, C. Euwens, B. Fuss, H. Bussow, K. Schilling, C. Steinhauser, and K. Willecke. 2003. Connexin 47 (Cx47)-deficient mice with enhanced green fluorescent protein reporter gene reveal predominant oligodendrocytic expression of Cx47 and display vacuolized myelin in the CNS. *J Neurosci* 23:4549-4559.

64. Menichella, D.M., D.A. Goodenough, E. Sirkowski, S.S. Scherer, and D.L. Paul. 2003. Connexins are critical for normal myelination in the CNS. *J Neurosci* 23:5963-5973.

65. Uhlenberg, B., M. Schuelke, F. Ruschendorf, N. Ruf, A.M. Kaindl, M. Henneke, H. Thiele, G. Stoltenburg-Didinger, F. Aksu, H. Topaloglu, P. Nurnberg, C. Hubner, B. Weschke, and J. Gartner. 2004. Mutations in the gene encoding gap junction protein alpha 12 (connexin 46.6) cause Pelizaeus-Merzbacher-like disease. *Am J Hum Genet* 75:251-260.

66. Orthmann-Murphy, J.L., A.D. Enriquez, C.K. Abrams, and S.S. Scherer. 2007. Loss-of-function GJA12/Connexin47 mutations cause Pelizaeus-Merzbacher-like disease. *Mol Cell Neurosci* 34:629-641.

67. Orthmann-Murphy, J.L., M. Freidin, E. Fischer, S.S. Scherer, and C.K. Abrams. 2007. Two distinct heterotypic channels mediate gap junction coupling between astrocyte and oligodendrocyte connexins. *J Neurosci* 27:13949-13957.

68. Lutz, S.E., Y. Zhao, M. Gulinello, S.C. Lee, C.S. Raine, and C.F. Brosnan. 2009. Deletion of astrocyte connexins 43 and 30 leads to a dysmyelinating phenotype and hippocampal CA1 vacuolation. *J Neurosci* 29:7743-7752.

69. Cameron, R.S., and P. Rakic. 1991. Glial cell lineage in the cerebral cortex: a review and synthesis. *Glia* 4:124-137.

70. Tekki-Kessaris, N., R. Woodruff, A.C. Hall, W. Gaffield, S. Kimura, C.D. Stiles, D.H. Rowitch, and W.D. Richardson. 2001. Hedgehog-dependent oligodendrocyte lineage specification in the telencephalon. *Development* 128:2545-2554.

71. Richardson, W.D., N. Kessaris, and N. Pringle. 2006. Oligodendrocyte wars. *Nat Rev Neurosci* 7:11-18.

72. Kessaris, N., M. Fogarty, P. Iannarelli, M. Grist, M. Wegner, and W.D. Richardson. 2006. Competing waves of oligodendrocytes in the forebrain and postnatal elimination of an embryonic lineage. *Nat Neurosci* 9:173-179.

73. Nishiyama, A., X.H. Lin, N. Giese, C.H. Heldin, and W.B. Stallcup. 1996. Co-localization of NG2 proteoglycan and PDGF alpha-receptor on O2A progenitor cells in the developing rat brain. *J Neurosci Res* 43:299-314.

74. Temple, S., and M.C. Raff. 1986. Clonal analysis of oligodendrocyte development in culture: evidence for a developmental clock that counts cell divisions. *Cell* 44:773-779.

75. Durand, B., and M. Raff. 2000. A cell-intrinsic timer that operates during oligodendrocyte development. *Bioessays* 22:64-71.

76. Gao, F.B., B. Durand, and M. Raff. 1997. Oligodendrocyte precursor cells count time but not cell divisions before differentiation. *Curr Biol* 7:152-155.

77. Calver, A.R., A.C. Hall, W.P. Yu, F.S. Walsh, J.K. Heath, C. Betsholtz, and W.D. Richardson. 1998. Oligodendrocyte population dynamics and the role of PDGF in vivo. *Neuron* 20:869-882.

78. Bjartmar, C., C. Hildebrand, and K. Loinder. 1994. Morphological heterogeneity of rat oligodendrocytes: electron microscopic studies on serial sections. *Glia* 11:235-244.

79. Butt, A.M., M. Ibrahim, F.M. Ruge, and M. Berry. 1995. Biochemical subtypes of oligodendrocyte in the anterior medullary velum of the rat as revealed by the monoclonal antibody Rip. *Glia* 14:185-197.

80. Butt, A.M., M. Ibrahim, and M. Berry. 1997. The relationship between developing oligodendrocyte units and maturing axons during myelinogenesis in the anterior medullary velum of neonatal rats. *J Neurocytol* 26:327-338.

81. Kirby, B.B., N. Takada, A.J. Latimer, J. Shin, T.J. Carney, R.N. Kelsh, and B. Appel. 2006. In vivo time-lapse imaging shows dynamic oligodendrocyte progenitor behavior during zebrafish development. *Nat Neurosci* 9:1506-1511.

82. ffrench-Constant, C., and H. Colognato. 2004. Integrins: versatile integrators of extracellular signals. *Trends Cell Biol* 14:678-686.

83. Jackson, E.L., J.M. Garcia-Verdugo, S. Gil-Perotin, M. Roy, A. Quinones-Hinojosa, S. VandenBerg, and A. Alvarez-Buylla. 2006. PDGFR alpha-positive B cells are neural stem cells in the adult SVZ that form glioma-like growths in response to increased PDGF signaling. *Neuron* 51:187-199.

84. Menn, B., J.M. Garcia-Verdugo, C. Yaschine, O. Gonzalez-Perez, D. Rowitch, and A. Alvarez-Buylla. 2006. Origin of oligodendrocytes in the subventricular zone of the adult brain. *J Neurosci* 26:7907-7918.

85. Ligon, K.L., S. Kesari, M. Kitada, T. Sun, H.A. Arnett, J.A. Alberta, D.J. Anderson, C.D. Stiles, and D.H. Rowitch. 2006. Development of NG2 neural progenitor cells requires Olig gene function. *Proc Natl Acad Sci U S A* 103:7853-7858.

86. Ligon, K.L., S.P. Fancy, R.J. Franklin, and D.H. Rowitch. 2006. Olig gene function in CNS development and disease. *Glia* 54:1-10.

87. Suh, H., W. Deng, and F.H. Gage. 2009. Signaling in adult neurogenesis. *Annu Rev Cell Dev Biol* 25:253-75.

88. Dimou, L., C. Simon, F. Kirchhoff, H. Takebayashi, and M. Gotz. 2008. Progeny of Olig2-expressing progenitors in the gray and white matter of the adult mouse cerebral cortex. *J Neurosci* 28:10434-10442.

89. Zhu, X., D.E. Bergles, and A. Nishiyama. 2008. NG2 cells generate both oligodendrocytes and gray matter astrocytes. *Development* 135:145-157.

90. Belachew, S., R. Chittajallu, A.A. Aguirre, X. Yuan, M. Kirby, S. Anderson, and V. Gallo. 2003. Postnatal NG2 proteoglycan-expressing progenitor cells are intrinsically multipotent and generate functional neurons. *J Cell Biol* 161:169-186.

91. Aguirre A.A., R. Chittajallu, S. Belachew, and V. Gallo. 2004. NG2-expressing cells in the subventricular zone are type C-like cells and contribute to interneuron generation in the postnatal hippocampus. *J Cell Biol* 165:575-589.

92. Dawson, M.R., A. Polito, J.M. Levine, and R. Reynolds. 2003. NG2-expressing glial progenitor cells: an abundant and widespread population of cycling cells in the adult rat CNS. *Mol Cell Neurosci* 24:476-488.

93. De Biase, L.M., A. Nishiyama, and D.E. Bergles. Excitability and Synaptic Communication within the Oligodendrocyte Lineage. *J Neurosci* 30:3600-3611.

94. Bergles, D.E., J.D. Roberts, P. Somogyi, and C.E. Jahr. 2000. Glutamatergic synapses on oligodendrocyte precursor cells in the hippocampus. *Nature* 405:187-191.

95. Tong, X.P., X.Y. Li, B. Zhou, W. Shen, Z.J. Zhang, T.L. Xu, and S. Duan. 2009. Ca(2+) signaling evoked by activation of Na(+) channels and Na(+)/Ca(2+) exchangers is required for GABA-induced NG2 cell migration. *J Cell Biol* 186:113-128.

96. Zhu, X., R. Szuki, and A. Nishiyama. 2008. The timing of NG2 cell differentiation in the brain. Program no. 124.9. *Neuroscience Meeting Planner*

97. He, Y., W. Cai, L. Wang, and P. Chen. 2009. A developmental study on the expression of PDGFalphaR immunoreactive cells in the brain of postnatal rats. *Neurosci Res* 65:272-279.

98. Chittajallu, R., A. Aguirre, and V. Gallo. 2004. NG2-positive cells in the mouse white and grey matter display distinct physiological properties. *J Physiol* 561:109-122.

99. Karadottir, R., N.B. Hamilton, Y. Bakiri, and D. Attwell. 2008. Spiking and nonspiking classes of oligodendrocyte precursor glia in CNS white matter. *Nat Neurosci* 11:450-456.

100. Ge, W.P., W. Zhou, Q. Luo, L.Y. Jan, and Y.N. Jan. 2009. Dividing glial cells maintain differentiated properties including complex morphology and functional synapses. *Proc Natl Acad Sci U S A* 106:328-333.

101. Karram, K., S. Goebbels, M. Schwab, K. Jennissen, G. Seifert, C. Steinhauser, K.A. Nave, and J. Trotter. 2008. NG2-expressing cells in the nervous system revealed by the NG2-EYFP-knockin mouse. *Genesis* 46:743-757.

102. Mason, J.L., and J.E. Goldman. 2002. A2B5+ and O4+ Cycling progenitors in the adult forebrain white matter respond differentially to PDGF-AA, FGF-2, and IGF-1. *Mol Cell Neurosci* 20:30-42.

103. Geurts, J.J., L. Bo, S.D. Roosendaal, T. Hazes, R. Daniels, F. Barkhof, M.P. Witter, I. Huitinga, and P. van der Valk. 2007. Extensive hippocampal demyelination in multiple sclerosis. *J Neuropathol Exp Neurol* 66:819-827.

104. Kujala, P., R. Portin, and J. Ruutiainen. 1997. The progress of cognitive decline in multiple sclerosis. A controlled 3-year follow-up. *Brain* 120 (Pt 2):289-297.

105. Ludwin, S.K. 1980. Chronic demyelination inhibits remyelination in the central nervous system. An analysis of contributing factors. *Lab Invest* 43:382-387.

106. Mason, J.L., A. Toews, J.D. Hostettler, P. Morell, K. Suzuki, J.E. Goldman, and G.K. Matsushima. 2004. Oligodendrocytes and progenitors become progressively depleted within chronically demyelinated lesions. *Am J Pathol* 164:1673-1682.

107. Franklin, R.J., and C. Ffrench-Constant. 2008. Remyelination in the CNS: from biology to therapy. *Nat Rev Neurosci* 9:839-855.

108. Jessberger, S., N. Toni, G.D. Clemenson, Jr., J. Ray, and F.H. Gage. 2008. Directed differentiation of hippocampal stem/progenitor cells in the adult brain. *Nat Neurosci* 11:888-893.

109. Agartz, I., J.L. Andersson, and S. Skare. 2001. Abnormal brain white matter in schizophrenia: a diffusion tensor imaging study. *Neuroreport* 12:2251-2254.

110. Ardekani, B.A., J. Nierenberg, M.J. Hoptman, D.C. Javitt, and K.O. Lim. 2003. MRI study of white matter diffusion anisotropy in schizophrenia. *Neuroreport* 14:2025-2029.

111. Hakak, Y., J.R. Walker, C. Li, W.H. Wong, K.L. Davis, J.D. Buxbaum, V. Haroutunian, and A.A. Fienberg. 2001. Genome-wide expression analysis reveals dysregulation of myelination-related genes in chronic schizophrenia. *Proc Natl Acad Sci U S A* 98:4746-4751.

112. Nadarajah, B., A.M. Jones, W.H. Evans, and J.G. Parnavelas. 1997. Differential expression of connexins during neocortical development and neuronal circuit formation. *J Neurosci* 17:3096-3111.

113. Bittman, K.S., and J.J. LoTurco. 1999. Differential regulation of connexin 26 and 43 in murine neocortical precursors. *Cereb Cortex* 9:188-195.

114. Bittman, K., D.F. Owens, A.R. Kriegstein, and J.J. LoTurco. 1997. Cell coupling and uncoupling in the ventricular zone of developing neocortex. *J Neurosci* 17:7037-7044.

115. Lo Turco, J.J., and A.R. Kriegstein. 1991. Clusters of coupled neuroblasts in embryonic neocortex. *Science* 252:563-566.

116. Fushiki, S., J.L. Perez Velazquez, L. Zhang, J.F. Bechberger, P.L. Carlen, and C.C. Naus. 2003. Changes in neuronal migration in neocortex of connexin43 null mutant mice. *J Neuropathol Exp Neurol* 62:304-314.

117. Owens, D.F., and A.R. Kriegstein. 1998. Patterns of intracellular calcium fluctuation in precursor cells of the neocortical ventricular zone. *J Neurosci* 18:5374-5388.

118. Duval, N., D. Gomes, V. Calaora, A. Calabrese, P. Meda, and R. Bruzzone. 2002. Cell coupling and Cx43 expression in embryonic mouse neural progenitor cells. *J Cell Sci* 115:3241-3251.

119. Cina, C., J.F. Bechberger, M.A. Ozog, and C.C. Naus. 2007. Expression of connexins in embryonic mouse neocortical development. *J Comp Neurol* 504:298-313.

120. Scemes, E., N. Duval, and P. Meda. 2003. Reduced expression of P2Y1 receptors in connexin43-null mice alters calcium signaling and migration of neural progenitor cells. *J Neurosci* 23:11444-11452.

121. Peinado, A., R. Yuste, and L.C. Katz. 1993. Extensive dye coupling between rat neocortical neurons during the period of circuit formation. *Neuron* 10:103-114.

122. Peinado, A., R. Yuste, and L.C. Katz. 1993. Gap junctional communication and the development of local circuits in neocortex. *Cereb Cortex* 3:488-498.

123. Naus, C.C., J.F. Bechberger, Y. Zhang, L. Venance, H. Yamasaki, S.C. Juneja, G.M. Kidder, and C. Giaume. 1997. Altered gap junctional communication, intercellular signaling, and growth in cultured astrocytes deficient in connexin43. *J Neurosci Res* 49:528-540.

124. Nadarajah, B., and J.G. Parnavelas. 1999. Gap junction-mediated communication in the developing and adult cerebral cortex. *Novartis Found Symp* 219:157-170; discussion 170-154.

125. Cheng, A., H. Tang, J. Cai, M. Zhu, X. Zhang, M. Rao, and M.P. Mattson. 2004. Gap junctional communication is required to maintain mouse cortical neural progenitor cells in a proliferative state. *Dev Biol* 272:203-216.

126. Leung, D.S., K. Unsicker, and B. Reuss. 2002. Expression and developmental regulation of gap junction connexins cx26, cx32, cx43 and cx45 in the rat midbrain-floor. *Int J Dev Neurosci* 20:63-75.

127. Rozental, R., M. Srinivas, S. Gokhan, M. Urban, R. Dermietzel, J.A. Kessler, D.C. Spray, and M.F. Mehler. 2000. Temporal expression of neuronal connexins during hippocampal ontogeny. *Brain Res Brain Res Rev* 32:57-71.

128. Kunze, A., M.R. Congreso, C. Hartmann, A. Wallraff-Beck, K. Huttmann, P. Bedner, R. Requardt, G. Seifert, C. Redecker, K. Willecke, A. Hofmann, A. Pfeifer, M. Theis, and C. Steinhauser. 2009. Connexin expression by radial glia-like cells is required for neurogenesis in the adult dentate gyrus. *Proc Natl Acad Sci U S A* 106:11336-11341.

129. Toeg, H.D. 2008. Role of connexin 30 in directing adult neural progenitor cell fate. In Department of Biochemistry, Microbiology and Immunology. University of Ottawa, Ottawa. 103.

Chapter 2: Neural progenitor cells express a wide repertoire of connexins that is modifiable by the extracellular matrix component laminin*

2.1 Objectives of this study

1) Determine which connexins are expressed by hippocampal-derived neural progenitor cells

2) Determine the cell types in which each connexin is expressed

3) Examine the effect of laminin on connexin protein expression and function

2.2 Statement of author contributions

SI and LGG performed the majority of the experimental work. SI, LGG, and SALB conceived and designed the experiments, analyzed the data, interpreted the results, and prepared the figures. CDS and RD carried out and interpreted the quantification of the lineage analysis with SI. CDS performed the immunogenic analyses on Cx36-/- neurospheres. LM participated in and interpreted the functional communication assays. AP performed the Cx45 RT-PCR and the comparison of different matrices on Cx43 expression. HDT participated in the Cx30 immunoassays and performed all of the flow cytometry experiments. ASM, KN, DLP, and AMS created and provided key study material and assisted in data analysis. DLP and AMS helped draft the manuscript. SI and SALB wrote the manuscript. SALB coordinated the study and provided financial support.

---

* A version of this chapter has been published in BMC Neuroscience:
Imbeault S*, Gauvin LG*, Toeg HD, Pettit A, Sorbara CD, Migahed L, DesRoches R, Menzies AS, Nishii K, Paul DL, Simon AM and Bennett SAL. (2009) The extracellular matrix controls gap junction protein expression and function in postnatal hippocampal progenitor cells. *BMC Neuroscience*. **10**(1):13.

2.3 The extracellular matrix controls gap junction protein expression and function in postnatal hippocampal neural progenitor cells

Sophie Imbeault[1*], Lianne G. Gauvin[1*], Hadi D. Toeg[1], Alexandra Pettit[1], Catherine D. Sorbara[1], Lamiaa Migahed[1], Rebecca DesRoches[1], A. Sheila Menzies[2], Kiyomasa Nishii[3], David L. Paul[2], Alexander M. Simon[4], and Steffany A.L. Bennett[1]

[*] Both authors contributed equally, [1]Neural Regeneration Laboratory and Ottawa Institute of Systems Biology, Dept. of Biochemistry, Microbiology and Immunology, University of Ottawa, ON, Canada, [2]Dept. of Neurobiology, Harvard Medical School, Boston, MA, USA, [3]Dept. of Cellular Neurobiology, Graduate School of Medicine, University of Tokyo, Tokyo, Japan, [4]Dept. of Physiology, University of Arizona, Tucson, AZ USA

Correspondence: Dr. Steffany Bennett, Neural Regeneration Laboratory, Department of Biochemistry, Microbiology and Immunology, University of Ottawa, 451 Smyth Rd., Ottawa, Ontario, Canada, K1H 8M5. Tel: 613 562-5800 x8372; Fax 613 562-5440; Email: sbennet@uottawa.ca

Acknowledgements: This work was supported by operating (#62826) and salary awards from the Canadian Institute of Health Research (CIHR) and the Ontario Mental Health Foundation (OMHF) to SALB, by NIH GM37751 and EY014127 to DLP, and by NIH HL64232 to AMS. SI, LGG, CDS, and HT were supported by Natural Sciences and Engineering Research Council (NSERC) graduate studentships. SI also received an Ontario Graduate Scholarship in Science and Technology. AP is supported by an OMHF graduate studentship. LM and RD received NSERC undergraduate student research awards. We thank James Bennett for editorial assistance.

2.4 Summary

Background: Gap junction protein and extracellular matrix signalling systems act in concert to influence developmental specification of neural stem and progenitor cells. It is not known how these two signalling systems interact. Here, we examined the role of ECM components in regulating connexin expression and function in postnatal hippocampal progenitor cells. **Results:** We found that Cx26, Cx29, Cx30, Cx37, Cx40, Cx43, Cx45 and Cx47 mRNA and protein but only Cx32 and Cx36 mRNA are detected in distinct neural progenitor cell populations cultured in the absence of exogenous ECM. Multipotential Type 1 cells express Cx26, Cx30, and Cx43 protein. Their Type 2a progeny but not Type 2b and 3 neuronally committed progenitor cells additionally express Cx37, Cx40, and Cx45. Cx29 and Cx47 protein is detected in early oligodendrocyte progenitors and mature oligodendrocytes respectively. Engagement with a laminin substrate markedly increases Cx26 protein expression, decreases Cx40, Cx43, Cx45, and Cx47 protein expression, and alters subcellular localization of Cx30. These changes are associated with decreased neurogenesis. Further, laminin elicits the appearance of Cx32 protein in early oligodendrocyte progenitors and Cx36 protein in immature neurons. These changes impact upon functional connexin-mediated hemichannel activity but not gap junctional intercellular communication. **Conclusions:** Together, these findings demonstrate a new role for extracellular matrix-cell interaction, specifically laminin, in the regulation of intrinsic connexin expression and function in postnatal neural progenitor cells.

2.5 Introduction

Juxtacrine signalling mechanisms, specifically cell-extracellular matrix (ECM) interactions and gap junctional intercellular communication (GJIC), act in concert to influence developmental specification of neural stem and progenitor cells (NPCs). The interaction of laminins with integrin receptors segregates proliferating units in the embryonic ventricular zone from migrating units in the overlying cortex (1) while GJIC within these ECM-defined boundaries ensures synchronous cellular activity between cells destined to become functional domains (2-4). Similarly, the interaction of laminin with receptors containing β1 integrin directs radial migration of proliferating neuroblasts from the embryonic ventricular zone and along the adult rostral migratory pathway (1, 5) while the presence of gap junction connexin proteins facilitates migration of neuroblasts along the axial processes of their radial glial guides during cortical lamination (6-8). Thus, available data suggest that ECM and connexin-mediated signalling systems act in concert to direct NPC specialization and migration.

Gap junction communication occurs through intercellular channels formed by connexins (9). Oligomerization of six connexins forms a hemichannel (connexon) when inserted into non-junctional plasma membranes (10). Connexons allow for the regulated passage of ions and small molecules (≤ 1 kDa) between the cytoplasm and the extracellular space (10). Alignment and docking of two connexons in adjacent cells creates an intercellular channel enabling direct cell-cell communication and possibly adhesion. Clusters of intercellular channels make up the morphologically defined gap junction (9). There are 20 different connexin proteins in mouse; 21 in humans (11). Fourteen (Cx26, Cx29, Cx30, Cx30.2, Cx31.1, Cx31.9, Cx32, Cx36, Cx37, Cx40, Cx43, Cx45, Cx47, Cx57) are detected in embryonic and/or adult central nervous system (12-15) but only select connexin combinations are capable of oligomerization, adhesion, and functional communication.

The impact of ECM components upon connexin expression in NPCs has not been tested. This is an important issue because NPCs are routinely expanded as neurospheres in the absence of exogenous ECM while functional assessment of cell-

cell signalling pathways often involves replating on adhesive substrates. Understanding the changes in NPC phenotype in 2D and 3D culture systems is necessary if we are to rigorously test and validate potential strategies involving NPC expansion and specification *in vitro* (16). It has already been demonstrated, in other cell types, that connexin expression and intercellular communication is strongly influenced by laminin-integrin interactions (17-19). In this study, we sought to identify the connexins intrinsically expressed by postnatal NPC populations and determine whether exposure to laminin or simple adhesion alters connexin expression and connexin-mediated GJIC and/or hemichannel activity. We show that subsets of NPCs exhibit a unique connexin profile and that this profile is altered by laminin but not poly-L-lysine impacting upon functional channel activity.

2.6 Methods

2.6.1 Mice

Breeding pairs of $Cx29^{-/-}$, $Cx36^{-/-}$, $Cx37^{-/+}$, $Cx40^{-/-}$, $Cx45^{F/F}$, and $Cx47^{-/-}$ animals were generated by our laboratories as described (20-25). $Cx32^{-/-}$ and $Cx30^{-/-}$ animals (26, 27) were kindly provided by Dr. Klaus Willecke (University of Bonn). Nestin-cre recombinase transgenics (28) were kindly provided by Dr. Ruth Slack (University of Ottawa). Each strain was backbred for 3-12 generations into a C57BL/6 lineage. All null-mutant mice were compared to congenic wild-type (WT) littermates. Mice were kept on a 12h light-dark cycle and allowed food and water *ad libitum*. Mice were genotyped using the primer pairs listed in Table 2.1. All experimental protocols were approved by the Animal Care Committee of the University of Ottawa according to guidelines set forth by the Canadian Council on Animal Care.

Table 2.1 Genotyping protocols

Gene	*Reaction Conditions*[a]	*Cycling & Amplicon sizes*
Cx29	*Cx29F: 5′-ATCTGTGCTGTGCTATTTGGAGT-3′* *Cx29R: 5′-ACAGGTTGTGCTGCCAATAC-3′* *lacZF: 5′-CCGACGGCACGCTGATTGAAG-3′* *lacZR: 5′-ATGCGGTCGCGTTCGGTTGC-3′* *Primer concentrations: 10 ng/μL each* *Volume of tail DNA: 5 μL* *Final reaction volume: 20 μL*	*95°C 5 m* *30 cycles:* *94°C 15 s* *66°C 15 s* *72°C 80 s* *(+ allele=700 bp)* *(- allele=1100 bp)*
Cx30	*F: 5′-GGTACCTCCTACTAATTAGCTTGG-3′* *lacZR: 5′-AGCGAGTAACAACCCGTCGGATTC-3′* *WTR: 5′-AGGTGGTACCCATTGTAGAGGAAG-3′* *Primer concentrations: 8 ng/μL each* *Volume of tail DNA: 1 μL* *Final reaction volume: 25 μL*	*94°C 5 m* *35 cycles:* *92°C 45 s* *60°C 45 s* *72°C 45 s* *72°C 10 m* *(+ allele=544 bp)* *(- allele=460 bp)*
Cx32	*F: 5′-ATACACCTTGCTCAGTGGCGTGAATCGGCA-3′* *R: 5′-TCATTCTGCTTGTATTCAGGTGAGAGGCGG-3′* *Primer concentrations: 8 ng/μL each* *Volume of tail DNA: 2.5 μL* *Final reaction volume: 12.5 μL*	*95°C 10 m* *30 cycles:* *95°C 60 s* *67°C 60 s* *72°C 60 s* *(+ allele=750 bp)*
	F: 5′-TCTTACTCCACACAGGCATAGAGTGTCTGC-3′ *R: 5′-TCATTCTGCTTGTATTCAGGTGAGAGGCGG-3′* *Primer concentrations: 8 ng/μL each* *Volume of tail DNA: 2.5 μL* *Final reaction volume: 12.5 μL*	*95°C 10 m* *30 cycles:* *95°C 60 s* *67°C 60 s* *72°C 60 s* *(- allele=1300 bp)*
Cx36	*F: 5′-AGCGGAGGGAGCAAACGAGAAG-3′* *R: 5′-CTGCCGAAATTGGGAACACTGAC-3′* *Primer concentrations: 8 ng/μL each* *Volume of tail DNA: 5 μL* *Final reaction volume: 25 μL*	*94°C 60s* *30 cycles:* *94°C 15 s* *69°C 15 s* *72°C 45 s* *(+ allele=533 bp)*
	PLAPF: 5′-GGTGAACCGCAACTGGTACT-3′ *PLAPR: 5′-CCCACCTTGGCTGTAGTCAT-3′* *Primer concentrations: 0.5 μM each* *Volume of tail DNA: 5 μL* *Final reaction volume: 20 μL*	*95°C 15m* *35 cycles:* *95°C 30s* *63°C 90s* *72°C 2m* *72°C 15m* *(- allele=187 bp)*
Cx37[b]	*F: 5′-TGCTAGACCAGGTCCAGGAAC-3′* *neoR: 5′-AGAGGCTATTCGGCTATGACT-3′* *WTR: 5′-GTCCCTTCGTGCCTTTATCTC-3′* *Primer concentrations: 125 nM each* *Volume of tail DNA: 1.5 μL* *Final reaction volume: 20 μL*	*94°C 3 m* *30 cycles:* *94°C 30 s* *63°C 30 s* *72°C 90 s* *72°C 5 m* *(+ allele=750 bp)* *(- allele=1300 bp)*

Table 2.1 (continued) Genotyping protocols

Cx40[c]	*F: 5'-TGGAGCCACAGTTGCAATGGT-3'* *neoR: 5'-GCACGAGACTAGTGAGACGTG-3'* *WTR: 5'-TCTCTGACTCCGAAAGGCAAG-3'* *Primer concentrations: 20 ng/μL each* *Volume of tail DNA: 2 μL* *Final reaction volume: 30 μL*	*94°C 3 m* *30 cycles:* *94°C 30 s* *64°C 30 s* *72°C 30 s* *72°C 4 m* *(+ allele=270 bp)* *(- allele=470 bp)*
Cx45[d]	*CreTK139F: 5'-ATTTGCCTGCATTACCGGTC-3'* *CreTK141R: 5'-ATCAACGTTTTGTTTTCGGA-3'* *Primer concentrations: 4 ng/μL each* *Volume of tail DNA: 2.5 μL* *Final reaction volume: 12.5 μL*	*94°C 5m* *30 cycles:* *94°C 30 s* *56°C 30 s* *72°C 60 s* *(Cre transgene=300 bp)*
	Cx45F: 5'-CTTGGCTTCCTTAATTACTTTA-3' *Cx45R: 5'-CTTCCCTACAAATGTCGAATG-3'* *neoR: 5'-AGGGGACGAAGACAGTAT3'* *Primer concentrations: 0.8 μg/μL each* *Volume of tail DNA: 2.5 μL* *Final reaction volume: 12.5 μL*	*94°C 5m* *30 cycles:* *94°C 30 s* *56°C 30 s* *72°C 60 s* *(+ allele=570 bp)* *(Flx allele=610 bp* *(- allele=820 bp)*
Cx47[e]	*F: 5'-AAGGCTGGTGCTGCTGGAAT-3'* *R: 5'-TGACCACCGTCTTGCCATCA-3'* *Primer concentrations: 0.4 μM each* *Volume of tail DNA: 5 μL* *Final reaction volume: 25 μL*	*95°C 5 m* *35 cycles:* *95°C 15 s* *67°C 15 s* *72°C 3 m* *(+ allele=1100 bp)*
	F: 5'-TCGCATTGTCTGAGTAGGTGTC-3' *R: 5'-CAGAGTTCCTCTGCACAGAGAT-3'* *Primer concentrations: 10 ng/μL each* *Volume of tail DNA: 5 μL* *Final reaction volume: 20 μL*	*95°C 15 m* *35 cycles:* *95°C 30 s* *64°C 90 s* *72°C 2 m* *72°C 15m* *(- allele=2200 bp)*

[a]*Unless otherwise stated, PCR reactions contain 1X Advantage 2 PCR buffer, 0.8 mM dNTPs and 0.4 μL of Advantage 2 Taq polymerase (Clontech)*

[b]*Final concentration of dNTPs is 0.2 mM.*

[c]*Final concentration of dNTPs is 0.2 mM. Reaction uses Titanium Taq Polymerase in 1X Titanium PCR Buffer*

[d]*Reactions use Titanium Taq Polymerase in 1X Titanium PCR Buffer.*

[e]*For the + allele, final Advantage 2 PCR buffer concentration is 0.8X.*

2.6.2 Neurosphere suspension culture

All chemical reagents were obtained from Sigma-Aldrich (St.-Louis, MO, USA) and all cell culture reagents were obtained from Invitrogen (Burlington, ON, Canada) unless otherwise stated. NPCs were cultured as described in (29) with some modifications. Briefly, cells were isolated from the hippocampi of postnatal day 0 - 2 (P0-P2) mouse pups. Animals were sacrificed by lethal injection with Euthansol (Schering-Plough Canada Inc., Pointe-Claire, QC, Canada) and 500 μm sections between Bregma -1.7 mm and -2.2 mm were prepared on a VT1000S vibratome (Leica Microsystems Inc.) in ice-cold artificial cerebral spinal fluid (26 mM $NaHCO_3$, 124 mM NaCl, 5 mM KCl, 2 mM $CaCl_2$, 1.3 mM $MgCl_2$, 10 mM D-glucose, 100 U/ml penicillin and 100 μg/ml streptomycin). Hippocampi from n=2-6 pups were pooled for each culture. Under a Leica MZ6 dissecting microscope, hippocampi were removed and dissected free of blood vessels and choroid plexus. Hippocampi were minced with a scalpel and enzymatically dissociated in: 26 mM $NaHCO_3$, 124 mM NaCl, 5 mM KCl, 0.1 mM $CaCl_2$, 3.2 mM $MgCl_2$, 10 mM D-glucose, 1% penicillin/streptomycin, 0.1 % neural protease, 0.01 % papain, and 0.01% DNase I for 45 minutes at 37°C. Single cells were resuspended in expansion media (Dulbecco's modified Eagle's medium F12 (DMEM/F12), 2 mM L-glutamine, 100 U/ml penicillin, 100 μg/ml streptomycin, 1X B27 supplement, 20 ng/ml human recombinant epidermal growth factor (EGF) and 10 ng/ml basic fibroblast growth factor (FGF-2)) in 60 mm Petri dishes (Fisher Scientific, Nepean, ON, Canada). Cell viability was established by Trypan Blue hemacytometer counts and cells plated at a density of $2.5x10^5$ viable cells/dish. This protocol typically yields 200 viable neurospheres/60 mm dish cultured in suspension. Cultures were maintained at 37°C in a 5% CO_2 atmosphere with fresh EGF and FGF-2 added every two days for 8 days *in vitro* (DIV).

2.6.3 Laminin, Matrigel, and Poly-L-Lysine Treatment

On DIV 8, neurospheres were plated in 10 cm tissue culture dishes containing laminin (15 μg/mL), Matrigel (Invitrogen), or poly-L-lysine (100 μg/ml)-coated

glass coverslips (Corning, NY, USA) and cultured in expansion media supplemented with EGF and FGF-2 or in differentiation media: DMEM/F12, 2 mM L-glutamine, 1 mM sodium pyruvate, 200 mM D-glucose, 100 U/ml penicillin, 100 µg/ml streptomycin, and 1X N2 supplement containing EGF and FGF-2 or 0.5 µM retinoic acid and 0.5% fetal bovine serum. The latter condition promotes astroglial specification (30). Cells were not dissociated to maintain the 3D topography of the cultures. Neurospheres adhered to each substrate and began to grow as monolayer colonies within 24 h of transfer. To maintain NPC proliferation, half the volume of media was removed and replenished every 2 days with fresh addition of EGF and FGF-2 to final concentrations of 10 and 20 ng/ml for 6 DIV (total 14 DIV). Some cultures were pulsed with 20 µg/mL 5'-bromo-2-deoxyuridine (BrdU, Roche Diagnostics, Laval, QC) 24 h prior to plating on laminin to determine the percentage of actively dividing cells in suspension that generated mature progeny. Cultures exposed to exogenous matrix or adhesive substrate were compared to cultures maintained in suspension in the same media supplemented with EGF and FGF-2. All immunocytochemistry and western analysis were performed on DIV 14.

2.6.4 Reverse transcriptase-polymerase chain reaction (RT-PCR)

Total RNA was isolated from WT, Cx29$^{-/-}$, Cx30$^{-/-}$, and Cx45$^{-/-}$ neurospheres and from adult and/P2 WT, Cx32$^{-/-}$, Cx36$^{-/-}$, Cx37$^{-/-}$, Cx40$^{-/-}$, and Cx47$^{-/-}$ mouse brain using Trizol Reagent (Invitrogen). RNA was collected from one dish per experiment. Each assessment was confirmed in duplicate or triplicate. Total RNA was treated with DNaseI (Promega, Madison, WI, USA). First-strand synthesis was performed using pdN_6 (Promega) random primers and Superscript II RT (BD Biosciences, San Jose, CA, USA) according to manufacturer's recommendations. PCR was performed using the primers and conditions listed in Table 2.2. The PCR reaction contained, in a final volume of 25 µl: 1X PCR buffer, 0.8 mM dNTPs, 1X Advantage 2 Polymerase (Clontech, Cambridge, ON, Canada). All reactions were carried out using the following cycling parameters: 94°C for 5 min, 35 cycles of 94°C for 25 sec, 59°C for 50 sec, and 72°C for 1 min 45 sec, and a final step at 72°C for 7

Table 2.2 RT-PCR protocols[a]

Gene	Primer Sequence	Primer Concentration	Amplicon length
Cx26 (GJB2)	F: 5′-GGATGTGGCAGTCAGTATCA R: 5′-TCTTGGCAGGAAGAAGTGTC	0.5 μM	368 bp
Cx29 (GJC3)	F: 5′-GGTTTTCGGCAATGAT R: 5′-AGAAGCTTGAGGCTTTTAGC	4 ng/μL	278 bp
Cx30 (GJB6)	F: 5′-GCCAGGGTGCAAGAACGTCTGC R: 5′-GGCATGGTTGGGTGGTTTCTC	10 ng/μL	535 bp
Cx32 (GJB1)[b]	F: 5′-GTGGCGTGAATCGGCACTCTAC R: 5′-CTCCGCCACGTTGAGGATAATG	10 ng/μL	593 bp
Cx36 (GJD2)	F: 5′-AGCGGAGGGAGCAAACGAGAAG R: 5′-CTGCCGAAATTGGGAACACTGAC	10 ng/μL	533 bp
Cx37 (GJA4)	F: 5′-AGAGCGGTTGCGGCAGAAAGAGG R: 5′-TGGATGAGAGCCCGTTGTAGGTG	10 ng/μL	551 bp
Cx40 (GJA5)	F: 5′-TTTGGCCAAGTCACGGCAGGG R: 5′-TTGTCACTGTGGTAGCCCTGAGG	4 ng/μL	311 bp
Cx43 (GJA1)	F: 5′-CCTGCCGCAATTACAACAAG R: 5′-AAGGTCGCTGATCCACGATA	10 ng/μL	201 bp
Cx45 (GJC1)[b]	F: 5′-GAGGTGGGCTTTCTAATAGGGCAG R: 5′-ATGGGGGTTGTTTTGGTGATGG	10 ng/μL	528 bp
Cx47 (GJC2)	F: 5′-GCTGGAGGAGATCCACAATCATTC R: 5′-GTGTGGAGATGACCACTATCTGGA	10 ng/μL	233 bp
GAPDH[b]	F: 5′-TGGTGCTGAGTATGTCGTGGAGT R: 5′-AGTCTTCTGAGTGGCAGTGATGG	0.2 μM	292 bp

[a]All reactions contained 1 μL of RT product, 0.8 mM dNTPs, 1X PCR Buffer, 1X Advantage 2 Taq Polymerase in a reaction volume of 25 μL except Cx32 and GAPDH reactions.
[b]1X Titanium Taq Polymerase was used.

min in a Whatman Biometra T-Gradient thermocycler (Montreal-Biotech Inc., Kirkland, QC, Canada).

2.6.5 Western blot analysis

Neurospheres were washed in PBS (10 mM PBS: 0.154 M NaCl, 0.0028 M NaH_2PO_4, 0.0072 M Na_2HPO_4, pH 7.2), pelleted, and resuspended in RIPA buffer (1% Nonidet P-40, 0.5% sodium deoxycholate, 0.1% sodium dodecyl sulphate (SDS), 1 mM sodium fluoride, 1 mM sodium orthovanadate, 50 μg/ml aprotinin, and 1 mg/mL phenylmethylsulphonylfluoride in PBS). Where western blot analysis of cultures grown on laminin substrate is indicated, adherent cultures were washed with PBS and RIPA buffer added directly to plates. Cells were collected using a cell scraper (Fisher), incubated on ice for 30 min, then centrifuged at 13 400 x g for 30 min. Protein was isolated from mouse brain homogenized in RIPA buffer using a Tissue Tearor (Biospec Products Inc., Bartlesville, OK, USA). Protein concentration was determined using the Bio-Rad DC protein assay kit (Bio-Rad, Hercules, CA, USA) according to manufacturer's protocol. Protein samples of 30 μg were separated by SDS-polyacrylamide gel electrophoresis and transferred to polyvinylidene difluoride membranes (Fisher). Membranes were blocked at room temperature for 1 h with 1% casein in PBS. Primary and secondary antibodies are listed in Table 2.3. Immunoreactivity was visualized using the SuperSignal West Pico Chemilunescent Substrate kit (Pierce Biotechnology Inc., Rockford, IL, USA). All assessments were performed in duplicate.

2.6.6 Immunocytochemistry

Neurospheres expanded in suspension or grown on laminin were fixed in 3.7% formaldehyde solution in PBS for 20 min. Following extensive washes in PBS, neurospheres were cryoprotected for 24 h with 15% sucrose in PBS + 0.001% NaN_3, flash-frozen, and serially sectioned (10 μm thickness) using a cryostat (Leica CM1900). Immunocytochemistry was carried out as previously described (31). Antibodies are listed in Table 2.3 and were diluted in 3% bovine serum

Table 2.3. Primary and secondary antibodies used in this study

Antibody	Type	Species	Source	Dilution Immuno	Dilution Western	Dilution Flow
Cx26	Polyclonal	Rabbit	Zymed	1:25	1:100	---
Cx29	Polyclonal	Rabbit	Dr.David Paul	1:20	---	---
Cx30	Monoclonal	Mouse	Zymed	1:50	---	1:25
Cx30	Polyclonal	Rabbit	Zymed	---	---	1:25
Cx32	Monoclonal	Mouse	Zymed	1 µg/mL	1:250	---
Cx36	Polyclonal	Rabbit	Zymed	5 µg/mL	1:100	---
Cx37	Polyclonal	Rabbit	Dr. Alex Simon	1:200	---	---
Cx40	Polyclonal	Rabbit	Zymed	1:50	---	---
Cx43	Monoclonal	Mouse	Chemicon	1:100	---	1:1000
Cx43	Polyclonal	Rabbit	Zymed	1:100	---	---
Cx45	Polyclonal	Rabbit	Chemicon	1:1000	---	---
Cx47	Polyclonal	Rabbit	Dr. David Paul	1:250	---	---
Actin	Monoclonal	Mouse	Sigma	---	1:1000	---
β-galactosidase	Polyclonal	Rabbit	Chemicon	1:1500	---	---
BrdU	Monoclonal	Mouse	Roche	6 µg/mL	---	---
DCX	Polyclonal	Guinea Pig	Chemicon	1:4000	---	---
GFAP	Polyclonal	Rabbit	Sigma	1:100	---	---
GFAP	Cy-3 conjugated	Mouse	Sigma	1:800	---	---
GFAP	Monoclonal	Rat	Zymed	1:40	---	1:25
Nestin	Monoclonal	Mouse	Chemicon	1:50	---	1:50
NCAM	Monoclonal	Mouse	Sigma	1:400	---	---
NG2	Polyclonal	Rabbit	Chemicon	1:200	---	---
NeuN	Monoclonal	Mouse	Chemicon	1:100	---	---
PDGFαR	Monoclonal	Rat	BD	1:300		
RIP	Monoclonal	Mouse	Chemicon	1:1000	---	---
TuJ1 (βIII-tubulin)	Monoclonal	Mouse	Research Diagnostics	1:250	---	---
Mouse IgG	Cy3-conjugated	Donkey	Jackson	1:800	---	---
Rabbit IgG	Cy3-conjugated	Donkey	Jackson	1:600	---	---
Mouse IgG	FITC-conjugated	Donkey	Jackson	1:100	---	---
Rabbit IgG	FITC-conjugated	Donkey	Jackson	1:100	---	1:50
Rat IgG	FITC-conjugated	Donkey	Jackson	1:80	---	---
Mouse IgG	HRP-conjugated	Donkey	Jackson	---	1:2000	---
Rabbit IgG	HRP-conjugated	Donkey	Jackson	---	1:5000	---
Mouse IgG	Cy5-conjugated	Goat	Invitrogen	---	---	1:50
Rat IgG	RPE-conjugated	Goat	Serotec	---	---	1:10
Rabbit IgG	AMCA-conjugated	Goat	Jackson	1:100	---	---
Mouse IgG	AMCA-conjugated	Donkey	Jackson	1:100	---	---

albumin + 0.3% Triton X-100 in PBS. Hoechst 33258 (1 μg/mL) was used as a nuclear counterstain. For suspension cells, the number of connexin$^+$ cells was expressed as the percentage of Hoechst$^+$ nuclei counted in serial sections of 10-50 neurospheres. For cultures plated on laminin, immunocytochemistry was performed directly on laminin-coated glass-coverslips. Connexin$^+$ cells/Hoechst$^+$ nuclei were established in five fields per neurosphere calculated for 5-10 neurospheres per connexin (n=25-50 fields per condition). Because cell density in the sphere core was such that individual cells could not be quantified or verified to be in contact with the laminin substrate, cell counts were performed over five defined peripheral cell fields shot at 40X magnification. All cell images were taken with a Leica DMXRA2 epifluorescence microscope and analyzed using Openlab software v5.05 (Improvision, Lexington, MA, USA).

2.6.7 Flow Cytometry

Cultures were expanded as neurospheres for 14 DIV before being suspended in 2% formaldehyde in 10 mM PBS and triturated to achieve a single cell suspension. Following two PBS washes and gentle centrifugation at 2000 rpm for 5 min, NPCs were suspended in PFN (2% fetal bovine serum, 0.1% NaN_3, 0.18% saponin in 10 mM PBS). Cell suspensions were separated into 1.5 ml microfuge tubes at a concentration of 1 x 10^6 cells per tube. Primary or isotype control antibodies were added directly to cell suspensions at appropriate concentrations followed by incubation at room temperature for 30 min on a shaker. Each sample was washed twice by the addition of 0.8 ml of PFN and gentle centrifugation. Secondary antibodies were added to cell suspensions at appropriate concentrations followed by incubation at room temperature for 30 min on a shaker and washed as described above. Cells were resuspended in 0.5 ml of PFN and analyzed using a Beckman Coulter FC500 Flow Cytometer (Beckman Coulter Canada Inc., Mississauga, ON) and Beckman Coulter CXP software.

2.6.8 GJIC and hemichannel assay

Dye uptake and dye transfer assays were assessed on 10 neurospheres/condition in two separate experiments per condition. For quantification, four fields were photographed per sphere. For dye coupling assays, photomicrographs represented two fields within the core of the neurosphere and two fields at the periphery where cells were in direct apposition and thus potentially coupled. To image cells within the core in direct contact with matrix, micrographs were obtained using a Leica DMIR epifluorescent inverted microscope equipped with a QICAM digital camera (Quorum Technologies, Guelph, ON, Canada) and captured using OpenLab software v5.05. For hemichannel assays, all four fields were shot along the periphery and were taken with a Leica DMXRA2 epifluorescence microscope and analyzed using Openlab software (v5.05). Cultures expanded in suspension as neurospheres for 8 DIV were plated on coverslips in expansion media containing (a) EGF and FGF-2 for 1 DIV to assess function prior to laminin-induced changes in connexin expression, (b) EGF and FGF-2 for 6 DIV to assess connexin function after laminin-induced changes, and (c) in differentiation media for 6 DIV supplemented with RA (0.5 μM) and FBS (0.5%) to promote glial differentiation. Hemichannel activity was assessed by comparing uptake of connexin channel-permeant Lucifer yellow (LY, 457 Da) and channel-impermeant rhodamine B isothiocyanate-dextran (RD, 10,000 Da) in the presence or absence of 50 μM flufenamic acid (FFA) or 100 μM 4,4′-diisothiocyanatostilbene-2,2′-disulfonic acid (DIDS) as previously described (32). Mechanical stimulation with glass microbeads was used to trigger hemichannel opening (32, 33). Cells positive for both LY and RD were excluded from the measurements to control for LY uptake resulting from loss of membrane integrity. For all assays, the number of LY^+/RD^- cells is expressed as a percentage of the total number of cells per microscopic field ± standard error of the mean (SEM). Dye transfer between cells indicative of GJIC was assessed by scrape loading in the presence or absence of the intercellular channel blocker 18α-glycyrrhetinic acid (GRA, 100 μM) or its inactive analog glycyrrhizic acid (GZA, 100 μM) as previously described (32). Dye transfer was quantified by

counting the number of LY^+/RD^- cells emanating from a LY^+/RD^+ cell adjacent to the scrape line. Data are expressed as the mean number of LY^+/RD^- cells ± SEM.

2.6.9 Statistics

Data were analyzed by analysis of variance (ANOVA) followed by *post hoc* Tukey tests or Student's *t* test where appropriate.

2.7 Results

2.7.1 ECM effects on postnatal NPC culture

To characterize neurosphere composition, we analysed marker expression in suspension and in cultures plated on a variety of adhesive substrates by immunofluorescence (Figure 2.1). Although each neurosphere is likely derived from a single NPC, progeny spontaneously adopt distinct developmental lineages in culture (Figure 2.2a). We found neurospheres cultured in the absence of exogenous ECM were primarily composed of $nestin^+$ cells (Figure 2.2i). Cells co-expressing the Type 1 NPC markers GFAP and nestin localized to the periphery of neurospheres (Figure 2.2b). Type 2a cells expressing nestin only were found in the core of cultures (Figure 2.2b). DCX^+, $NCAM^+$, and $TuJ1^+$ neuroblasts and immature neurons were detected in clusters throughout the neurosphere structure (Figure 2.2c-e). $NG2^+$ and $PDGF\alpha R^+$ oligodendrocyte progenitor cells (OPCs) and RIP^+ oligodendrocytes were found at the periphery of neurospheres with rare cells detected in the core (Figure 2.2f-h). When cultures were plated on laminin, we observed a significant increase in the percentage of cells that retained a $nestin^+$ NPC identity and a significant decrease in the percentage of cells that specified to neuroblasts, immature neurons, and/or OPCs (Figure 2.2i). No change in the number of astrocytes was detected but a small increase in RIP^+ oligodendrocytes was observed in laminin-plated cultures (Figure 2.2i).

Figure 2.1 Schematic representation of the neurosphere culture protocol and analysis. A graphic depiction of the protocol employed to culture and analyze neurospheres in the presence and absence of laminin.

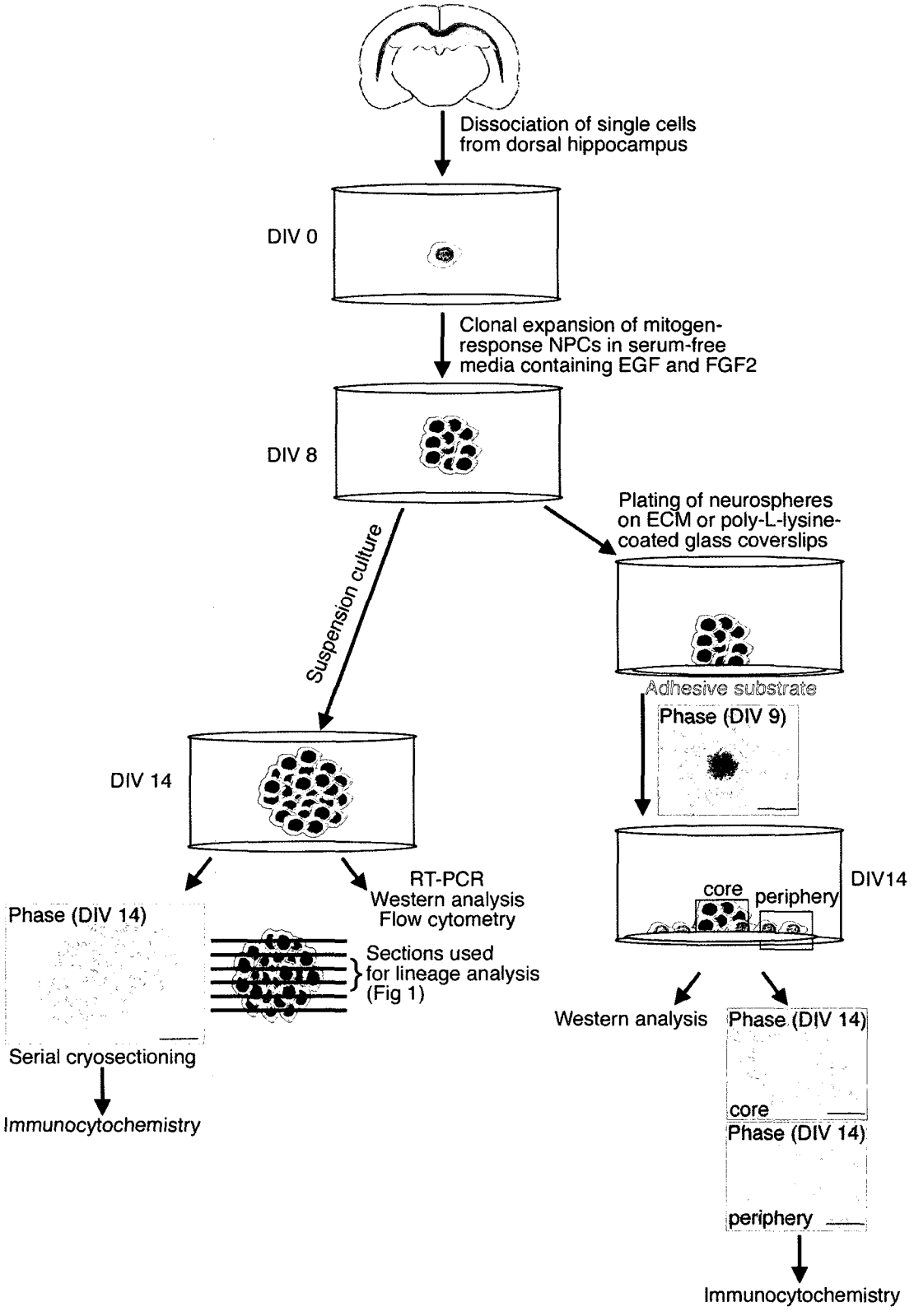
Dissociation of single cells
from dorsal hippocampus
DIV 0
Clonal expansion of mitogen-
response NPCs in serum-free
media containing EGF and FGF2
DIV 8
Plating of neurospheres
on ECM or poly-L-lysine-
coated glass coverslips
Suspension culture
Adhesive substrate
Phase (DIV 9)
DIV 14
RT-PCR
Western analysis
Flow cytometry
DIV14
core
periphery
Phase (DIV 14)
Sections used
for lineage analysis
(Fig 1)
Western analysis
Phase (DIV 14)
Serial cryosectioning
core
Phase (DIV 14)
periphery
Immunocytochemistry
Immunocytochemistry

Figure 2.1

Figure 2.2 Postnatal hippocampal-derived neurospheres are composed of subpopulations of progenitor and immature cell types. Schematic of spontaneous specification over the course of neurosphere expansion *in vitro*. Pertinent lineage markers are indicated (a). Representative digital micrographs depicting antigenic lineage analysis of NPC populations through the central sections of serial cryosections of neurospheres cultured in the absence of laminin are depicted in b-h. Scale bars, 50 μm, insets 25 μm. Type 1 NPCs expressing GFAP and nestin localized to the periphery of spheres (b, arrows and inset); Type 2a NPCs expressing nestin were found toward the centre of the core (b, arrowhead). Type 3 neuroblasts (c,d, arrows and inset) and immature neurons (d,e, arrows and inset) were found in clusters throughout serial sections. $NG2^+$ (f, arrows and inset) and $PDGF\alpha R^+$ (g, arrows and inset) OPCs and RIP^+ oligodendrocytes (h, arrows and inset) tended to be found along the neurosphere periphery. Culture on a laminin matrix increased the percentage of NPCs that retained a $nestin^+$ NPC identity and decreased the percentage of cells that specified to neuroblasts, immature neurons, and OPCs (i). Data represent mean of 5-15 sections counted over n=5-10 cultures/condition $\pm$ standard error of measurement (SEM). *$p<0.05$, **$p<0.01$, ANOVA, *post-hoc* Tukey test.

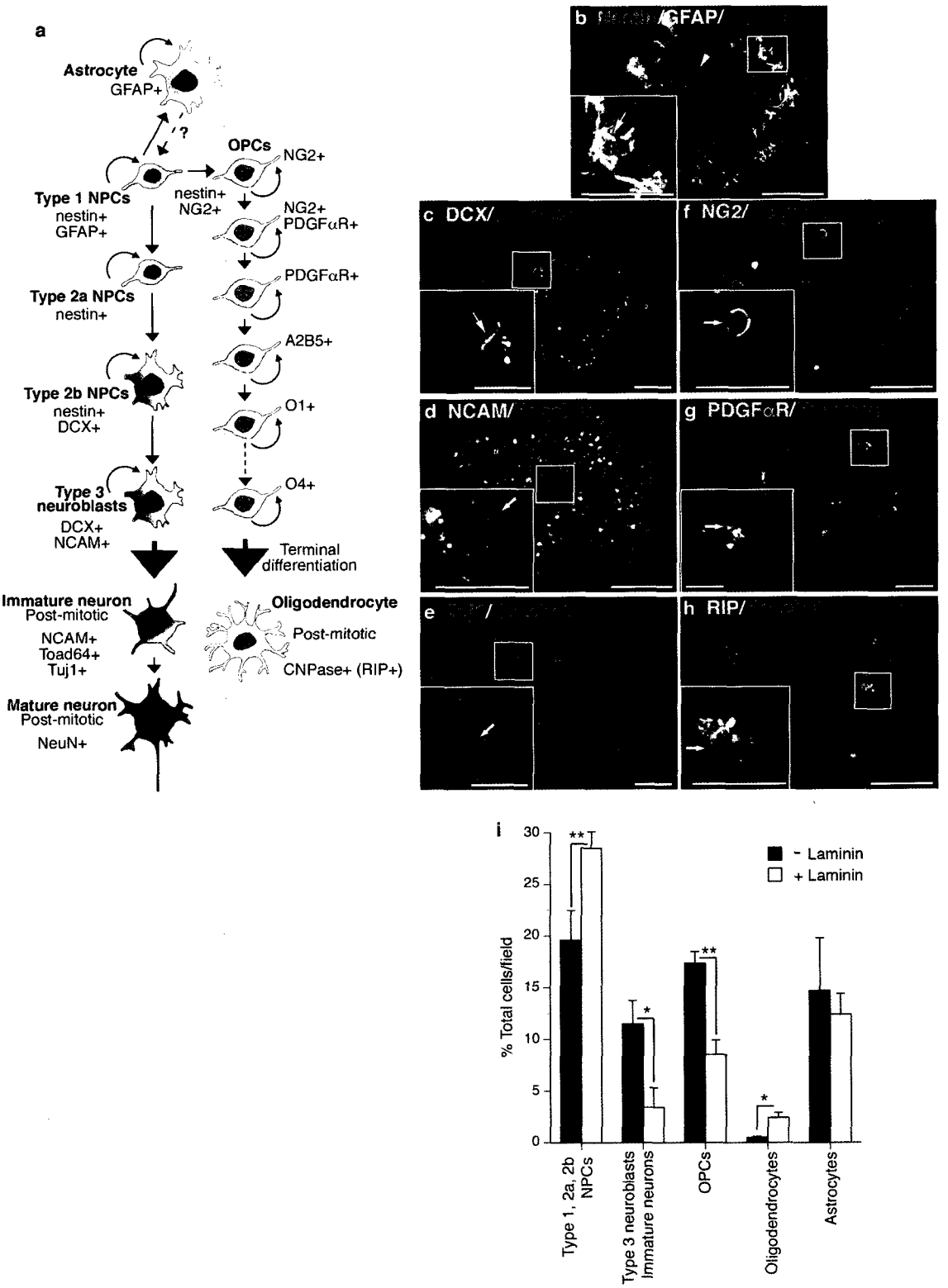
a
Astrocyte
GFAP+
?
Type 1 NPCs
nestin+
GFAP+
OPCs
NG2+
nestin+
NG2+
NG2+
PDGFαR+
Type 2a NPCs
nestin+
PDGFαR+
A2B5+
Type 2b NPCs
nestin+
DCX+
O1+
Type 3
neuroblasts
DCX+
NCAM+
O4+
Terminal
differentiation
Immature neuron
Post-mitotic
NCAM+
Toad64+
Tuj1+
Oligodendrocyte
Post-mitotic
CNPase+ (RIP+)
Mature neuron
Post-mitotic
NeuN+
b GFAP/
c DCX/
f NG2/
d NCAM/
g PDGFαR/
e /
h RIP/
i
- Laminin
+ Laminin
% Total cells/field
30
25
20
15
10
5
0
**
*
**
*
Type 1, 2a, 2b NPCs
Type 3 neuroblasts Immature neurons
OPCs
Oligodendrocytes
Astrocytes

Figure 2.2

2.7.2 Intrinsic connexin mRNA expression

To identify the connexins expressed by postnatal progenitor cells in the absence of exogenous ECM we performed RT-PCR. Fourteen connexins (Cx26, Cx29, Cx30, Cx30.2, Cx31.1, Cx31.9, Cx32, Cx36, Cx37, Cx40, Cx43, Cx45, Cx47, Cx57) are expressed in the mammalian CNS (12-15). Transcripts for ten of these connexins (Cx26, Cx29, Cx30, Cx32, Cx36, Cx37, Cx40, Cx43, Cx45, and Cx47) were detected in neurosphere culture (Figure 2.3a-j). Cx29, Cx30, and Cx36 expression was further confirmed by analysis of the reporter gene products present in null-mutant lines. In $Cx29^{-/-}$ and $Cx30^{-/-}$ mice, the *lacZ* open reading frame replaces the connexin coding sequences (26, 34) whereas a bicistronic reporter cassette containing *lacZ*, an internal ribosome entry site, and placental alkaline phosphatase replaces the connexin coding sequence in $Cx36^{-/-}$ mice (21). β-galactosidase expression was readily detected in neurosphere cultures from these three null-mutant lines (Figure 2.3b,c,e).

2.7.3 Differential expression of connexins in subsets of NPCs

We used immunofluorescence to localize connexins to NPC subtypes grown in the absence of exogenous laminin (Figure 2.4-2.8). For all connexins except Cx26, cultures from null-mutant mice served as negative controls to ensure antibody specificity. For Cx26, where deletion is embryonic lethal (35), antibody specificity was determined by western blot (Figure 2.6a, inset). Four distinct connexin protein profiles were detected:

(I) Cx30 (Figure 2.4a) and Cx43 (Figure 2.4d) were expressed by the majority of cells (>60%) throughout the structure of the sphere. Punctate membrane-associated immunoreactivity characteristic of gap junction labelling was evident in $nestin^+$ and $GFAP^+$ cells (Figure 2.4b-f). We used flow cytometry to quantify Cx30 expression in $nestin^+/GFAP^+$ Type 1 NPCs, $nestin^+$ Type 2a NPCs, and $GFAP^+/nestin^-$ astrocytes (Figure 2.5). We found that all of the Type 1 NPCs ($93\pm6\%$) and the vast majority of Type 2a NPCs ($83\pm2\%$) expressed Cx30.

Figure 2.3 Connexin mRNA expression in postnatal hippocampal neurospheres cultured in the absence of exogenous ECM. RT-PCR analysis of Cx26 (a), Cx29 (b), Cx30 (c), Cx32 (d), Cx36 (e), Cx37 (f), Cx40 (g), Cx43 (h), Cx45 (i), and Cx47 (j) of random-primed RNA extracted from 100-150 pooled neurosphere cultures (+RT). GAPDH was amplified to confirm template integrity. Positive controls were: Total RNA isolated from adult and/or P1 WT whole brain. Negative controls included RT-PCR reactions performed on total RNA from null-mutant neurospheres ($Cx29^{-/-}$, $Cx30^{-/-}$, and $Cx45^{-/-}$) or adult brain ($Cx32^{-/Y}$, $Cx36^{-/-}$, $Cx40^{-/-}$, $Cx37^{-/-}$, and $Cx47^{-/-}$), and reactions processed in the absence of template (NT). Potential contamination by genomic DNA was assessed by omitting the RT enzyme from the reactions (-RT). In a, c, and e, panels depict neurosphere cryosections derived from $Cx29^{-/-}$, $Cx30^{-/-}$, and $Cx36^{-/-}$ animals processed for β-galactosidase immunocytochemistry. The *LacZ* gene replaces the connexin coding sequence in each of these null-mutant animals. Insets are antibody controls demonstrating WT sections are negative for the β-galactosidase marker. Scale bars, 50 μm.

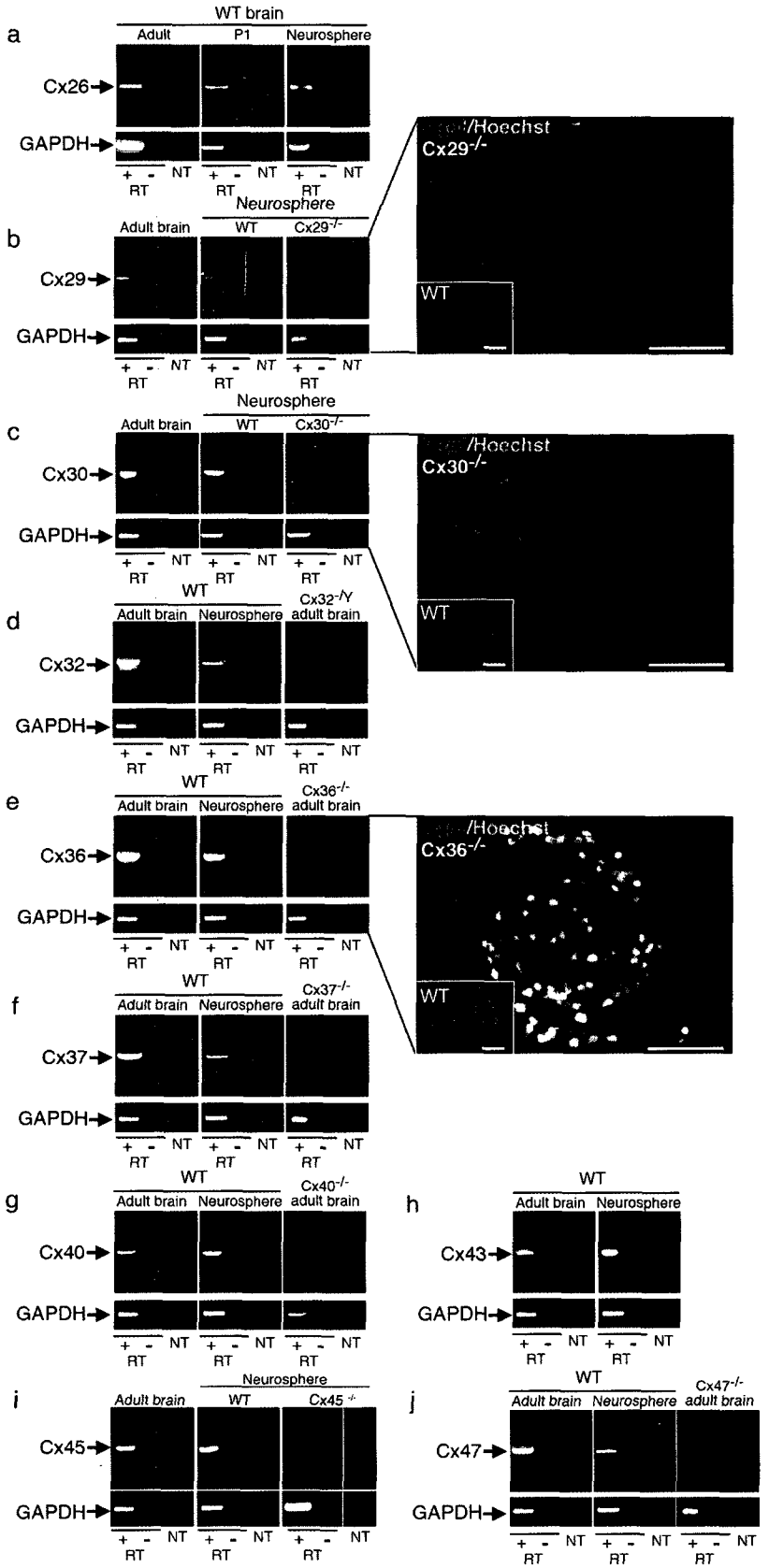
a
WT brain
Adult
P1
Neurosphere
Cx26
GAPDH
+ - NT
RT
b
Neurosphere
Adult brain
WT
Cx29-/-
Cx29
/Hoechst
Cx29-/-
WT
c
Cx30
Cx30-/-
/Hoechst
Cx30-/-
d
Cx32-/Y adult brain
Cx32
e
Cx36-/- adult brain
Cx36
/Hoechst
Cx36-/-
f
Cx37-/- adult brain
Cx37
g
Cx40-/- adult brain
Cx40
h
Cx43
i
Cx45 -/-
Cx45
j
Cx47-/- adult brain
Cx47

Figure 2.3

Figure 2.4 Cx30 and Cx43 are expressed by Type 1 and Type 2a NPCs and are responsive to laminin. Cx30 and Cx43 was detected in the majority of cells within neurospheres (a,d, arrows) and localized to cells expressing nestin (b,e, insets) and GFAP (c,f, insets). Inset in (a) demonstrates lack of Cx30 immunostaining on null-mutant neurospheres confirming antibody specificity. Adherence to laminin did not impact on the frequency of $Cx30^+$ cells (g) although a change in subcellular localization was observed (compare punctate membrane staining (a, arrows) with diffuse cytoplasmic staining (i, arrows)). A decrease in the frequency of $Cx43^+$ cells (arrows) was detected following culture on laminin (j). Cx43 was present at the plasma membrane between cells in direct apposition in the presence (a) or absence (b, small arrows) of laminin. Scale bars, 50 μm, insets in a,b,c,f, 25 μm, inset in e 10 μm. Data represent mean of 5-15 sections (- laminin) or field (+ laminin) counted over n=5-10 cultures/condition ± SEM (g,j). **$p<0.01$ Student's *t*-test.

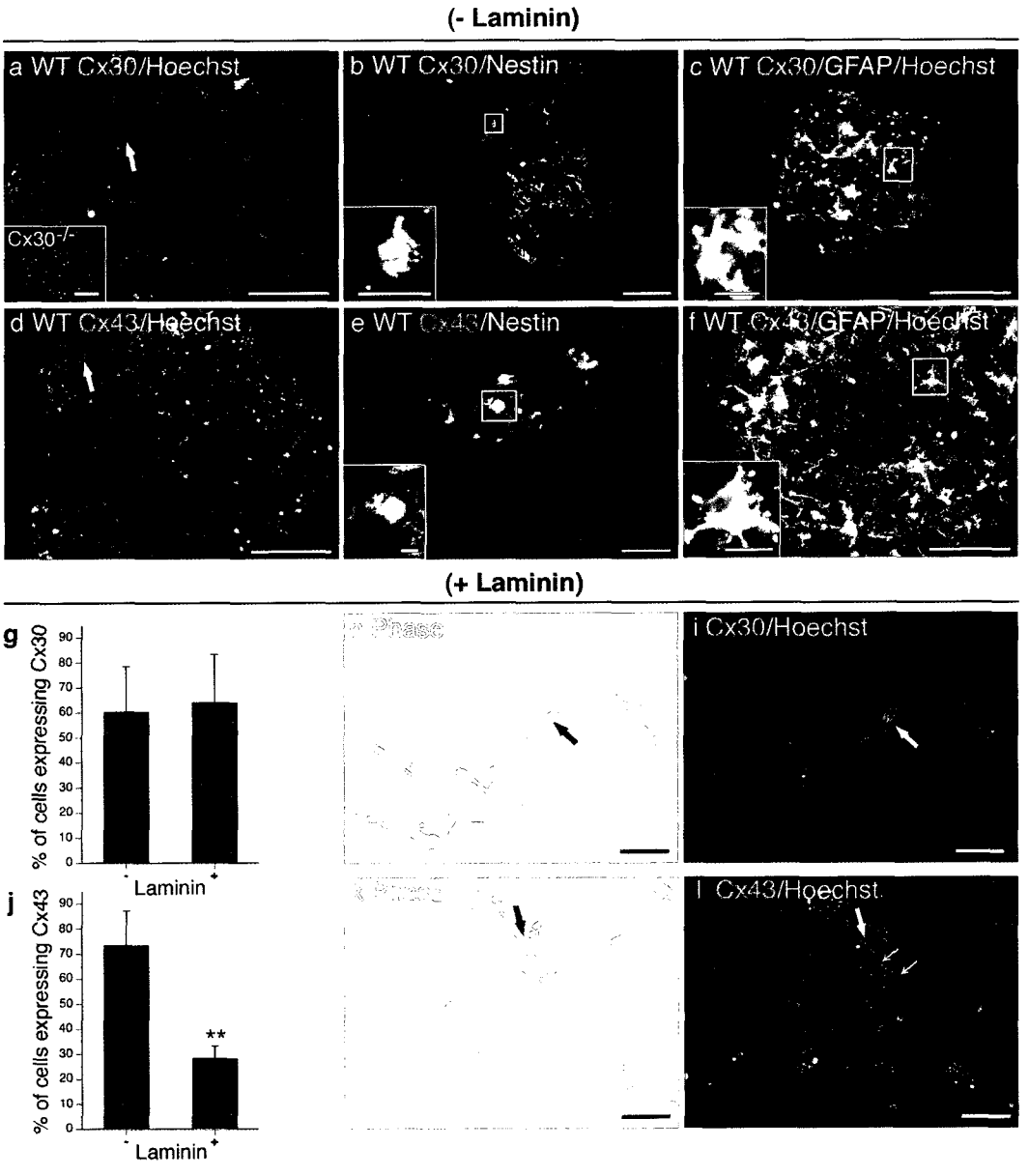
(- Laminin)
a WT Cx30/Hoechst
Cx30-/-
b WT Cx30/Nestin
c WT Cx30/GFAP/Hoechst
d WT Cx43/Hoechst
e WT Cx43/Nestin
f WT Cx43/GFAP/Hoechst
(+ Laminin)
g
% of cells expressing Cx30
Laminin
h Phase
i Cx30/Hoechst
j
% of cells expressing Cx43
**
Laminin
k Phase
l Cx43/Hoechst

Figure 2.4

Figure 2.5 Cx30 is expressed by Type 1 and 2a NPCs. (a) Hippocampal NPCs cultured as neurospheres were dissociated on DIV 14 and triple-labelled for Cx30, nestin, and GFAP. Two and three dimensional histograms from a representative flow cytometry analysis are presented for both isotype control (left panel) and experimental (right panel) reactions. The quadrant percentages represent the percentage of total cells expressing corresponding cell markers. (b) Quantitative analysis of Cx30 expression in Type 1 (GFAP+/nestin+) NPCs, Type 2a (GFAP-/nestin+) NPCs, and committed astrocytes (GFAP+/nestin-). The percentage of cells co-expressing Cx30 was calculated divided by the total percentage of each cell type by the total percentage of cells within each cell type expressing Cx30 in triple-labelling studies. Data are presented as mean$\pm$SEM and represent the average of three independent flow cytometric analyses/cultures.

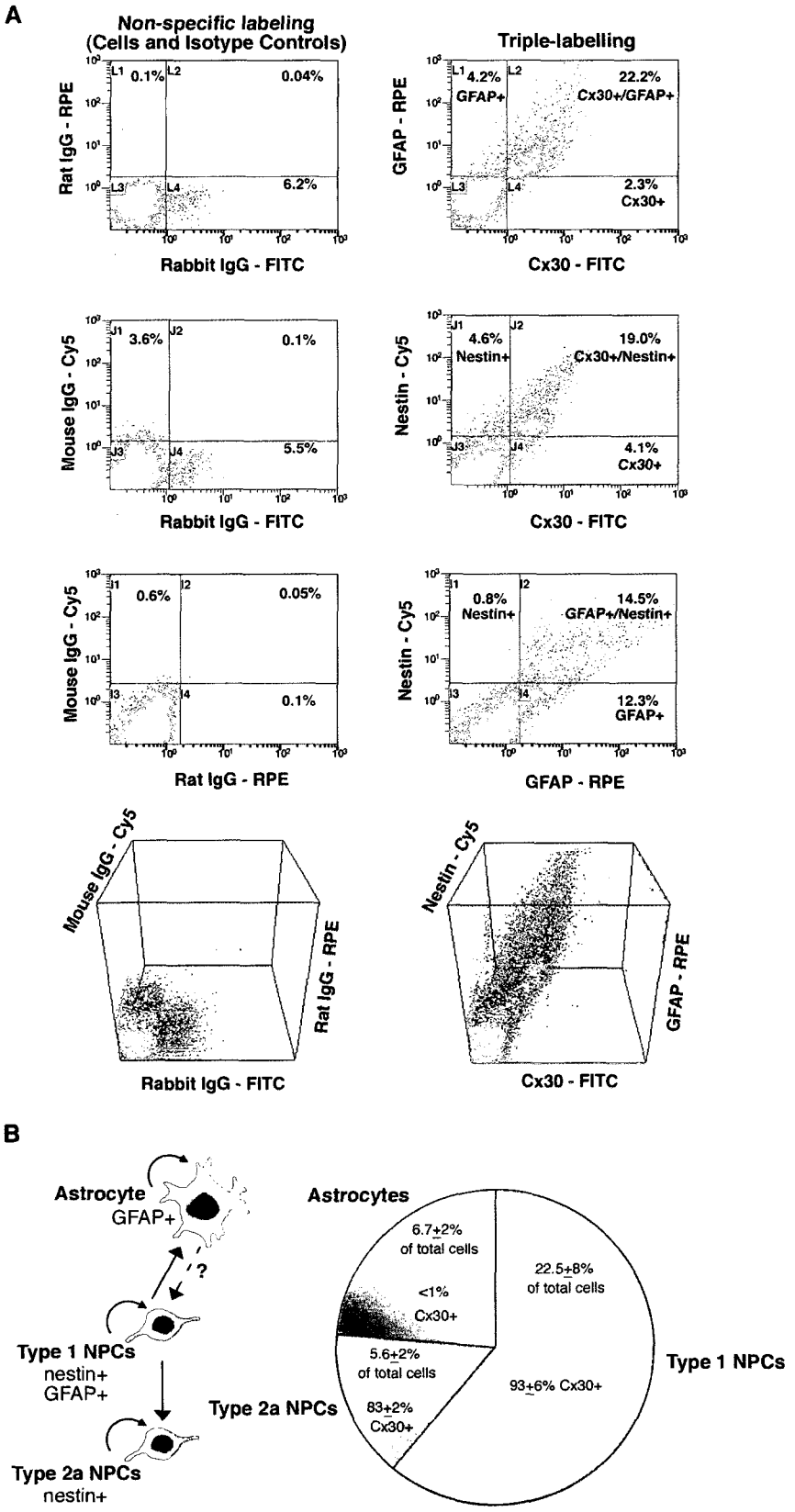
A
Non-specific labeling
(Cells and Isotype Controls)
Triple-labelling
Rat IgG - RPE
Rabbit IgG - FITC
0.1%
0.04%
6.2%
GFAP - RPE
Cx30 - FITC
4.2%
GFAP+
22.2%
Cx30+/GFAP+
2.3%
Cx30+
Mouse IgG - Cy5
3.6%
0.1%
5.5%
Nestin - Cy5
4.6%
Nestin+
19.0%
Cx30+/Nestin+
4.1%
Cx30+
0.6%
0.05%
0.1%
0.8%
Nestin+
14.5%
GFAP+/Nestin+
12.3%
GFAP+
B
Astrocyte
GFAP+
Type 1 NPCs
nestin+
GFAP+
Type 2a NPCs
nestin+
Astrocytes
6.7±2%
of total cells
<1%
Cx30+
22.5±8%
of total cells
5.6±2%
of total cells
83±2%
Cx30+
93±6% Cx30+
Type 1 NPCs
Type 2a NPCs

Figure 2.5

Surprisingly, few if any committed GFAP$^+$/nestin$^-$ astrocytes were Cx30$^+$ (<0.1%) (Figure 2.5) These results were further substantiated by triple-labelling for Cx30, Cx43, and GFAP (Figure 2.6). Cx43 but not Cx30 was detected in all GFAP$^+$ cell types suggesting ubiquitous localization of Cx43 in GFAP$^+$ NPCs and astroglia but a more restricted distribution of Cx30 to subsets of multipotential Type 1 GFAP$^+$ NPCs.

(II) Cx26 (Figure 2.7a), Cx29 (Figure 2.8a), Cx37 (Figure 2.8c), and Cx40 (Figure 2.8e) were expressed in a minority of cells (~10%) localizing to both the sphere core and periphery in the absence of laminin. Cx26 and Cx29 exhibited membrane-associated staining but rarely in apposition with neighbouring cells expressing the same connexin (Figure 2.7a, 2.8a arrows, 2.7b, 2.8b inset). Cx26 localized to nestin$^+$ and GFAP$^+$ Type 1 NPCs (Figure 2.7b,c) at the periphery of the sphere and nestin$^+$ Type 2a NPCs within the core (Figure 2.7b) as well as GFAP$^+$/nestin$^-$ astrocytes (Figure 2.7b,c). Cx29 localized to PDGFαR$^+$ OPCs (Figure 2.8b, inset). Cx37 and Cx40 labelling appeared to be largely intracellular (Figure 2.8c, e, arrows) suggesting these connexins are not forming gap junction channels at the plasma membrane. Both Cx37 and Cx40 were expressed primarily by nestin$^+$ Type 2a cells (Figure 2.8d, f, insets).

(III) Cx45 (Figure 2.9a) and Cx47 (Figure 2.9c) were expressed by rare cells (<10%) restricted primarily to the periphery of neurospheres cultured in the absence of laminin. These connexins were often expressed in adjoining cells (Figure 2.9a,c, large arrows) where contiguous labelling was detected at the plasma membrane (Figure 2.9a,c, small arrows). Cx45 localized to nestin$^+$ Type 2a NPCs (Figure 2.9b, inset) and was not detected in GFAP$^+$ cells (data not shown). Cx47 expression was restricted to RIP$^+$ oligodendrocytes (Figure 2.9d, inset).

(IV) Both Cx32 and Cx36 were detected at the mRNA level (Figure 2.3d,e) but no immunodetection of protein was observed (Figure. 2.9k, o). Antibody efficacy was confirmed by western analysis (Figure 2.9k, o, insets).

Figure 2.6 Cx43 but not Cx30 is detected in all GFAP$^+$ cell types. A 10 μm cyrosection through a neurosphere harvested on DIV 14 triple-labelled for Cx30, Cx43, and GFAP is presented. Yellow arrow points to cells expressing GFAP/Cx30/ and Cx43. Purple arrow identifies cells expressing Cx43 and Cx30 but not GFAP. White arrows indicate cells expressing GFAP and Cx43 but not Cx30. Scale bar, 50 μm.

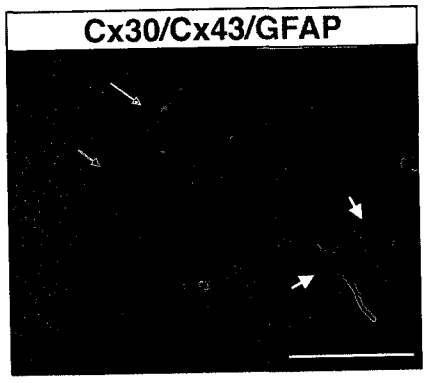

Figure 2.6

Figure 2.7 Cx26 is expressed Type 1 and Type 2a NPCs and is responsive to laminin. Cx26 was expressed by a small population of cells within neurospheres (a, arrow) and localizes to both cells expressing nestin (b, inset and arrow) and GFAP (c, inset and arrow). Inset in (a) depicts western blotting on protein derived from adult, P1 and neurospheres cultured in the absence of laminin to confirm antibody specificity. A marked increase in the frequency of $Cx26^+$ cells was detected when cultured on laminin (d,e,f, arrows). Data represent mean of 5-15 sections (- laminin) or field (+ laminin) counted over n=5-10 cultures/condition $\pm$ SEM. (d). Scale bars, 50 μm, insets, 25 μm. **$p<0.01$ Student's *t*-test.

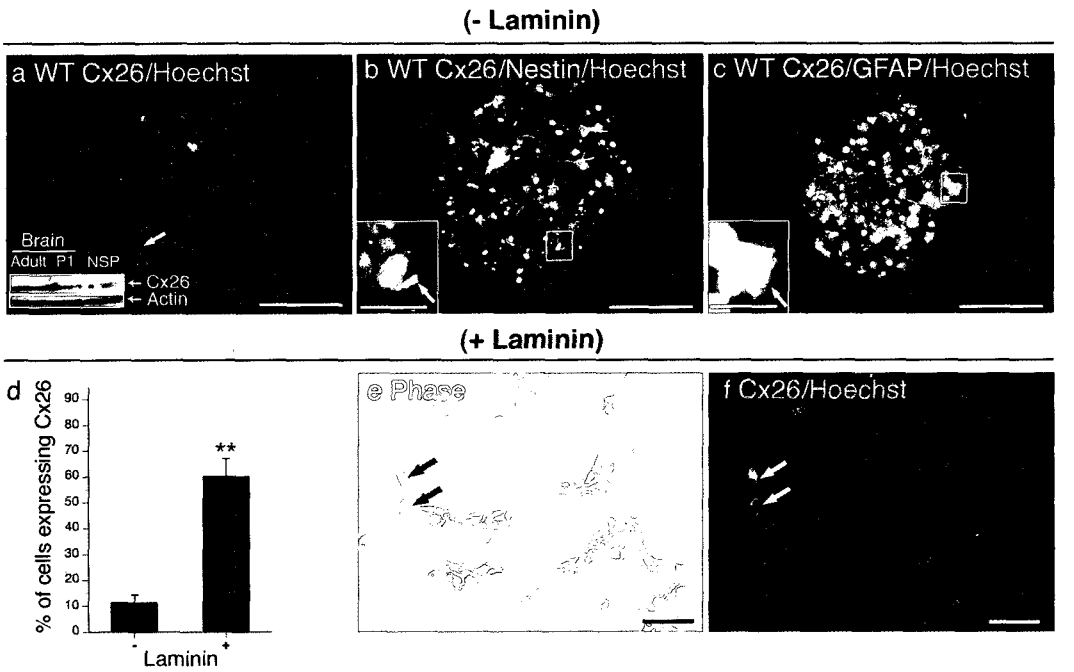
(- Laminin)
a WT Cx26/Hoechst
b WT Cx26/Nestin/Hoechst
c WT Cx26/GFAP/Hoechst
Brain
Adult P1 NSP
← Cx26
← Actin
(+ Laminin)
d
% of cells expressing Cx26
90
80
70
60
50
40
30
20
10
0
**
-
+
Laminin
e Phase
f Cx26/Hoechst

Figure 2.7

Figure 2.8 Cx29, Cx37, and Cx40 are expressed by discrete cell populations with only Cx40 responsive to laminin. Cx29 (a, arrow), Cx37 (c, arrow) and Cx40 (e, arrow) were found in a small number of cells within neurospheres. Insets depict immunostaining performed on null-mutant controls demonstrating antibody specificity. Cx29 was expressed by PDGFαR$^+$ OPCs (b). Cx37 and Cx40 expression were detected in nestin$^+$ Type 2a cells (d, f). Laminin did not alter the frequency of Cx29$^+$ (g-I, arrows) or Cx37$^+$ (j-l, arrows) cells but decreased the number of Cx40$^+$ cells detected in culture (m-o, arrows). Data represent mean of 5-15 sections (- laminin) or field (+ laminin) counted over n=5-10 cultures/condition $\pm$ SEM (g,j.m). Scale bars, 50 μm. Inset in b, 10 μm. Inset in d,f, 25 μm. * $p<0.05$ Student's *t*-test.

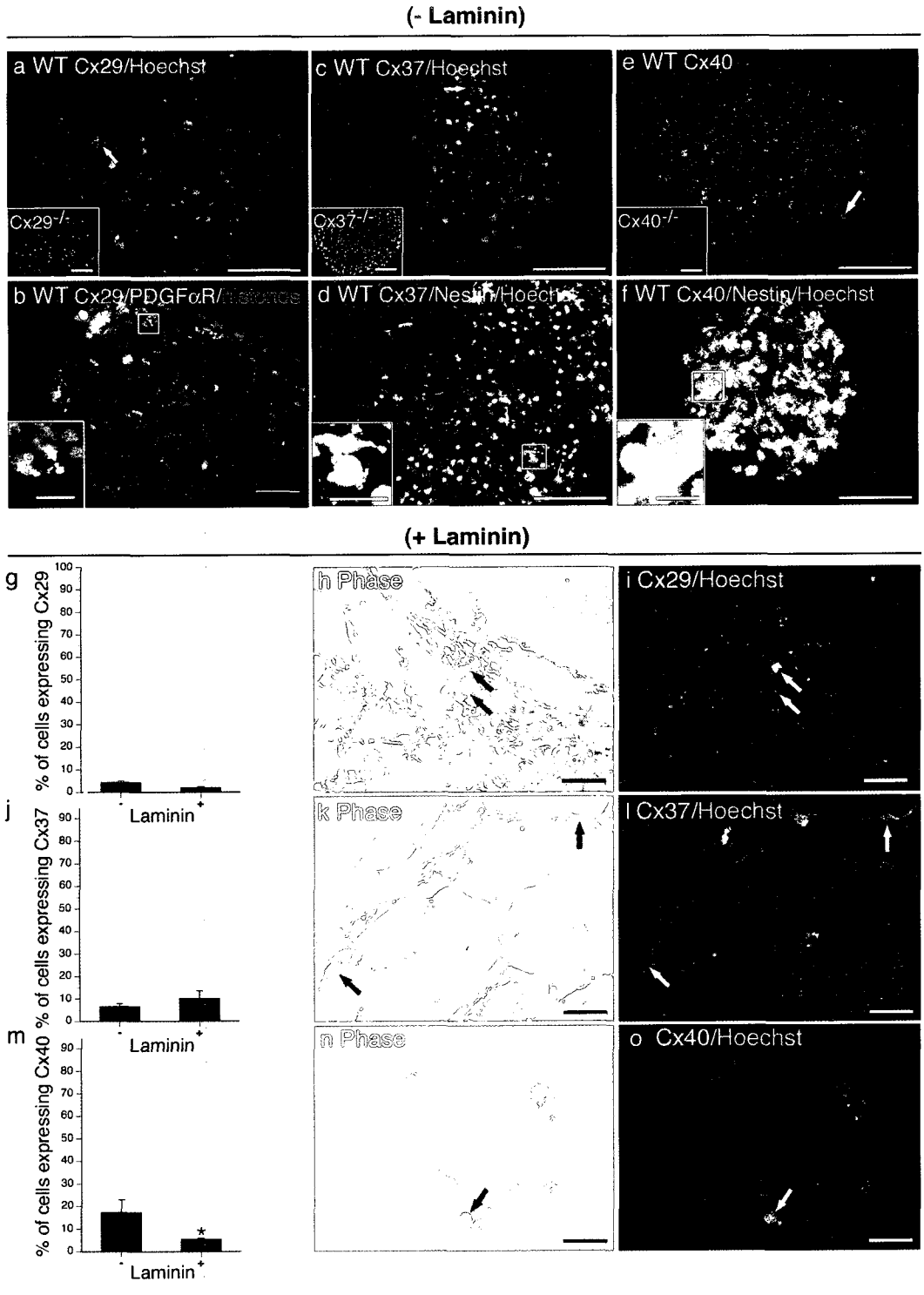
(- Laminin)
a WT Cx29/Hoechst
Cx29-/-
c WT Cx37/Hoechst
Cx37-/-
e WT Cx40
Cx40-/-
b WT Cx29/PDGFαR/
d WT Cx37/Nestin/Hoechst
f WT Cx40/Nestin/Hoechst
(+ Laminin)
g
% of cells expressing Cx29
Laminin
h Phase
i Cx29/Hoechst
j
% of cells expressing Cx37
Laminin
k Phase
l Cx37/Hoechst
m
% of cells expressing Cx40
Laminin
n Phase
o Cx40/Hoechst

Figure 2.8

Figure 2.9 Cx32, Cx36, Cx45, and Cx47 are expressed by rare cells and are laminin-responsive. Cx45 (a, arrows) and Cx47 (c, arrows) were expressed in rare populations of cells. Cx45 was detected in Type 2a nestin$^+$ cells (b, inset). Cx47 was restricted to RIP$^+$ oligodendrocytes (d, inset). Both connexins were downregulated when plated on a laminin substrate (Cx45 e-g, Cx47 h-j). Cx32 (k) and Cx36 (o) protein was not detected in the absence of laminin but was induced following adherence to substrate (Cx32 (l-n) and Cx36 (p-r)). To confirm the lack of Cx32 protein in suspension cultures, western analysis was performed using adult WT brain as a positive control (k, inset). Similarly, western analysis was carried out to confirm Cx36 expression in the + laminin condition and to verify antibody specificity (p, inset). Adult WT and null-mutant (KO) brain served as positive and negative controls. Actin immunoblotting was performed as a loading control. Scale bars, 50 μm, Insets, 25 μm. ** $p<0.01$ Student's *t*-test.

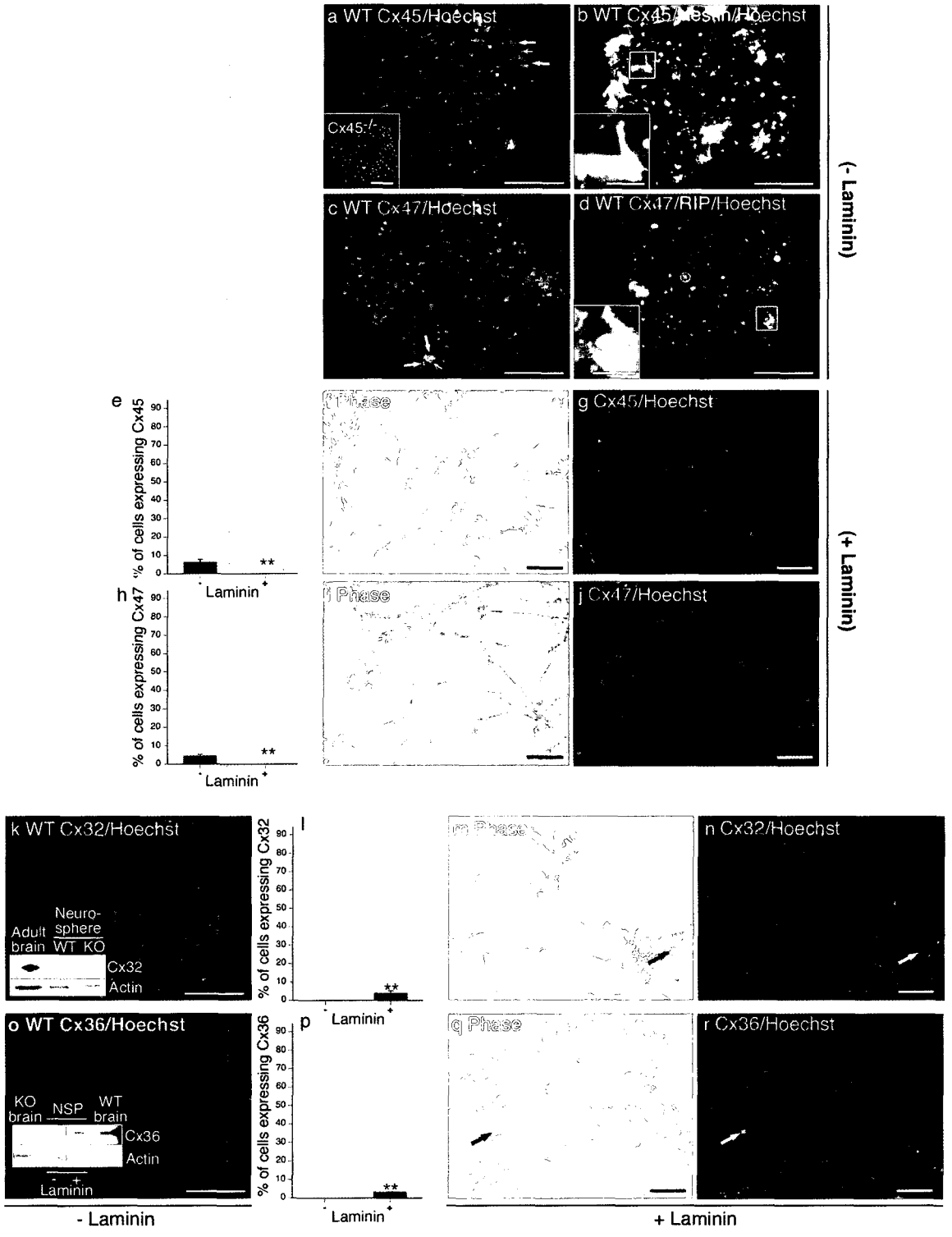
a WT Cx45/Hoechst
Cx45-/-
b WT Cx45/Hoechst
c WT Cx47/Hoechst
d WT Cx47/RIP/Hoechst
(- Laminin)
e
% of cells expressing Cx45
Laminin
f Phase
g Cx45/Hoechst
h
% of cells expressing Cx47
Laminin
i Phase
j Cx47/Hoechst
(+ Laminin)
k WT Cx32/Hoechst
Adult brain
Neuro-sphere
WT KO
Cx32
Actin
l
% of cells expressing Cx32
Laminin
m Phase
n Cx32/Hoechst
o WT Cx36/Hoechst
KO brain
NSP
WT brain
Cx36
Actin
Laminin
p
% of cells expressing Cx36
Laminin
q Phase
r Cx36/Hoechst
- Laminin
+ Laminin

Figure 2.9

2.7.4 Exposure to exogenous laminin substrate alters NPC expression of most connexins

To assess the effect of ECM on connexin expression, NPCs were expanded for 8 DIV in suspension before plating on laminin-coated glass coverslips (Figure. 2.1). Cultures exposed to laminin rapidly adhered to the ECM substrate. Cells at the periphery of the neurosphere migrated from the core as adherent monolayers over 6 DIV. Fewer $Cx43^+$ cells (Figure 2.4j-l) and $Cx40^+$ cells (Figure 2.8m-o) and no $Cx45^+$ (Figure 2.9e-g) or $Cx47^+$ (Figure 2.9h-j) cells were observed when NPCs were cultured on laminin substrate. Laminin increased the number of $Cx26^+$ cells (Figure 2.7d-f) and induced Cx32 (Figure 2.9l-n) and Cx36 (Figure 2.9p-r) protein. $Cx32^+$ cells exhibited small nuclei (Figure 2.9m,n, arrow) and were immunopositive for the OPC marker NG2 (data not shown). Cx36 was expressed in refractile cells with neuritic extensions (Figure 2.9r,s, arrow) and were immunoreactive for the neuronal marker Tuj1-βIII tubulin (data not shown). Although exposure to the ECM substrate did not alter the percentage of cells expressing Cx30 (Figure 2.4g), a change in subcellular localization was observed. Immunoreactivity was markedly less punctate (compare Figure 2.4a and i) with protein detected throughout the cytosol of laminin-treated cultures (Figure 2.4h,i, arrows). Contact with laminin did not change the number of cells expressing Cx29 (Figure 2.8g-i), Cx30 (Figure 2.4g-i), or Cx37 (Figure 2.8j-l). An alternative explanation for these changes lies in the mechanical impact of NPC plating to an adhesive substrate (16, 36, 37). To test this, we plated neurospheres on poly-L-lysine, laminin, or a Matrigel mixture containing the following ECM components (56% laminin, 31% collagen IV, 8% entactin) and assessed Cx43 expression (Figure 2.10). The same reduction in Cx43-expressing cells was observed following engagement with Matrigel as plating on laminin alone. Plating on poly-L-lysine had no effect on Cx43 expression. Taken together, these data provide converging evidence for a laminin-specific regulation of connexin expression as compared to a physico-mechanical influence of culture condition.

Figure 2.10 Laminin and laminin-ECM mixtures but not poly-L-lysine alter the expression of Cx43. The number of Cx43 expressing cells was reduced when NPCs were plated on laminin or a Matrigel matrix composed of laminin/ collagen/ entactin but not when cultures were plated on poly-L-lysine. * $p<0.05$, ANOVA, *post-hoc* Dunnett's *t*-test compared to neurospheres cultured in the absence of matrix.

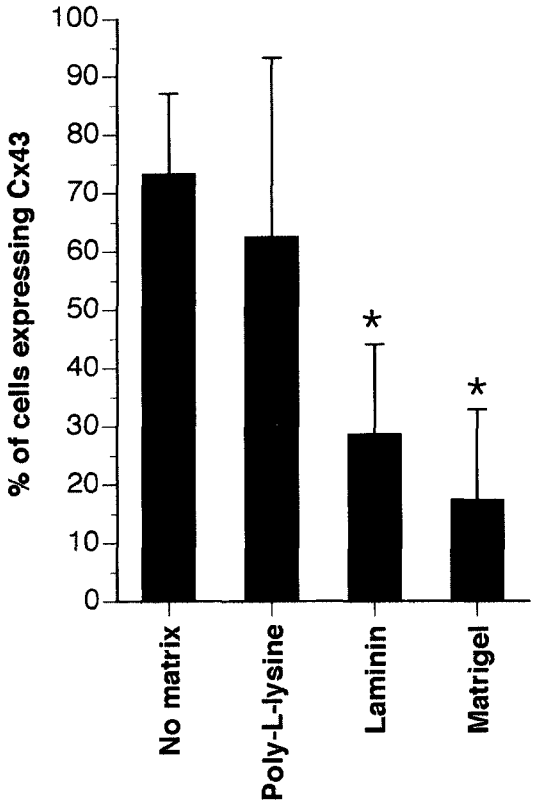
% of cells expressing Cx43
100
90
80
70
60
50
40
30
20
10
0
*
*
No matrix
Poly-L-lysine
Laminin
Matrigel

Figure 2.10

2.7.5 Impact of laminin-induced changes in connexin expression on cell-cell and hemichannel communication

Transmembrane flux of the low molecular mass fluorescent dye, LY, was used to assess hemichannel activity in neurosphere cultures. RD was used to control for uptake resulting from plasma membrane damage. Hemichannel opening was induced by mechanical stimulation with glass microbeads as previously described (32). Cultures were expanded in suspension for 8 DIV, then plated and analyzed immediately after adherence (Figure 2.11a, DIV 1) prior to any detectable change in connexin protein expression (data not shown) or after 6 DIV in contact with laminin (Figure 2.11a, DIV 6) following the observed changes in connexin expression (Figure 2.4-2.8). Mechanical stimulation elicited a significant increase in dye uptake on DIV 1 (Figure 2.11a, DIV 1) that was largely inhibited by the dual-specificity chloride channel and connexin/pannexin-channel blocker FFA (33, 38) but not the chloride channel inhibitor DIDS (Figure 2.11a, DIV 1). Hemichannel activity was lost when NPCs were cultured on laminin for 6 DIV (Figure 2.11a, DIV 6). We cannot, however, rule out that these changes are due to an effect of ECM on pannexin channel formation as we have determined that NPCs cultured in suspension express both pannexin 1 and 2 mRNA (data not shown) yet we have not investigated impact of laminin on this expression at the protein level. Biochemical coupling indicative of GJIC was assessed by scrape loading. Little to no dye transfer was observed on DIV 1 or DIV 6 (Figure 2.11b, Proliferative conditions, DIV 1 and DIV 6,). These data were surprising given the ubiquitous Cx30 and Cx43 expression detected in the majority of cells prior to laminin engagement. As a positive control, we differentiated NPCs to a predominantly nestin$^-$/GFAP$^+$ astrocytic lineage (Figure 2.12). Robust GJIC was detected in these cultures and was inhibited by gap junction channel blocker GRA but not its inactive analog GZA (Figure 2.11b). To provide mechanistic insight into the lack of LY transfer in NPC cultures, we assessed Cx43 phosphorylation status and found, in neurospheres cultured without laminin, that the P2, P3, and hyperphosphorylated forms of Cx43 predominated (Figure 2.13). Previous studies have indicated that the degree of LY dye coupling is

Figure 2.11 Laminin engagement alters functional hemichannel but not GJIC activity. *Functional hemichannel activity was assessed by anionic* LY dye uptake (a) of cultures exposed to laminin for 1 DIV (prior to any changes in connexin expression) or 6 DIV (following changes in connexin expression). Spontaneous LY uptake was observed at low levels after 1 and 6 DIV. Open hemichannel activity could be induced by mechanical stimulation with glass microbeads within 1 DIV but not 6 DIV. Dye uptake was inhibited by the hemichannel/chloride channel inhibitor FFA but not the chloride channel blocker DIDS. LY^+/RD^- cells is expressed as a percentage of the total number of cells per microscopic field ± standard error of the mean (SEM) counted in n=5 fields per experiment conducted in triplicate experiments. GJIC was assayed using the scrape-loading method (b). Significant LY^+/RD^- dye transfer was not observed after 1 or 6 DIV when NPCs were cultured in the presence of mitogens (proliferative conditions). As a positive control, we performed the same experiment in a condition known to promote glial cell differentiation and obtained robust GJIC which was significantly inhibited by the gap junction blocker GRA but not the inactive analog GZA (glial differentiation). In GJIC assays, the number of LY^+/RD^- cells along the scrape line was established in serial photographs taken along the entire length of the scrape (9–14 photos/coverslip) over triplicate cultures. Two coverslips were assessed per culture for a total of n=54–84 measurements per condition. Data are expressed as the mean number of LY^+/RD^- cells $\pm$ SEM. *$p<0.05$, **$p<0.01$, ANOVA, *post-hoc* Tukey test.

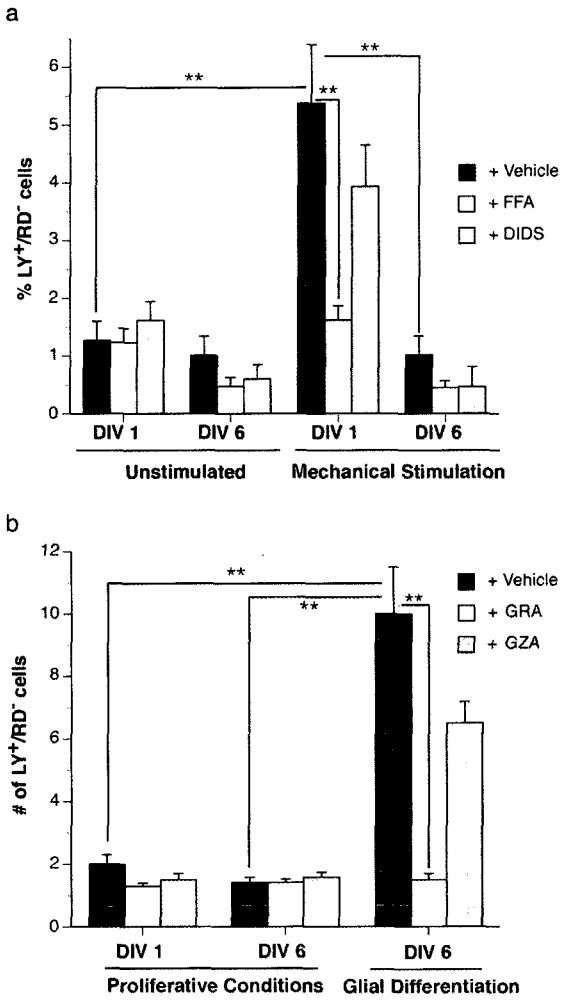
a
% LY+/RD- cells
0
1
2
3
4
5
6
**
**
**
+ Vehicle
+ FFA
+ DIDS
DIV 1
DIV 6
DIV 1
DIV 6
Unstimulated
Mechanical Stimulation
b
# of LY+/RD- cells
0
2
4
6
8
10
12
**
**
**
+ Vehicle
+ GRA
+ GZA
DIV 1
DIV 6
DIV 6
Proliferative Conditions
Glial Differentiation

Figure 2.11

Figure 2.12 Culture composition following mitogen or glial differentiating conditions. Cultures were pulsed with BrdU 24 h prior to plating on a laminin substrate in the presence of EGF and FGF-2 (proliferative conditions) or RA and FBS (glial differentiation). Data are expressed as the percentage of cells actively proliferating at the time of plating that retained a Type1/2a NPC identity or specified to astrocytes, oligodendrocytes, or neurons. *$p<0.05$, **$p<0.01$, ANOVA, *post-hoc* Tukey test.

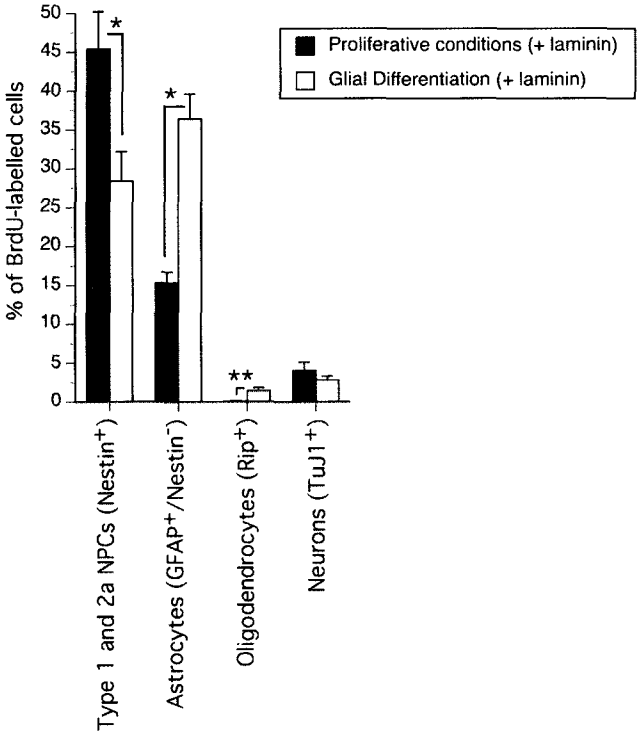
% of BrdU-labelled cells
50
45
40
35
30
25
20
15
10
5
0
Proliferative conditions (+ laminin)
Glial Differentiation (+ laminin)
*
*
**
Type 1 and 2a NPCs (Nestin+)
Astrocytes (GFAP+/Nestin-)
Oligodendrocytes (Rip+)
Neurons (TuJ1+)

Figure 2.12

Figure 2.13 Phosphorylation status of Cx43 in NPCs cultured as neurospheres. Protein lysates were prepared from neurosphere cultures on DIV 14. Two predominant phosphoisoforms were detected corresponding to the P2 and P3 phosphovariants as well as hyperphosphorylated forms. Very low levels of the faster migrating unphosphorylated (NP) and little to no of the P1 phosphoisoform was detected. Data are representative of two independent cultures.

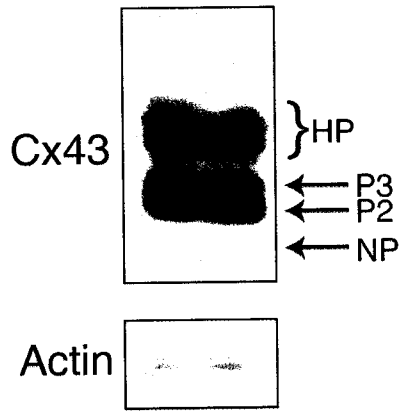

Figure 2.13

inversely correlated with phosphorylation state (39) suggesting that post-translation modification of Cx43 in NPC cultures may account for this lack of dye transfer. Taken together, these data indicate that postnatal NPC cultures do not establish gap junctions permeable to LY, but do exhibit hemichannel activity that is suppressed upon exposure to laminin.

2.8 Discussion

Our data indicate hippocampal-derived postnatal progenitor cells express a broad array of connexin genes and that connexin expression, intracellular distribution, and channel activity are regulated by ECM-cell interactions. When cultured as neurospheres in the absence of exogenous ECM, postnatal NPCs express Cx26, Cx29, Cx30, Cx37, Cx40, Cx43, Cx45, and/or Cx47 mRNA and protein as well as Cx32 and/or Cx36 mRNA. Exposure to a laminin substrate markedly increases the number of $Cx26^+$ cells present in culture and elicits the appearance of Cx32 and Cx36 protein. Conversely, laminin treatment decreases the frequency of $Cx40^+$, $Cx43^+$, and $Cx45^+$ cells without impacting on the number of $Cx29^+$, $Cx30^+$, or $Cx37^+$ NPCs. Surprisingly, we found that, while postnatal NPC cultures exhibit hemichannel activity, they do not transfer LY, a well-established hallmark of junctional communication, until differentiated to a mature astroglial lineage. The lack of dye transfer is likely the result of post-translational modification of the connexin proteins, specifically Cx43. Further, hemichannel activity is suppressed by plating on laminin. Together, these findings suggest a new role for ECM-cell interaction, specifically laminin, in the regulation of intrinsic connexin expression and function in postnatal NPC cultures. This regulation may predispose postnatal NPCs toward channel-independent connexin communication as recently demonstrated in the developing CNS wherein channel-independent connexin adhesion influences the migration of newly born neurons along radial glia (7).

2.8.1 Localization of connexins to discrete subsets of postnatal hippocampal progenitor cells

The repertoire of connexins identified here is much larger than that reported by Wörsdöfer *et al.*, (40) who demonstrated expression of seven connexin transcripts but protein for only Cx31, Cx43, and Cx45. However, these studies used ECM components and not suspension-grown neurospheres. Furthermore, they used embryonic stem (ES) cells rather than postnatal NPCs. Thus, the differences in connexin expression patterns likely reflect the unique connexin signature of the different stem and progenitor cell populations present in these cultures as well as the impact of ECM adhesion on connexin expression. Here, we show that Type 1 and Type 2a multipotential NPCs express Cx26, Cx30, and Cx43. Cx26 and Cx43 have been previously observed in embryonic NPC populations (41, 42) but this is the first demonstration that Cx30, exclusively expressed postnatally (8, 43), is also expressed by multipotential Type 1 NPCs. We found that progression to a Type 2a lineage is associated with *de novo* Cx37, Cx40, and Cx45 protein expression. Further commitment to an oligodendrocyte lineage is accompanied by the loss of all of the connexins identified in multipotential NPCs and *de novo* expression of connexins associated with mature oligodendrocytes (Cx29, Cx32, Cx47) (22). Surprisingly, Cx32 transcript but not protein was detected in OPCs and oligodendroglia in the absence of laminin. The presence of Cx32 transcript but not protein is also observed in ES cells (40) with unknown consequence on cell fate. Taken together, these data provide evidence of intrinsic connexin signatures expressed by progenitor cell subsets over the course of commitment *in vitro*.

2.8.2 Effect of laminin on connexin expression and function

Exposure of NPCs to a laminin substrate altered connexin protein expression and/or stability, intracellular distribution, and functional channel activity. The simplest explanation for these changes is that this profile mirrors the effect of laminin on the differentiation of NPCs. Plating of NPCs on ECM is known to alter the rate of spontaneous specification and survival of embryonic stem cell cultures (44-46). Indeed, we found more cells retained a multipotential Type 1/2 phenotype

in laminin-treated cultures than those expanded in the absence of laminin. An alternative explanation is a direct effect of laminin/integrin signalling on the regulation of connexin protein expression or stability in NPCs. Certainly, laminin has been shown to alter connexin expression and function in other cell types (17-19). The consequence of these changes have only begun to be appreciated. In CNS, the recent finding that gap junctional plaques formed by Cx26 or Cx43 are required for migration of neuronal progenitors along radial glial cells during cortical development in the mouse (7) suggests that ECM regulation of connexin expression is involved in cortical lamination and thus is likely to influence postnatal NPC migration. This hypothesis represents an unexplored role for ECM-connexin interactions *in vivo*.

The changes in connexin profile detected in the presence of laminin are not restricted to NPCs. OPC and neuronal profiles are also altered. Cx32 and Cx36 protein, not observed in the absence of exogenous ECM, are present following laminin engagement. Cx32 null-mutation has previously been shown to delay terminal differentiation of $NG2^+$ OPCs in adult hippocampus (31). Here, we find that the induction of Cx32 protein in $NG2^+$ OPCs by laminin is associated with a moderate increase in the frequency of RIP^+ oligodendrocytes suggesting enhanced oligodendrogenesis. Surprisingly, these new oligodendrocytes did not express Cx47 in the presence of laminin suggesting that perhaps different functional subset of cells are generated. Recent studies indicate that Cx32 and Cx47 do not oligomerize and do not form the same heterotypic intercellular channels taken as evidence for functional differences between these connexins and perhaps between subsets of oligodendrocytes (47, 48). Finally, the induction of Cx36 protein in $TuJ1^+$ neurons in the face of reduced neurogenesis was equally surprising. This observation may recapitulate the changes observed between early and late phases of embryonic neurogenesis. Cx36 mRNA is initially detected in multipotential neural stem cells during early but not late neurogenesis where expression is restricted to their neuronal progeny (8, 49). It may be that the functional changes in channel activity

observed following engagement of neurosphere cultures with laminin regulate NPC and OPC commitment.

At no point did we detect cell-cell coupling with respect to the passage of the anionic dye LY. While surprising given that embryonic progenitor populations are coupled during early neurogenesis (50-52) our data agree with the findings of Duval *et al.* who demonstrated GJIC in astrocytes but not in other NPC-derived cells (53). Here, we show passage of LY only when NPC cultures are induced to differentiate towards a primarily astroglial lineage and likely corresponds with a shift in the phosphorylation status of Cx43. Conversely, robust transmembrane dye flux indicative of functional hemichannel activity is evident prior to ECM-induced changes in connexin protein profiles. Laminin engagement suppresses this activity. It is tempting to speculate that connexin (or pannexin)-mediated hemichannel activity promotes specification whereas channel-independent adhesion supports the migration through ECM-defined domains in postnatal hippocampus. However, care must be taken in directly extrapolating our results to the *in vivo* situation given the complex three dimensional character of the developing hippocampus where many different matrices and cellular scaffolds are present given evidence of different cell phenotypes within 2D and 3D culture systems (16). Clearly, it will be important to establish the impact of ECM control of connexin protein expression on postnatal NPC proliferation, migration, and specification *in vivo*.

We have identified the repertoire of connexins expressed by postnatal hippocampal NPCs over the course of commitment *in vivo*. We have demonstrated that ECM engagement, more specifically laminin, can alter not only the fate of cultured postnatal hippocampal NPCs, but also their connexin expression profile and related channel function. Taken together, these data suggest that ECM control of connexin expression and signalling may play a role in the direction of multipotential NPCs towards a neuronal or glial lineage.

2.9 References

1. Lathia, J.D., B. Patton, D.M. Eckley, T. Magnus, M.R. Mughal, T. Sasaki, M.A. Caldwell, M.S. Rao, M.P. Mattson, and C. ffrench-Constant. 2007. Patterns of laminins and integrins in the embryonic ventricular zone of the CNS. *J Comp Neurol* 505:630-643.

2. Peinado, A. 2001. Immature neocortical neurons exist as extensive syncitial networks linked by dendrodendritic electrical connections. *J Neurophysiol* 85:620-629.

3. Peinado, A., R. Yuste, and L.C. Katz. 1993. Gap junctional communication and the development of local circuits in neocortex. *Cereb Cortex* 3:488-498.

4. Russo, R.E., C. Reali, M. Radmilovich, A. Fernandez, and O. Trujillo-Cenoz. 2008. Connexin 43 delimits functional domains of neurogenic precursors in the spinal cord. *J Neurosci* 28:3298-3309.

5. Belvindrah, R., S. Hankel, J. Walker, B.L. Patton, and U. Muller. 2007. Beta1 integrins control the formation of cell chains in the adult rostral migratory stream. *J Neurosci* 27:2704-2717.

6. Fushiki, S., J.L. Perez Velazquez, L. Zhang, J.F. Bechberger, P.L. Carlen, and C.C. Naus. 2003. Changes in neuronal migration in neocortex of connexin43 null mutant mice. *J Neuropathol Exp Neurol.* 62:304-314.

7. Elias, L.A., D.D. Wang, and A.R. Kriegstein. 2007. Gap junction adhesion is necessary for radial migration in the neocortex. *Nature* 448:901-907.

8. Cina, C., J.F. Bechberger, M.A. Ozog, and C.C. Naus. 2007. Expression of connexins in embryonic mouse neocortical development. *J Comp Neurol* 504:298-313.

9. Simon, A.M., and D.A. Goodenough. 1998. Diverse functions of vertebrate gap junctions. *Trends Cell Biol* 8:477-483.

10. Stout, C., D.A. Goodenough, and D.L. Paul. 2004. Connexins: functions without junctions. *Curr Opin Cell Biol* 16:507-512.

11. Sohl, G., and K. Willecke. 2004. Gap junctions and the connexin protein family. *Cardiovasc Res* 62:228-232.

12. Rouach, N., E. Avignone, W. Meme, A. Koulakoff, L. Venance, F. Blomstrand, and C. Giaume. 2002. Gap junctions and connexin expression in the normal and pathological central nervous system. *Biol. Cell.* 94:457-475.

13. Kreuzberg, M.M., J. Deuchars, E. Weiss, A. Schober, S. Sonntag, K. Wellershaus, A. Draguhn, and K. Willecke. 2008. Expression of connexin30.2 in interneurons of the central nervous system in the mouse. *Mol Cell Neurosci* 37:119-134.

14. Dere, E., Q. Zheng-Fischhofer, D. Viggiano, U.A. Gironi Carnevale, L.A. Ruocco, A. Zlomuzica, M. Schnichels, K. Willecke, J.P. Huston, and A.G. Sadile. 2008. Connexin31.1 deficiency in the mouse impairs object memory and modulates open-field exploration, acetylcholine esterase levels in the striatum, and cAMP response element-binding protein levels in the striatum and piriform cortex. *Neuroscience* 153:396-405.

15. Vandecasteele, M., J. Glowinski, and L. Venance. 2006. Connexin mRNA expression in single dopaminergic neurons of substantia nigra pars compacta. *Neurosci Res* 56:419-426.

16. Pampaloni, F., E.G. Reynaud, and E.H. Stelzer. 2007. The third dimension bridges the gap between cell culture and live tissue. *Nat Rev Mol Cell Biol* 8:839-845.

17. Lampe, P.D., B.P. Nguyen, S. Gil, M. Usui, J. Olerud, Y. Takada, and W.G. Carter. 1998. Cellular interaction of integrin alpha3beta1 with laminin 5 promotes gap junctional communication. *J Cell Biol* 143:1735-1747.

18. Guo, Y., C. Martinez-Williams, C.E. Yellowley, H.J. Donahue, and D.E. Rannels. 2001. Connexin expression by alveolar epithelial cells is regulated by extracellular matrix. *Am J Physiol Lung Cell Mol Physiol* 280:L191-202.

19. Isakson, B.E., C.E. Olsen, and S. Boitano. 2006. Laminin-332 alters connexin profile, dye coupling and intercellular Ca2+ waves in ciliated tracheal epithelial cells. *Respir Res* 7:105.

20. Altevogt, B.M., K.A. Kleopa, F.R. Postma, S.S. Scherer, and D.L. Paul. 2002. Connexin29 is uniquely distributed within myelinating glial cells of the central and peripheral nervous systems. *J Neurosci* 22:6458-6470.

21. Deans, M.R., J.R. Gibson, C. Sellitto, B.W. Connors, and D.L. Paul. 2001. Synchronous activity of inhibitory networks in neocortex requires electrical synapses containing connexin36. *Neuron* 31:487-485.

22. Menichella, D.M., D.A. Goodenough, E. Sirkowski, S.S. Scherer, and D.L. Paul. 2003. Connexins are critical for normal myelination in the CNS. *J. Neurosci.* 23:5963-5973.

23. Simon, A.M., D.A. Goodenough, E. Li, and D.L. Paul. 1997. Female infertility in mice lacking connexin 37. *Nature* 385:525-529.

24. Simon, A.M., D.A. Goodenough, and D.L. Paul. 1998. Mice lacking connexin40 have cardiac conduction abnormalities characteristic of atrioventricular block and bundle branch block. *Curr Biol* 8:295-298.

25. Nishii, K., M. Kumai, K. Egashira, T. Miwa, K. Hashizume, Y. Miyano, and Y. Shibata. 2003. Mice lacking connexin45 conditionally in cardiac myocytes display embryonic lethality similar to that of germline knockout mice without endocardial cushion defect. *Cell Commun Adhes* 10:365-369.

26. Teubner, B., V. Michel, J. Pesch, J. Lautermann, M. Cohen-Salmon, G. Sohl, K. Jahnke, E. Winterhager, C. Herberhold, J.P. Hardelin, C. Petit, and K. Willecke. 2003. Connexin30 (Gjb6)-deficiency causes severe hearing impairment and lack of endocochlear potential. *Hum Mol Genet* 12:13-21.

27. Nelles, E., C. Buetzler, D. Jung, A. Temme, H.D. Gabriel, U. Dahl, O. Traub, F. Stuempel, K. Jungermann, J. Zielasek, K.V. Toyka, R. Dermietzel, and K. Willecke. 1996. Defective propagation of signals generated by sympathetic nerve stimulation in the liver of connexin32-deficient mice. *Proc. Natl. Acad. Sci. USA.* 93:9565-9570.

28. Berube, N.G., M. Mangelsdorf, M. Jagla, J. Vanderluit, D. Garrick, R.J. Gibbons, D.R. Higgs, R.S. Slack, and D.J. Picketts. 2005. The chromatin-remodeling protein ATRX is critical for neuronal survival during corticogenesis. *J Clin Invest* 115:258-267.

29. Bennett, S.A., and L. Melanson-Drapeau. 2003. Primary culture of adult neural progenitors. *Methods Mol Med* 79:397-404.

30. Song, H.J., C.F. Stevens, and F.H. Gage. 2002. Neural stem cells from adult hippocampus develop essential properties of functional CNS neurons. *Nat Neurosci* 5:438-445.

31. Melanson-Drapeau, L., S. Beyko, S. Davé, A.L.O. Hebb, D.J. Franks, C. Sellito, D.L. Paul, and S.A.L. Bennett. 2003. Oligodendrocyte progenitor enrichment in the connexin32 null-mutant mouse. *J Neurosci* 23:1759-1768.

32. Boucher, S., and S.A.L. Bennett. 2003. Differential connexin expression, gap junction intercellular coupling, and hemichannel formation in NT2/D1 human neural progenitors and terminally differentiated hNT neurons. *J. Neurosci. Res.* 72:393-404.

33. Stout, C.E., J.L. Costantin, C.C. Naus, and A.C. Charles. 2002. Intercellular calcium signaling in astrocytes via ATP release through connexin hemichannels. *J. Biol. Chem.* 22:10482-10488.

34. Altevogt, B.M., and D.L. Paul. 2004. Four classes of intercellular channels between glial cells in the CNS. *J Neurosci* 24:4313-4323.

35. Filippov, M.A., S.G. Hormuzdi, E.C. Fuchs, and H. Monyer. 2003. A reporter allele for investigating connexin 26 gene expression in the mouse brain. *Eur J Neurosci* 18:3183-3192.

36. Csete, M. 2005. Oxygen in the cultivation of stem cells. *Ann N Y Acad Sci* 1049:1-8.

37. Ruiz, A., L. Buzanska, D. Gilliland, H. Rauscher, L. Sirghi, T. Sobanski, M. Zychowicz, L. Ceriotti, F. Bretagnol, S. Coecke, P. Colpo, and F. Rossi. 2008. Micro-stamped surfaces for the patterned growth of neural stem cells. *Biomaterials* 29:4766-4774.

38. Suadicani, S.O., C.F. Brosnan, and E. Scemes. 2006. P2X7 receptors mediate ATP release and amplification of astrocytic intercellular Ca2+ signaling. *J Neurosci* 26:1378-1385.

39. Lampe, P.D., and A.F. Lau. 2000. Regulation of gap junctions by phosphorylation of connexins. *Arch Biochem Biophys* 384:205-215.

40. Worsdorfer, P., S. Maxeiner, C. Markopoulos, G. Kirfel, V. Wulf, T. Auth, S. Urschel, J. von Maltzahn, and K. Willecke. 2008. Connexin expression and functional analysis of gap junctional communication in mouse embryonic stem cells. *Stem Cells* 26:431-439.

41. Nadarajah, B., A.M. Jones, W.H. Evans, and J.G. Parnavelas. 1997. Differential expression of connexins during neocortical development and neuronal circuit formation. *J Neurosci* 17:3096-3111.

42. Bittman, K.S., and J.J. LoTurco. 1999. Differential regulation of connexin 26 and 43 in murine neocortical precursors. *Cereb Cortex* 9:188-195.

43. Rochefort, N., N. Quenech'du, P. Ezan, C. Giaume, and C. Milleret. 2005. Postnatal development of GFAP, connexin43 and connexin30 in cat visual cortex. *Brain Res Dev Brain Res* 160:252-264.

44. Flaim, C.J., S. Chien, and S.N. Bhatia. 2005. An extracellular matrix microarray for probing cellular differentiation. *Nat Methods* 2:119-125.

45. Goetz, A.K., B. Scheffler, H.X. Chen, S. Wang, O. Suslov, H. Xiang, O. Brustle, S.N. Roper, and D.A. Steindler. 2006. Temporally restricted substrate interactions direct fate and specification of neural precursors derived from embryonic stem cells. *Proc Natl Acad Sci U S A* 103:11063-11068.

46. Philp, D., S.S. Chen, W. Fitzgerald, J. Orenstein, L. Margolis, and H.K. Kleinman. 2005. Complex extracellular matrices promote tissue-specific stem cell differentiation. *Stem Cells* 23:288-296.

47. Orthmann-Murphy, J.L., M. Freidin, E. Fischer, S.S. Scherer, and C.K. Abrams. 2007. Two distinct heterotypic channels mediate gap junction coupling between astrocyte and oligodendrocyte connexins. *J Neurosci* 27:13949-13957.

48. Kleopa, K.A., J.L. Orthmann, A. Enriquez, D.L. Paul, and S.S. Scherer. 2004. Unique distributions of the gap junction proteins connexin29, connexin32, and connexin47 in oligodendrocytes. *Glia* 47:346-357.

49. Gulisano, M., R. Parenti, F. Spinella, and F. Cicirata. 2000. Cx36 is dynamically expressed during early development of mouse brain and nervous system. *Neuroreport* 11:3823-3828.

50. Lo Turco, J.J., and A.R. Kriegstein. 1991. Clusters of coupled neuroblasts in embryonic neocortex. *Science* 252:563-566.

51. Bittman, K., D.F. Owens, A.R. Kriegstein, and J.J. LoTurco. 1997. Cell coupling and uncoupling in the ventricular zone of developing neocortex. *J Neurosci* 17:7037-7044.

52. Kandler, K. 1997. Coordination of neuronal activity by gap junctions in the developing neocortex. *Semin Cell Dev Biol* 8:43-51.

53. Duval, N., D. Gomes, V. Calaora, A. Calabrese, P. Meda, and R. Bruzzone. 2002. Cell coupling and Cx43 expression in embryonic mouse neural progenitor cells. *J Cell Sci* 115:3241-3251.

Chapter 3: Connexin 29 regulates oligodendrogenesis in postnatal hippocampal culture*

3.1 Objective of study

Determine the localization and role of Cx29 in proliferation and specification of neural progenitor cells using a loss-of-function (Cx29 null-mutant mice) approach in hippocampal-derived postnatal neural progenitor cell primary culture.

3.2 Statement of author contributions

SI and SALB wrote the manuscript and prepared the figures. SI, LGG, and SALB conceived and designed the experiments. SI performed all the experimental work except: immunocytochemistry from Figure 2b,e and the data from Figure 4c-e, which were done by LGG. SALB also helped to quantify the data appearing in Figure 4c-e.

* A version of this chapter has been submitted to the Journal of Neuroscience

3.3 Connexin29 regulates postnatal hippocampal neural progenitor cell oligodendrogenesis

Sophie Imbeault, Lianne G. Gauvin, and Steffany A.L. Bennett
Neural Regeneration Laboratory and Ottawa Institute of Systems Biology, Dept. of Biochemistry, Microbiology and Immunology, University of Ottawa, ON, Canada

Running title: Cx29 regulates hippocampal oligodendrogenesis

Correspondence: Dr. Steffany Bennett, Neural Regeneration Laboratory, Department of Biochemistry, Microbiology and Immunology, University of Ottawa, 451 Smyth Rd., Ottawa, Ontario, Canada, K1H 8M5. Tel: 613 562-5800 x8372; Fax 613 562-5440; Email: sbennet@uottawa.ca

Acknowledgements: This research was supported by operating grants from CIHR (MOP-62826) and Genome Canada to SALB. SI and LG were supported by OGSST and NSERC graduate scholarships. We thank Dr David Paul for providing the Cx29 antibodies and Cx29$^{-/-}$ breeding pairs, Dr William Stallcup for supplying the NG2 antibody, and Dr. Leigh Anne Swayne for optimization of the flow cytometry protocols. The excellent technical support of Mark Akins and the editorial assistance of Jim Bennett are gratefully acknowledged.

3.4 Summary

Cognitive dysfunction in multiple demyelinating and neuropsychiatric disorders is attributed, in part, to hippocampal oligodendrocyte loss precipitated by the failure of resident oligodendrocyte progenitor cells (OPCs) to restore oligodendrocyte number. Enhancing this capacity would be of substantive benefit. The neural progenitor cells (NPCs) present in the subgranular zone of the dentate gyrus of the hippocampus represent an alternative source of oligodendrocytes; however these cells are intrinsically directed towards an oligodendrocyte lineage and away from an astrocyte or neuronal lineage, the capacity of which remains unclear. We found the loss of a single connexin protein, connexin29, was sufficient to impair NPC oligodendrogenesis in neurosphere culture and to redirect the OPC-like progeny towards an astrocytic lineage without changing NPC proliferation, clonal expansion, or survival. Together, these data identify a new oligodendrogenic fate determinant in multipotential NPCs that directs glial specification *in vitro*.

3.5 Introduction

In the postnatal brain, oligodendrocyte number is primarily maintained by resident oligodendrocyte progenitor cells (OPCs). These cells are born embryonically, migrate throughout the developing central nervous system (CNS), and activate postnatally (1, 2). In fact, platelet-derived growth factor α receptor (PDGFαR) and chondroitin sulphate proteoglycan NG2-expressing OPCs comprise the majority of cycling cells in the CNS (3). Following white matter injury, these cells are able to repopulate affected areas (4). However, in demyelinating conditions such as multiple sclerosis (MS), failure to remyelinate occurs once the regenerative capacity of resident OPCs is exhausted (5). Enhancing oligodendrogenesis by mobilizing alternate progenitor pools represents a novel therapeutic strategy for MS and neuropsychiatric disorders where cognitive deficits are attributed, in part, to hippocampal oligodendrocyte loss (5-8). Validation will require a comprehensive understanding of how NPC oligodendrogenic fate is determined *in vitro* and *in vivo*.

Multipotential postnatal neural stem/progenitor cells (NPCs) represent an alternative source of hippocampal oligodendrocytes. NPCs can be directed towards an oligodendrocyte lineage by ectopic expression of *Ascl1* and by direct cell-cell contact with hippocampal neurons (9, 10). Furthermore, the loss of the gap junction protein connexin 32 (Cx32) in adult mouse hippocampus leads to an increase in $NG2^+$ OPCs (11). Connexins (Cxs) have also been implicated in the control of NPC cell cycle, specification (11-13) and in the migration of immature neuroblasts (14). Signaling involves both gap junction-dependent and -independent mechanisms. Cx hexamerization forms voltage and pH-gated single membrane channels ("connexons") enabling communication with the extracellular milieu. The alignment of two connexons at junctional cell membranes creates a functional channel, enabling the passage of ions and small metabolites ≤ 1 kDa between cells. Channel-independent signaling occurs through protein-protein interactions (15) or the formation of "adhesion domains" between NPCs and neighbouring instructive cells (14). Signal specificity is dictated by the repertoire of Cxs expressed. Only select combinations are capable of oligomerization, docking, or adhesion.

Of the 20 murine Cx proteins, three are detected in oligodendrocytes (Cx29, Cx32, Cx47) (16) but only two (Cx29 and Cx32) are expressed by NPC-derived OPCs (17). Cx32 has already been implicated in the control of hippocampal $NG2^+$ proliferation and specification (11). Here, we asked whether Cx29 expression alters hippocampal NPC fate. Using neurospheres as a simple model of hippocampal development, we show the loss of Cx29 is sufficient to inhibit NPC specification to a $PDGF\alpha R^+$ OPC and RIP^+ oligodendrocyte lineage by promoting astrocytic commitment without altering proliferative or apoptotic indices. Together, these data identify a new target through which NPC oligodendrogenesis can be controlled *in vitro*.

3.6 Methods

3.6.1 Mice

Breeding pairs of $Cx29^{-/-}$ mice mice (16) were provided by Dr David Paul (Harvard Medical School). Mice were backbred for six generations (N6) to a C57Bl/6 background and compared to congenic N6 $Cx29^{+/+}$ mice. Genotyping was carried out as described in Imbeault *et al.* (17). All animal procedures were approved by the University of Ottawa Animal Care Committee in accordance with guidelines set forth by the Canadian Council on Animal Care.

3.6.2 Neurosphere cultures

Primary neurosphere suspension cultures were prepared from single hippocampal NPCs isolated on postnatal day 0-3 as described in Imbeault *et al.* (17) in expansion medium for 14 days *in vitro* (DIV) with addition of fresh epidermal growth factor (EGF: 20 ng/ml) and fibroblast growth factor-2 (FGF2: 10 ng/ml) every two days. To label proliferating NPCs, cultures were pulsed with 5'-bromo-2-deoxyuridine (BrdU; 20 μg/mL, Roche) on DIV 7 or DIV 13 for 24 h as indicated. NPCs were induced to differentiate by plating on laminin on DIV 8 in DMEM/F12

containing 1 mM sodium pyruvate, 200 mM D-glucose, 1% penicillin/streptomycin, 2% N2 supplement, retinoic acid (RA; 0.5 μM), and fetal bovine serum (FBS; 0.5%). Control cultures were grown in the same media containing EGF and FGF2 in place of RA and FBS.

3.6.3 Reverse transcriptase-polymerase chain reaction (RT-PCR)

Total RNA was isolated using Trizol (Invitrogen, Burlington, ON) from 100-150 neurospheres pooled on DIV 14 or adult mouse cerebrum (positive control). Samples were treated with RQ1 DNAse (Promega, Madison, WI). Total RNA (2 μg) was subjected to random hexamer (pdN6, Promega) primed-reverse transcription (RT) using Superscript II RT (BD Biosciences, Burlington, ON). Polymerase chain reaction was performed in a final volume of 25 μl containing: 1X PCR buffer, 0.8 mM dNTPs, 1X Advantage 2 Polymerase (Clontech, Cambridge, ON), 4 ng/μL Cx29 primers (F: 5'-GGTTTTCGGCAATGAT, R: 5'-GGCATGGTTGGGTGGTTTCTC, amplicon length 278 bp) or 0.2 μM GAPDH primers (F: 5'-TGGTGCTGAGTATGTCGTGGAGT, R: 5'-AGTCTTCTGAGTGGCAGTGATGG, amplicon length 292 bp). Cycling parameters were: 94°C for 5 min, 35 cycles of 94°C for 25 sec, 59°C for 50 sec, and 72°C for 1 min 45 sec, and a final step at 72°C for 7 min in a Whatman Biometra T-Gradient thermocycler (Montreal-Biotech Inc., Kirkland, QC).

3.6.4 Immunocytochemistry

On DIV 14, cells were fixed at room temperature in 3.7% formaldehyde solution in 10 mM phosphate buffered saline (PBS, 0.154 M NaCl, 0.0028 M NaH_2PO_4, 0.0072 M Na_2HPO_4, pH 7.2) for 20 min as described in Imbeault *et al.* (17) and immunocytochemistry performed as described in Melanson-Drapeau *et al.* (11). All antibodies (Table 3.1) were diluted in Antibody (Ab) buffer (3% BSA + 0.3% Triton-X 100 in PBS). Hoechst 33258 (0.5 μg/mL) or immunolabelling for histones was performed as a nuclear counterstain. For BrdU staining, slides were incubated with 2 N HCl at 37°C for 30 min, rinsed 2 x 5 min with 0.1 M Borate Buffer, and 3 x 4

min with PBS prior to primary antibody incubation. In fate-tracking experiments, immunocytochemistry was performed on neurospheres expanded for 8 DIV before plating on laminin-coated coverslips and cultured for 6 further DIV in differentiation or maintenance media.

3.6.5 Terminal deoxynucleotidyl transferase (TdT)-mediated dUTP nick end labelling (TUNEL)

Neurosphere sections were hydrated in PBS for 5 min prior to permeabilization with 0.1% Triton X-100 and 0.1% sodium citrate for 5 min on ice. Sections were washed 2 min with PBS and incubated for 1 h at 37°C with FITC-dUTP in TdT buffer (140 mM sodium cacodylate, 1 mM cobalt chloride in 30 mM Tris-HCl pH 7.2) and TdT enzyme according to manufacturer's protocol (Roche).

3.6.6 Flow cytometry

On DIV 14, neurospheres were collected, centrifuged 5 min at 300 x g, and resuspended in versene (Invitrogen). Cells were gently triturated using a series of pipettes with decreasing tip apertures until a single-cell suspension was obtained (verified by hemacytometer counts). Formaldehyde was added to the versene suspension to a final concentration of 2% and incubated on ice for 20 min. Fixed single cell suspensions were washed twice in 2% FBS in PBS (PBS/FBS) followed by resuspension in 0.18% saponin in PBS/FBS (sapPBS/FBS). Approximately 2-5 x 10^5 cells/200 µL of sapPBS/FBS were used per condition. Cells were sequentially incubated with primary and secondary antibodies (including isotype controls) as specified in Table 3.1 for 30 min with shaking. Between incubations, cells were washed with PBS/FBS and centrifuged at 300 x g. Cells were resuspended in 600 µL of PBS/FBS prior to analysis on a Beckman Coulter FC500 Flow Cytometer using CXP software (Beckman Coulter Canada Inc., Mississauga, ON). A blank (PBS/FBS) followed by a 'cells alone' control provided the initial gate for the cellular population of each condition. Detector sensitivity was determined using positive controls for each antigen-antibody combination. Parameters (initial gating, detector

Table 3.1 Primary and secondary antibodies used for immunocytochemistry and flow cytometry

Antibody	Type	Species	Source	Dilution Immuno	Dilution Flow
Cx29	Polyclonal	Guinea Pig	Dr. David Paul	1:20	---
Cx29	Polyclonal	Rabbit	Dr.David Paul	1:20	1:20
β-galactosidase	Polyclonal	Rabbit	Chemicon	1:1500	---
BrdU	Monoclonal	Rat	BD	1:50	---
GFAP	Polyclonal	Rabbit	Sigma	1:100	---
Histones	Monoclonal	Mouse	Chemicon	1:500	---
Nestin	Monoclonal	Mouse	Chemicon	1:50	---
NG2	Polyclonal	Rabbit	Chemicon	1:200	1:200
NG2	Polyclonal	Guinea Pig	Dr. William Stallcup	1:200	---
PDGFαR	Monoclonal	Rat	BD Pharmingen	1:300	1:200
Phospho-histone H3	Polyclonal	Rabbit	BD Pharmingen	1:1000	---
RIP	Monoclonal	Mouse	Chemicon	1:1000	1:800
TuJ1 (βIII-tubulin)	Monoclonal	Mouse	Research Diagnostics	1:250	---
Mouse IgG	Cy3-conjugated	Donkey	Jackson	1:800	---
Rabbit IgG	Cy3-conjugated	Donkey	Jackson	1:600	---
Guinea Pig IgG	Cy3-conjugated	Donkey	Jackson	1:1000	---
Mouse IgG	FITC-conjugated	Donkey	Jackson	1:100	1:100
Rabbit IgG	FITC-conjugated	Donkey	Jackson	1:100	1:100
Rat IgG	FITC-conjugated	Donkey	Jackson	1:80	---
Rat IgG	RPE-conjugated	Goat	Serotec	---	1:100

voltage, and signal gain) were kept constant throughout all conditions. Data from 3-4 independent experiments (litters) per genotype were averaged and compared. All data were corrected for background fluorescence signal.

3.6.7 Quantification and statistical analyses

For immunocytochemical assessments, each parameter was assessed n=10-50 individual neurospheres prepared over n=2-4 experiments. Data represent the number of positive cells for a specified antigen expressed as a percentage of the total number of Hoechst 33258$^+$ or anti-histone$^+$ nuclei per section. For non-nuclear antigens, only cells having over 50% of the nucleus surrounded by specific immunoreactivity were counted. Neurosphere volumes were calculated according to the formula $V=4/3(\pi r^3)$. Cell density/per section was calculated as the average number of Hoechst 33258$^+$ or anti-histone$^+$ nuclei per section. Average cell area was determined by dividing the section area by the total number of nuclei therein. All measurements were made using the Advanced Measurement module of OpenLab software (v.5.05, Improvision, Perkin-Elmer, Waltham, MA). Data represent averages ± standard error of the mean (SEM) also expressed, in some cases, as fold change relative to wild-type. Statistics were Student's *t*-tests, Mann-Whitney U tests (where n>5 (n=3-4)), or ANOVA followed by *post-hoc* Tukey test using Instat (v3.0, GraphPad, LaJolla, CA).

3.7 Results

3.7.1 Cx29 is expressed by early OPCs

Both Cx29 mRNA (Figure 3.1a) and protein (Figure 3.1b) were detected in primary postnatal hippocampal NPC neurosphere cultures after 14 DIV. In wild-type cultures, Cx29 protein was expressed by approximately 4% of cells as determined by immunolabelling of cryosections (Figure. 3.1c) and flow cytometry of dissociated cultures (Figure. 3.1d). Specificity was confirmed by immunolabelling for β-galactosidase (β-gal) in Cx29 null-mutant cultures wherein the *lacZ* gene replaces the Cx29 coding sequence (Figure. 3.1b, inset).

Figure 3.1 Cx29 is expressed by a subset of cells in postnatal hippocampal-derived neurospheres. **(A)** RT-PCR was performed on total RNA from 100-150 pooled neurosphere cultures or mouse cerebrum in the presence (+) or absence (-) of reverse transcriptase or template (NT). M, molecular size marker. **(B)** Immunostaining for Cx29 in a 10 μm section through the equatorial region of a neurosphere culture. Scale bar, 50 μm. Upper inset depicts higher magnification of the $Cx29^{+}$ cell indicated by arrows. Scale bar, 10 μm. Lower inset depicts β-gal immunostaining in a $Cx29^{-/-}$ neurosphere. Scale bar, 50 μm. Quantification of $Cx29^{+}$ cells was performed by **(C)** immunostaining (n=9 neurospheres) and **(D)** flow cytometry of n=100-150 neurospheres per analysis conducted in replicate. Isotype controls are shown in grey. The specific Cx29 signal quantified is indicated in light green.

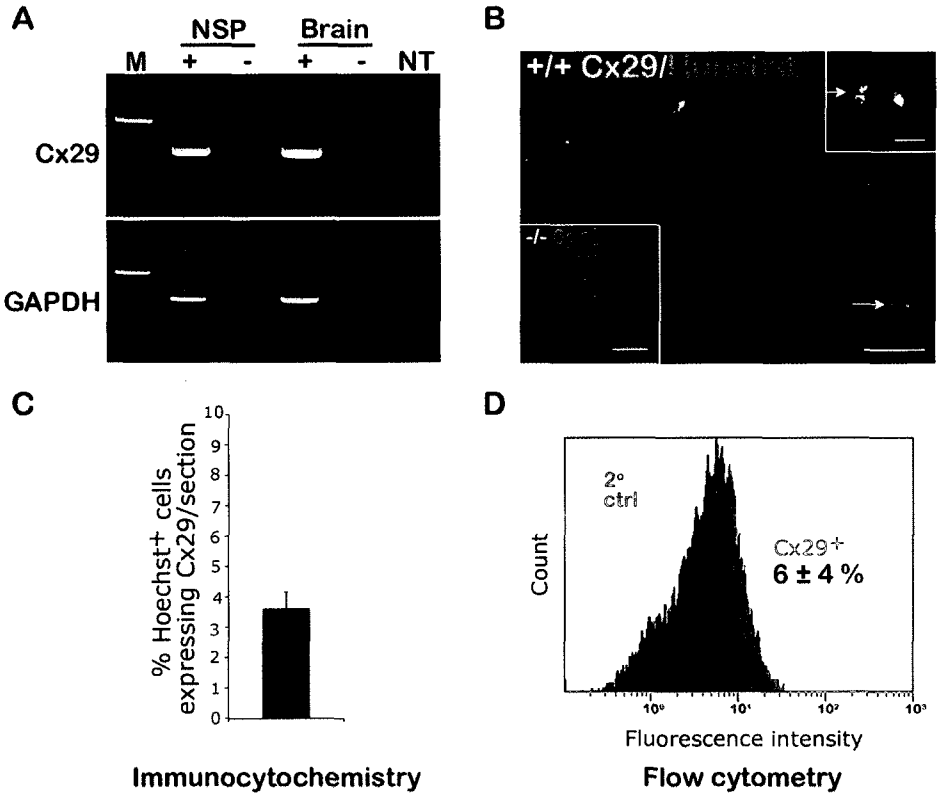
A
NSP
Brain
M
+
-
+
-
NT
Cx29
GAPDH
B
+/+ Cx29/
-/-
C
% Hoechst+ cells expressing Cx29/section
0
1
2
3
4
5
6
7
8
9
10
Immunocytochemistry
D
2°
ctrl
Cx29+
6 ± 4 %
Count
Fluorescence intensity
Flow cytometry

Figure 3.1

Although each neurosphere is derived from a single nestin$^+$ NPC (Figure 3.2a), daughter cells spontaneously adopt distinct lineages in culture recapitulating many of the neurogenic and gliogenic stages observed in the postnatal hippocampus (Figure 3.2a). Cx29$^+$ cells were identified by double-immunostaining for the antigenic lineage markers listed in Figure 3.2a and either Cx29 or β-gal in wild-type and null-mutant cultures respectively. Expression was not detected in nestin$^+$ NPCs (Figure 3.2b, arrowhead) but was evident in subsets of daughter cells expressing the OPC-like lineage markers NG2$^+$ (Figure 3.2c, arrow) and PDGFαR$^+$ (Figure 3.2d, arrow and insets) as well as in their progeny, RIP$^+$ oligodendrocytes (Figure 3.2e). Cx29$^+$/NG2$^+$ cells localized primarily to polar sections of neurosphere cultures (Figure 3.2c). Cx29$^+$/PDGFαR$^+$ OPC-like cells were present throughout polar and equatorial regions of the neurosphere cultures. This localization was confirmed by β–gal and PDGFαR immunostaining in Cx29$^{-/-}$ cultures (Figure 3.2d).

3.7.2 Cx29 does not regulate proliferation or survival of NPCs or their progeny

To assess the functional consequences of Cx29 expression over the course of NPC oligodendrogenesis, we compared proliferative, apoptotic, and specification indices in congenic wild-type and null-mutant cultures. Loss of Cx29 did not affect the ability of Type 1 NPCs to clonally expand as neurospheres. No difference in neurosphere volume (+/+ 0.014 ± 0.003 mm^3 and -/- 0.013 ± 0.002 mm^3), cell density (+/+ 493 ± 55 cells/section and -/- 474 ± 44 cells/section), or average cell size (area) per section (+/+ 82 ± 3 μm^2/cell and -/- 78 ± 6 μm^2/cell) was observed between genotypes (Figure 3.3a-e). Furthermore, Cx29 null-mutation did not alter cell proliferative indices as assessed by BrdU-labelling of cells in S-phase (+/+ 9 ± 3% and -/- 7 ± 2% cells/section) or phospho-histone H3 (pHH3) immunolabelling of cells in M-phase (+/+ 0.4 ± 0.1% and -/- 0.3 ± 0.1% cells/section) (Figure 3.3c-e). Finally, no difference in the basal apoptotic index was detected in wild-type and null-mutant cultures indicating that loss of Cx29 did not significantly impact upon the survival of NPCs or their progeny (Figure 3.3f).

Figure 3.2 Cx29 is expressed by early OPC-like cells. (A) Schematic of NPC oligodendrogenesis in postnatal hippocampal neurosphere culture indicating the antigenic lineage markers used to distinguish progenitor populations. **(B)** Cx29 protein (arrowhead) was not detected in nestin$^+$ NPCs (arrow). Inset depicts these cells at higher magnification. **(C)** Cx29 was also present in a subset of NG2$^+$ OPC-like cells (arrow). A section through the polar region of neurosphere is shown. Inset depicts these cells at higher magnification. **(D)** Cx29 was expressed by a subset of PDGFαR$^+$ cells (arrow and upper inset) confirmed by the co-expression of the PDGFαR and β-gal reporter in Cx29$^{-/-}$ cultures (D, lower inset). **(E)** Co-expression of Cx29 and the oligodendrocyte marker RIP is observed at DIV 14 (arrow and inset). Scale bars, 50 μm. Upper inset scale bars, 10 μm. Lower inset scale bars, 5 μm.

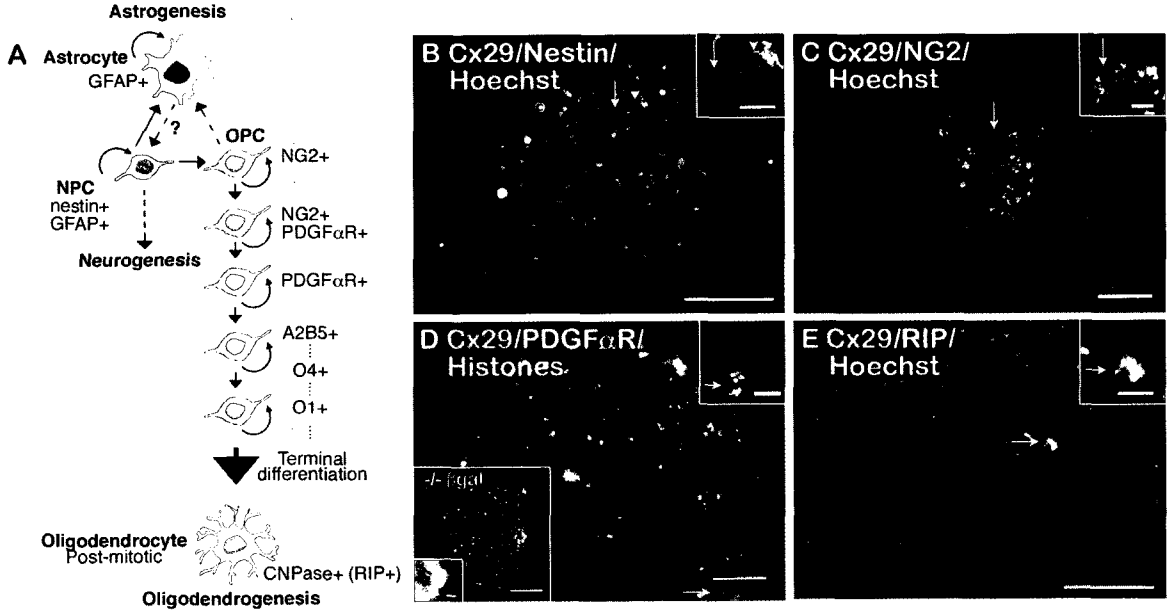
Astrogenesis
A
Astrocyte
GFAP+
?
OPC
NG2+
NPC
nestin+
GFAP+
NG2+
PDGFαR+
Neurogenesis
PDGFαR+
A2B5+
O4+
O1+
Terminal
differentiation
Oligodendrocyte
Post-mitotic
CNPase+ (RIP+)
Oligodendrogenesis
B Cx29/Nestin/
Hoechst
C Cx29/NG2/
Hoechst
D Cx29/PDGFαR/
Histones
E Cx29/RIP/
Hoechst

Figure 3.2

Figure 3.3 Loss of Cx29 does not affect cell number, cell size, or cell proliferation of NPC neurosphere cultures. (A,B) Representative phase contrast images of neurospheres derived from $Cx29^{+/+}$ and $Cx29^{-/-}$ mice. Scale bars, 50 μm; insets,10 μm. **(C,D)** Representative immunocytochemistry for BrdU in the same cultures presented in **(A,B)** labelled for 24 h with BrdU on DIV 13 and processed on DIV 14. Immunostaining using a pan-histones antibody was used to assess total cell number. Insets show phosphohistone H3 $(pHH3)^{+}$ cells, a marker of cells in M-phase assessed in separate cultures. **(E)** Quantitation of neurosphere volume, cell density, average cell size, and % of cells in S-phase and M-phase. All data are expressed as fold change relative to $Cx29^{+/+}$ cultures. No statistically significant change was observed in any parameter as a result of Cx29 null-mutation (Student's *t*-test).

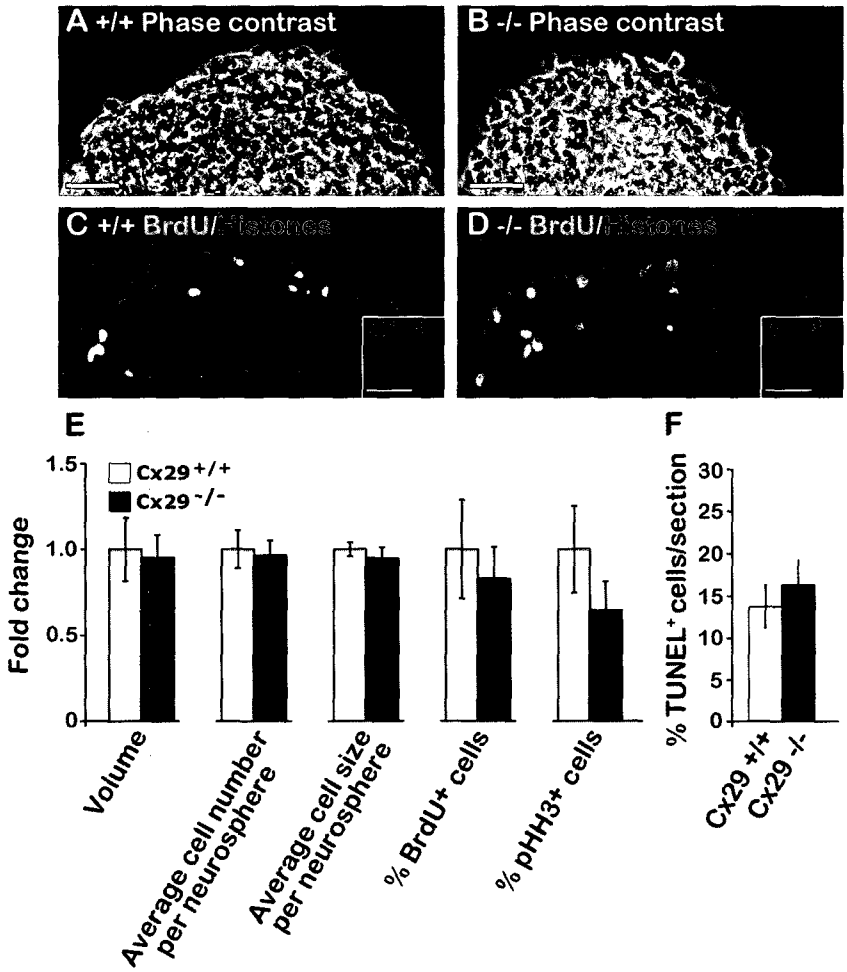
A +/+ Phase contrast
B -/- Phase contrast
C +/+ BrdU/Histones
D -/- BrdU/Histones
E
F
Fold change
1.5
1.0
0.5
0
Cx29+/+
Cx29-/-
Volume
Average cell number per neurosphere
Average cell size per neurosphere
% BrdU+ cells
% pHH3+ cells
% TUNEL+ cells/section
30
25
20
15
10
5
0
Cx29 +/+
Cx29 -/-

Figure 3.3

3.7.3 Cx29 directs progenitor cells towards an oligodendrocyte lineage

Although survival of progenitors and their progeny was not altered, spontaneous oligodendrocyte differentiation was reduced by 55% in $Cx29^{-/-}$ cultures with a concomitant 33% reduction in NPC-derived early OPCs (Figure 3.4a,b). Closer examination revealed the impairment in NPC oligodendrogenesis lay in the transition of $NG2^+$ OPCs to a $PDGF\alpha R^+$ lineage (Figure 3.4b). No difference was found in the number of $nestin^+$ NPCs (Figure 3.4b). Further, no difference was found in the ability of Type 1 NPCs to specify to an $NG2^+$ OPC-like lineage assessed by both immunocytochemistry (+/+ 7 ± 1% and -/- 8 ± 1% $NG2^+$ cells/section, n=15 neurospheres, Figure 3.4b) and flow cytometry (+/+ 45 ± 3% and -/- 33 ± 6% $NG2^+$ cells/culture, n=4 and 3 cultures of ~250 neurospheres/culture per genotype). A significant decrease was evident in the number of early OPCs expressing $PDGF\alpha R$ (+/+ 9 ± 1% and -/- 3.1 ± 0.3% cells/section, Figure 3.4b). Placed in context with evidence of comparable clonal expansion (Figure 3.3a-e), proliferation (Figure 3.3a-e), and survival (Figure 3.3f), these data suggested that the $NG2^+$ progeny of Type 1 NPCs adopt a non-oligodendrocytic fate in the absence of Cx29.

To test this hypothesis directly, we asked whether loss of Cx29 was sufficient to prevent NPCs and their progeny from specifying to oligodendrocytes even in the presence of differentiating factors. NPCs were expanded as neurospheres for 8 DIV, pulsed for 24 h with BrdU to label actively proliferating cells, plated on laminin-coated coverslips, and cultured in media containing either FGF2 and EGF to maintain BrdU-labelled cells in an undifferentiated state or RA and FBS to promote differentiation. The fate of labelled cells was established after a further 6 DIV by immunocytochemistry. Consistent with our previous data (Figure 3.3f), loss of Cx29 did not affect the survival of BrdU-labelled cells whether cultured in NPC maintenance media or differentiating media (Figure 3.4c). Oligodendrogenic specification was significantly reduced in $Cx29^{-/-}$ cultures to half that of control cultures (Figure 3.4d). These data are in keeping with our observation that Cx29 is expressed by a subpopulation of OPCs (Figures 3.1 and 3.2) and thus loss of function does not completely block NPC oligodendrogenesis. In the absence of

Figure 3.4 Loss of Cx29 redirects NG2+ OPCs to adopt an astrocytic fate. (*A*) Loss of Cx29 resulted in a significant reduction in the percentage of cells expressing the early OPC lineage markers NG2 and/or PDGFαR and the mature oligodendrocyte marker RIP as assessed by flow cytometry (n=3-4 independent experiments assessing 100-150 pooled neurosphere cultures per experiment). * $p \leq 0.05$, **$p < 0.01$, Mann Whitney U. ***(B)*** Closer examination by immunocytochemistry revealed that the PDGFαR+ early OPCs and the RIP+ mature oligodendrocyte populations but not the $NG2^+$ early OPC or $nestin^+$ NPC populations were affected. *$p < 0.05$, ***$p < 0.001$, Student's *t*-test. Scale bars, 50 μm. Scale bars in inset, 8 μm. (***C***) Fate tracking of BrdU labelled cells was performed by labelling neurospheres on DIV 7 plating on laminin-coated coverslips, and assessing survival and fate on DIV 14. No difference in the survival of BrdU-labelled cells was detected between genotypes whether cells were cultured in media that maintained NPCs in their undifferentiated state (EGF+FGF2) or promoted terminal differentiation (RA+FBS). ***(D)*** Oligodendrogenesis was significantly inhibited under both spontaneous differentiating conditions (EGF-FGF2) and directed differentiation (RA+FBS) in $Cx29^{-/-}$ cultures (ANOVA, *post-hoc* Tukey, * $p < 0.05$, **$p < 0.01$). ***(E)*** Loss of Cx29 redirected BrdU-labelled cells to adopt an astrocyte fate at the expense of oligodendrogenesis in cultures exposed to differentiated media. Neurogenesis was not affected. (Student's *t* test, * $p < 0.05$).

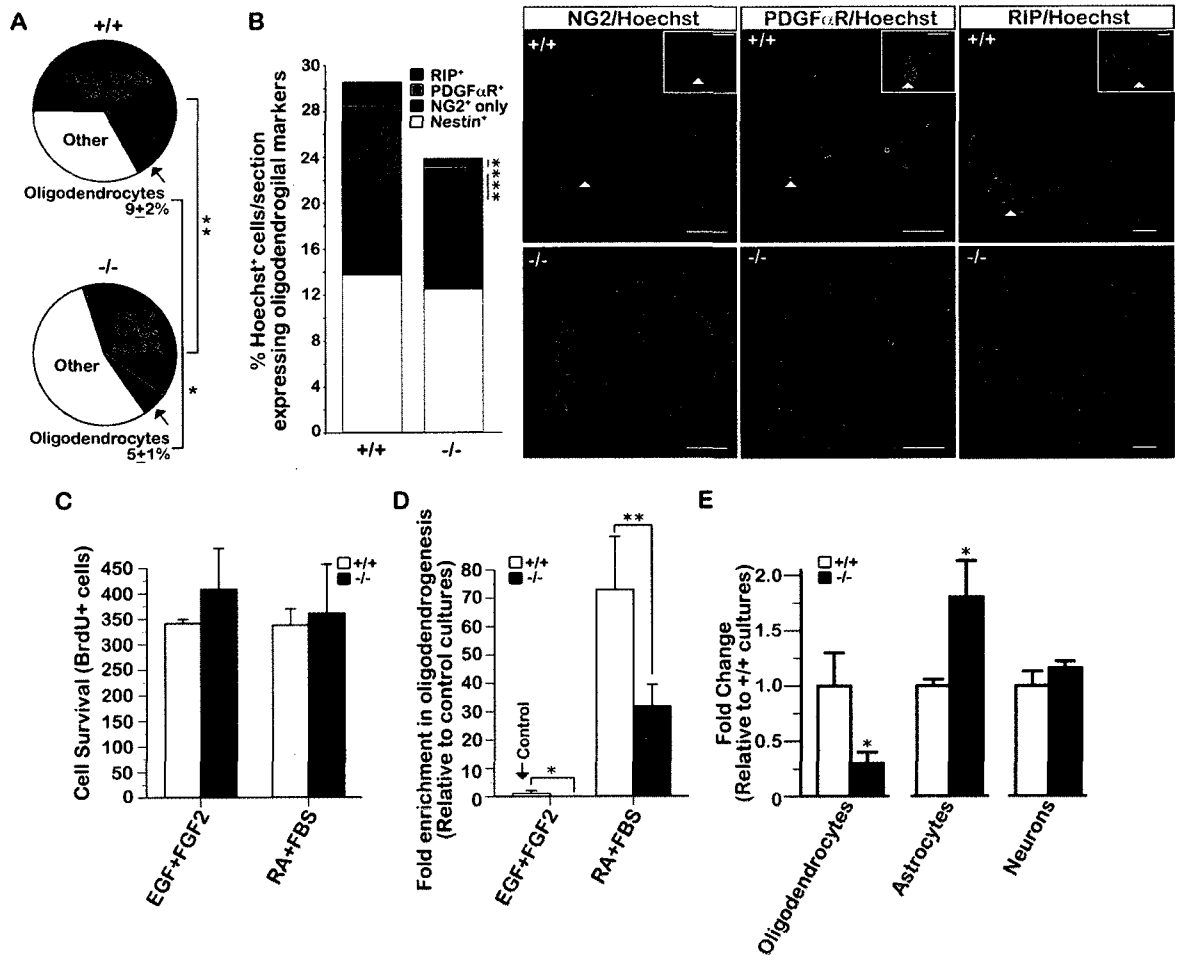
A
+/+
Other
Oligodendrocytes
9±2%
-/-
Other
Oligodendrocytes
5±1%
B
% Hoechst+ cells/section expressing oligodendroglial markers
RIP+
PDGFαR+
NG2+ only
Nestin+
+/+
-/-
NG2/Hoechst
PDGFαR/Hoechst
RIP/Hoechst
C
Cell Survival (BrdU+ cells)
EGF+FGF2
RA+FBS
D
Fold enrichment in oligodendrogenesis (Relative to control cultures)
Control
E
Fold Change (Relative to +/+ cultures)
Oligodendrocytes
Astrocytes
Neurons

Figure 3.4

Cx29, more BrdU-labelled cells adopted an astrocytic fate at the expense of oligodendrocytes (Figure 3.4e). No difference in neurogenesis was detected between genotypes (Figure 3.4e). Taken together, these data provide strong evidence that Cx29 expression directs a subset of OPCs to adopt an oligodendrocytic fate whereas in the absence of Cx29 these cells specify to astrocytes.

3.8 Discussion

Here, we show the gap junction protein Cx29 is an intrinsic regulator of hippocampal NPC oligodendrogenesis. Our data indicate that a subset of $NG2^+$ and $PDGF\alpha R^+$ early OPC-like progeny of Type 1 hippocampal NPCs express Cx29. Using a loss of function approach, we found this expression is required for approximately half of these NPC-derived $NG2^+$cells in primary neurosphere culture to specify to a $PDGF\alpha R^+$ early OPC-like lineage. This impairment in oligodendrogenesis was independent of any defect in postnatal hippocampal NPC self-renewal, clonal expansion, proliferation, or survival. Rather, Cx29 expression was apparently sufficient to direct OPC-like cells to adopt an oligodendrocytic fate whereas, in the absence of Cx29, more NPC progeny differentiated into astrocytes.

Previous reports have demonstrated Cx29 expression in myelinating fibers within the CNS and peripheral nervous system (18-20). While mRNA expression is detected by P7 in the mouse brain (21), immunofluorescence studies show Cx29 is restricted to mature $CNPase^+$ cells in the corpus callosum by P8 (22). However, most studies restricted their investigations to post-mitotic oligodendrocyte markers. Recently, Li *et al.* used a β-gal reporter mouse to show Cx29 expression as early as E12.5 in the spinal cord (23). They further demonstrated, using primary cultures from both wild-type and knock-out reporter mice, Cx29 expression during the transition from multipotential neural crest cells to Schwann cell progenitors. In contrast to our data, loss of Cx29 did not alter the specification of Schwann cells precursors to more mature cell types (23). The authors thus present Cx29 as a novel marker of the Schwann cell progenitor stage but do not explore what function Cx29 may have in these precursors. Here, we show a similar dynamic expression during

the transition of multipotential nestin$^+$ hippocampal NPCs to an NG2$^+$ cell lineage and further demonstrate that, in hippocampal cultures, loss of Cx29 is sufficient to alter the transition of OPCs to a more mature cell fate thereby affecting the balance of NPC gliogenesis.

While our data clearly show that, in the absence of Cx29, oligodendrogenesis is impaired in over half the NPC-derived NG2$^+$ glial progenitors, it is also important to note that not all NG2$^+$ NPC-progeny require Cx29 for oligodendrogenesis. While we have yet to define the underlying molecular mechanisms by which Cx29 directs NG2$^+$ cells away from an astrocytic fate, our data underline the plasticity of hippocampal NPCs and the potential of these cells to serve as an alternative source of oligodendrocytes. One possible mechanism involves the formation of hemichannels. In mature myelinating cells of the CNS, Cx29 is associated with the juxtaparanodal region and the inner mesaxon (18). Due to this localization in non-junctional membranes, and to experiments showing Cx29 cannot form gap junction channels (18, 24), it is likely that Cx29 forms hemichannels. Furthermore, in the peripheral nervous system, Cx29 is intriguingly located across from Kv1.2 channels on axons where it is thought to help sequester K^+ from the periaxonal space although this possibility has yet to be directly tested (18, 25). On the other hand, Li *et al.* (23) hinted at a possible structural role for Cx29 in neuronal/glial interactions involving protein-protein interactions. Our data fit with both these hypothesized roles. If Cx29 indeed forms hemichannels, loss of channel activity may lead to an inability to respond to trophic messengers from neighbouring cells, notably neurons, given evidence that NPC-neuron co-cultures promote oligodendrogenesis (10). Alternatively, Cx29 may help localize other proteins, such as PDGFαR, to the cell surface. Loss of Cx29 would thus lead to loss of PDGFαR signaling and of responses normally associated with this receptor. Certainly, both hypotheses will require further empirical testing. Our data, however, clearly demonstrate the potential of transiently altering the connexin profile of NPCs in order to overcome or induce fate restrictions *in vitro*. This approach could be exploited to increase

oligodendrocyte specification and supplement or enhance oligodendrocyte number, which has important implications for *in vivo* remyelination strategies in MS.

3.9 References

1. Zhu, X., D.E. Bergles, and A. Nishiyama. 2008. NG2 cells generate both oligodendrocytes and gray matter astrocytes. *Development* 135:145-157.

2. Peters, A., and C. Sethares. 2004. Oligodendrocytes, their progenitors and other neuroglial cells in the aging primate cerebral cortex. *Cereb Cortex* 14:995-1007.

3. Dawson, M.R., A. Polito, J.M. Levine, and R. Reynolds. 2003. NG2-expressing glial progenitor cells: an abundant and widespread population of cycling cells in the adult rat CNS. *Mol Cell Neurosci* 24:476-488.

4. Gensert, J.M., and J.E. Goldman. 1997. Endogenous progenitors remyelinate demyelinated axons in the adult CNS. *Neuron* 19:197-203.

5. Franklin, R.J., and C. Ffrench-Constant. 2008. Remyelination in the CNS: from biology to therapy. *Nat Rev Neurosci* 9:839-855.

6. Geurts, J.J., L. Bo, S.D. Roosendaal, T. Hazes, R. Daniels, F. Barkhof, M.P. Witter, I. Huitinga, and P. van der Valk. 2007. Extensive hippocampal demyelination in multiple sclerosis. *J Neuropathol Exp Neurol* 66:819-827.

7. Fields, R.D. 2008. White matter in learning, cognition and psychiatric disorders. *Trends Neurosci* 31:361-370.

8. Jessberger, S., and F.H. Gage. 2009. Fate plasticity of adult hippocampal progenitors: biological relevance and therapeutic use. *Trends Pharmacol Sci* 30:61-65.

9. Jessberger, S., N. Toni, G.D. Clemenson, Jr., J. Ray, and F.H. Gage. 2008. Directed differentiation of hippocampal stem/progenitor cells in the adult brain. *Nat Neurosci* 11:888-893.

10. Song, H., C.F. Stevens, and F.H. Gage. 2002. Astroglia induce neurogenesis from adult neural stem cells. *Nature* 417:39-44.

11. Melanson-Drapeau, L., S. Beyko, S. Dave, A.L. Hebb, D.J. Franks, C. Sellitto, D.L. Paul, and S.A. Bennett. 2003. Oligodendrocyte progenitor enrichment in the connexin32 null-mutant mouse. *J Neurosci* 23:1759-1768.

12. Bittman, K., D.F. Owens, A.R. Kriegstein, and J.J. LoTurco. 1997. Cell coupling and uncoupling in the ventricular zone of developing neocortex. *J Neurosci* 17:7037-7044.

13. Pearson, R.A., N. Dale, E. Llaudet, and P. Mobbs. 2005. ATP released via gap junction hemichannels from the pigment epithelium regulates neural retinal progenitor proliferation. *Neuron* 46:731-744.

14. Elias, L.A., D.D. Wang, and A.R. Kriegstein. 2007. Gap junction adhesion is necessary for radial migration in the neocortex. *Nature* 448:901-907.

15. Herve, J.C., N. Bourmeyster, D. Sarrouilhe, and H.S. Duffy. 2007. Gap junctional complexes: from partners to functions. *Prog Biophys Mol Biol* 94:29-65.

16. Altevogt, B.M., and D.L. Paul. 2004. Four classes of intercellular channels between glial cells in the CNS. *J Neurosci* 24:4313-4323.

17. Imbeault, S., L.G. Gauvin, H.D. Toeg, A. Pettit, C.D. Sorbara, L. Migahed, R. DesRoches, A.S. Menzies, K. Nishii, D.L. Paul, A.M. Simon, and S.A. Bennett. 2009. The extracellular matrix controls gap junction protein expression and function in postnatal hippocampal neural progenitor cells. *BMC Neurosci* 10:13.

18. Altevogt, B.M., K.A. Kleopa, F.R. Postma, S.S. Scherer, and D.L. Paul. 2002. Connexin29 is uniquely distributed within myelinating glial cells of the central and peripheral nervous systems. *J Neurosci* 22:6458-6470.

19. Kleopa, K.A., J.L. Orthmann, A. Enriquez, D.L. Paul, and S.S. Scherer. 2004. Unique distributions of the gap junction proteins connexin29, connexin32, and connexin47 in oligodendrocytes. *Glia* 47:346-357.

20. Nagy, J.I., A.V. Ionescu, B.D. Lynn, and J.E. Rash. 2003. Coupling of astrocyte connexins Cx26, Cx30, Cx43 to oligodendrocyte Cx29, Cx32, Cx47: Implications from normal and connexin32 knockout mice. *Glia* 44:205-218.

21. Sohl, G., J. Eiberger, Y.T. Jung, C.A. Kozak, and K. Willecke. 2001. The mouse gap junction gene connexin29 is highly expressed in sciatic nerve and regulated during brain development. *Biol Chem* 382:973-978.

22. Nagy, J.I., A.V. Ionescu, B.D. Lynn, and J.E. Rash. 2003. Connexin29 and connexin32 at oligodendrocyte and astrocyte gap junctions and in myelin of the mouse central nervous system. *J Comp Neurol* 464:356-370.

23. Li, J., H.W. Habbes, J. Eiberger, K. Willecke, R. Dermietzel, and C. Meier. 2007. Analysis of connexin expression during mouse Schwann cell development identifies connexin29 as a novel marker for the transition of neural crest to precursor cells. *Glia* 55:93-103.

24. Ahn, M., J. Lee, A. Gustafsson, A. Enriquez, E. Lancaster, J.Y. Sul, P.G. Haydon, D.L. Paul, Y. Huang, C.K. Abrams, and S.S. Scherer. 2008. Cx29 and Cx32, two connexins expressed by myelinating glia, do not interact and are functionally distinct. *J Neurosci Res* 86:992-1006.

25. Rash, J.E. 2009. Molecular disruptions of the panglial syncytium block potassium siphoning and axonal saltatory conduction: pertinence to neuromyelitis optica and other demyelinating diseases of the central nervous system. *Neuroscience*

Chapter 4: Glial connexins partly regulate oligodendrocyte progenitor cell fate in the postnatal dentate gyrus

4.1 Objectives of the study

1) Determine the *in vivo* cell-type localization of Cx29, Cx32 and Cx47 within the dentate gyrus of the hippocampus

2) Using single-, double-, and triple-null mutations in Cx29, Cx32, and, Cx47, determine the role these proteins play in progenitor cell proliferation and specification in the hippocampal niche.

4.2 Statement of author contributions

SI and SALB conceived and designed the experiments. SI performed all the experimental work and produced the figures. SI and SALB wrote the manuscript. CDS contributed wild-type tissue sections for the staining in Figures 4.1-4.3.

4.3 A glial connexin network regulates oligodendrocyte progenitor cell proliferation in the subgranular zone of the dentate gyrus

Sophie Imbeault, Catherine D. Sorbara and Steffany A.L. Bennett
Neural Regeneration Laboratory and Ottawa Institute of Systems Biology, Department of Biochemistry, Microbiology and Immunology, University of Ottawa, ON, Canada

Running Title: Cxs regulate OPC proliferation in the hippocampus

Corresponding Author: Dr. Steffany Bennett, Neural Regeneration Laboratory, Department of Biochemistry, Microbiology and Immunology, University of Ottawa, 451 Smyth Rd., Ottawa, Ontario, Canada, K1H 8M5. Tel: 613 562-5800 x8372; Fax 613 562-5440; Email: sbennet@uottawa.ca

Acknowledgements
The authors would like to thank Mark Akins and Stefan Petrescu for technical assistance with animal colony maintenance and genotyping. Confocal imaging was made possible thanks to partial equipment funding from the Heart and Stroke Foundation Centre for Stroke Recovery.

4.4 Summary

Oligodendrocytes are crucial to proper cognitive function. Failure of oligodendrocyte progenitor cells (OPCs) to properly differentiate into oligodendrocytes is one of the reasons for sustained demyelination in multiple sclerosis. An alternative source of progenitors might prove useful for therapeutic applications, however we must first understand what factors influence OPC proliferation and specification. Previous work from our laboratory has shown a role for connexins in specification of OPCs, whereby loss of Cx32 in the adult dentate gyrus results in an increased pool of $NG2^+$ OPCs. Aside from Cx32, hippocampal-derived OPCs also express Cx29 *in vitro* and this connexin is important for specification of these OPCs to oligodendrocytes. Furthermore, oligodendrocytes express Cx29, Cx32 and Cx47 *in vivo*. Here we investigate the localization of Cx29, Cx32 and Cx47 within the dentate gyrus of the hippocampus and whether these connexins play a role in oligodendrocyte progenitor cell proliferation. We find the novel localization of Cx29 to $NG2^+$ OPCs and to platelet-derived growth factor receptor alpha $(PDGF\alpha R)^+$ OPCs while Cx32 is expressed in $NG2^+PDGF\alpha R^-$ cells. Loss of this differential expression results in significantly increased proliferation of $NG2^+$ cells and $GFAP^+$ astrocytes in Cx29 null-mutant mice whereas loss of Cx32 results in a very significant expansion of only the $NG2^+$ cell population. Together these data implicate both Cx29 and Cx32 in the regulation of OPC type-specification and proliferation within the dentate gyrus.

4.5 Introduction

The hippocampal formation is vital for learning and memory processes and thus for proper cognitive function. Loss of not only hippocampal neurons, but also of glia, as a result of injury or disease impairs function leading to cognitive deficits. Specifically, progressive loss of hippocampal oligodendrocytes in multiple sclerosis has been reported to underlie some of the cognitive impairments observed in patients (1). Cell replacement strategies to restore neurons but also oligodendrocytes therefore represent a novel therapeutic approach that, however, depends upon a comprehensive understanding of how new cells are born in the adult brain.

The hippocampus is one of the regions that boasts a robust neurogenic and gliogenic niche in the adult brain - the subgranular zone (SGZ) of the dentate gyrus. The neural progenitor cells (NPCs) contained therein have been shown to be multipotential *in vitro* and have also demonstrated fate plasticity *in vivo*. Recently, Jessberger *et al.* (2) have succeeded in switching the *in vivo* fate of adult hippocampal neural progenitor cells (NPCs) from granule neurons to oligodendrocytes by viral overexpression of the transcription factor Ascl1. In addtion to Ascl1, previous work in our laboratory has also implicated connexin-mediated communication in the direction of NPCs towards specific glial lineages. We have shown *in vitro* that connexin 29 (Cx29), which is expressed in oligodendrocyte progenitor cells (OPCs) derived from multipotential hippocampal NPCs (3), plays a role in directing NPC progeny towards an oligodendrocytic lineage and away from an astrocytic lineage (4, manuscript submitted). Furthermore, we have shown *in vivo* and *in vitro* the specification of a subset of $NG2^+$ OPCs in the hippocampus is impaired in Cx32 null-mutant mice (5).

Connexins are the building blocks of connexons or "hemichannels" which are the functional units of connexin-mediated signalling. A hemichannel allows the passage of ions and metabolites ($\leq$ 1kDa) from the cytosol to the extracellular environment and vice-versa. Two adjacent cells can each contribute a connexon to form an intercellular channel in traditional gap junctional intercellular coupling.

Channel-independent modes of Cx-mediated signalling include protein-protein interactions through the C-terminus and the formation of adhesion domains allowing cellular migration (6). Connexins are a protein superfamily comprising 20 members in the mouse (7). In the central nervous system, fourteen Cxs are expressed (Cx26, Cx29, Cx30, Cx30.2, Cx31.1, Cx31.9, Cx32, Cx36, Cx37, Cx40, Cx45, and Cx47)(8-11). It is generally agreed oligodendrocytes express three connexins: Cx29, Cx32 and Cx47 (12). Within the dentate gyrus, it has been shown adult $NG2^+$ OPCs express Cx32 (5). However, despite *in vitro* evidence, it has not been explored whether hippocampal OPCs express other Cxs. Here, we examined the expression of Cx29, Cx32, and Cx47 in the oligodendrocyte cell lineage. Then, using a genetic dissection approach and taking advantage of single, double, and triple null-mutant mice, we investigated the role of these connexins in regulating hippocampal progenitor cell fate *in vivo*.

4.6 Methods

4.6.1 Mice

Breeding pairs of Cx29 (13) and Cx47 (14) null-mutant mice were obtained from Dr. David Paul (Harvard Medical School). The Cx32 null-mutant line (15) was originally generated by Dr Klaus Willecke (University of Bonn) and backbred in our laboratory onto a C57Bl/6 lineage. Double and triple null-mutant mice were generated through heterozygote matings. Animals were between generations N4-N6 and were compared to congenic littermate-derived control mice in all experiments. Due to the postnatal lethal phenotype of $Cx32^{-/Y}Cx47^{-/-}$ (14) and $Cx29^{-/-}Cx32^{-/Y}Cx47^{-/-}$ mice, all experiments were carried out on mice aged between postnatal day 27 and 34 (P27-34). All animals were provided with food and water *ad libitum* and kept under a 12h light-dark cycle. All animal protocols were approved by the University of Ottawa Animal Care Committee according to guidelines set forth by the Canadian Council on Animal Care.

4.6.2 5-bromo-2'-deoxyuridine (BrdU) treatment

Mice were injected five times over 3 days with 5-bromo-2'-deoxyuridine (50 mg/kg, Roche Diagnostics, Laval, QC) and sacrificed 24 h following the last injection.

4.6.3 BrdU Immunostaining

Chemical reagents were obtained from Sigma-Aldrich (St.-Louis, MO, USA) unless otherwise stated. Animals were injected with a lethal dose of Euthansol (Schering-Plough Canada Inc., Pointe-Claire, QC, Canada) and transcardially perfused with 10 mM PBS (PBS: 0.154 M NaCl, 0.0028 M NaH_2PO_4, 0.0072 M Na_2HPO_4, pH 7.2) followed by 3.7% formaldehyde solution in PBS. Brains were post-fixed overnight, cryoprotected in 20% sucrose in 10 mM PB + 0.001% NaN_3, and 10 µm-thick sections were serially cut on a Leica CM1900 cryostat (Leica Microsystems Inc.). Sections were stored at -20°C until further use. Slides were thawed at room temperature (RT) for 10 min in PBS. For BrdU staining, sections were incubated in 2 N HCl at 37°C for 1 h. Sections were then washed 2 x 5 min in 0.1 M Borate Buffer pH 8.5 and 3 x 5 min in PBS, both at RT, prior to primary antibody incubation overnight at 4°C in a humid chamber. The following day (all steps performed at RT), sections were rinsed 3 x 5 min in PBS and incubated 1 h in a humid chamber with secondary antibody. Sections were again washed 3 x 5 min in PBS and mounted using antifade medium. The same procedure was followed for double labelling of BrdU with cell-type specific markers found in Table 4.1. All antibodies were diluted in Ab buffer (0.3% Triton X-100, 3% BSA in PBS, pH 7.2). Images were acquired using a Leica DMXRA2 epifluorescence microscope and analyzed using Openlab software (version 5.0.2, Improvision, Lexington, MA, USA).

4.6.4 Connexin imunostaining

Tissue sections were treated with ice-cold methanol for 3 min followed by a 5 min PBS wash at RT. Permeabilization was carried out using 0.2% Triton X-100 in PBS for 20 min at RT followed by a PBS wash. Blocking was done in 5% normal

Table 4.1 Primary and secondary antibodies used for immunostaining

Antibody	Type	Species	Source	Dilution Immuno
Cx29	Polyclonal	Rabbit	Dr.David Paul	1:20
Cx32	Monoclonal	Mouse	Zymed (13-8200)	1:250
Cx47	Polyclonal	Rabbit	Dr. David Paul	1:1000
BrdU	Monoclonal	Mouse	Roche	6 μg/mL
BrdU FITC-conjugated	Monoclonal	Rat	BD	1:50
β-galactosidase	Monoclonal	Mouse	Promega	1:20
β-galactosidase	Polyclonal	Rabbit	Chemicon	1:1500
GFAP	Polyclonal	Rabbit	Sigma	1:400
Nestin	Monoclonal	Mouse	Chemicon	1:50
Nestin	Polyclonal	Rabbit	Covance	1:500
NG2	Polyclonal	Rabbit	Chemicon	1:200
NG2	Polyclonal	Guinea Pig	Dr. William Stallcup	1:200
PDGFαR	Monoclonal	Mouse	Spring Bioscience	undiluted
PDGFαR	Monoclonal	Rat	BD Pharmingen	1:300
RIP	Monoclonal	Mouse	Chemicon	1:1000
Guinea Pig IgG	Cy3-conjugated	Donkey	Jackson	1:1000
Mouse IgG	Cy3-conjugated	Donkey	Jackson	1:800
Mouse IgG	FITC-conjugated	Donkey	Jackson	1:100
Rabbit IgG	Alexa488-conjugated	Goat	Invitrogen	1:400
Rabbit IgG	AMCA-conjugated	Donkey	Jackson	1:100
Rabbit IgG	Cy3-conjugated	Donkey	Jackson	1:600
Rat IgG	FITC-conjugated	Donkey	Jackson	1:80
Rat IgG	Cy3-conjugated	Donkey	Jackson	1:800

donkey serum in PBS for 10 min at RT followed by a PBS wash prior to primary antibody incubation (diluted in Ab buffer) for 1 h at RT in a humid chamber. Following 3 x 5 min washes in PBS, secondary antibody incubation was performed in the same fashion. Slides were again washed 3 x 5min in PBS and mounted in antifade medium. Hoechst 33258 (1 μg/mL) was included in the 2nd PBS wash following secondary antibody incubation as a nuclear counterstain. Imaging was performed using a Zeiss LSM 510 Meta (Carl Zeiss Canada Ltd., Toronto, ON) followed by processing using Zeiss AxioVision software (version 4.7.2) and Adobe Photoshop (version 11.0.1, Adobe Systems Inc. USA). A Gaussian blur with a radius of 0.4 pixels was applied to all images.

4.6.5 In vivo cell proliferation and antigenic analysis

A minimum of 5 animals per genotype were assessed per condition. Using OpenLab software, an area of interest was established that encompassed the dorsal dentate gyrus in each hemisphere (the first two inner cell layers of the superior and inferior blades of the granule cell layer as well as the polymorphic layer) per animal. Immunolabelling was quantified bilaterally over two adjacent 10 μm sections to yield four measurements per animal. Counts performed in each dentate gyrus were expressed as number of cells per 0.1 mm^2. All sections analyzed were between Bregma -1.60 mm and -2.10 mm. The total number of $BrdU^+$ cells and the number of $BrdU^+$ cells expressing specific antigenic lineage markers were determined by investigators blinded to the genotypes of the animals.

4.6.6 Immunoreactivity quantification

Immunoreactivity for RIP, a marker of post-mitotic oligodendrocytes, was quantified and expressed as the percentage of the area of interest exhibiting immunoreactive signal above background using Image J software (version 1.41, National Institute of Health, USA). As above, to ensure accuracy, immunoreactivity was quantified bilaterally in two adjacent sections and these four measurements averaged to yield one measurement per animal.

4.6.7 Statistical analysis

All data are presented as mean ± standard error of the mean (S.E.M.). Data were analysed using one-way analysis of variance (ANOVA) followed by a *post-hoc* Tukey test (GraphPad InStat version 3.0b, LaJolla, CA).

4.7 Results

4.7.1 OPCs express Cx32 and Cx29 but not Cx47

Our previous studies indicate Cx29 and Cx32 but not Cx47 are dynamically expressed by OPCs *in vitro* (3). Here, we sought to expand these results *in vivo* using immunostaining and confocal microscopy to assess the cell-type specific expression of Cx32, Cx29, and Cx47 in the SGZ and in the polymorphic layer (PO) of the dentate gyrus of the hippocampus in mice aged P30 using the cell-type specific markers highlighted in Figure 4.1a.

Cx32 immunoreactivity generally appeared uniform and was detected both intracellularly and at the plasma membrane of the soma and processes of cells. At higher magnification, $Cx32^+$ puncta, characteristic of connexin labelling, were observed, notably along cell processes (Figure 4.1b,c, yellow arrows). Protein was clearly expressed by RIP^+ oligodendrocytes as expected (16-18) but also in RIP-negative cells with a stellate morphology reminiscent of OPCs. To further identify OPC populations expressing Cx32 in the hippocampus, we performed dual immunofluorescence for Cx32 and either PDGFαR or NG2, two markers of early OPCs (Figure 4.1b,c). Surprisingly, Cx32 immunolabelling was restricted to the $NG2^+$ population and was not detected in $PDGF\alpha R^+$ OPCs (Figure 4.1b, arrowheads). Co-expression was most prominent in the processes of these cells (Figure 4.1c, arrows). Cx32 was not detected in $nestin^+$ NPCs, however proximity of $Cx32^+$ processes to $nestin^+$ cells was frequently observed (Figure 4.1d, asterisks).

Like Cx32, Cx29 immunoreactivity was detected on the cell soma and on both proximal and distal cellular processes (Figure 4.2a,c,e,g). Immunolabelling was often

Figure 4.1 Cx32 is expressed by NG2$^+$ oligodendrocyte progenitor cells of the dentate gyrus. A) Schematic diagram of postnatal hippocampal generation of oligodendrocytes from nestin$^+$/GFAP$^+$ neural progenitor cells and relevant cell-type specific markers used to identify oligodendrocytes and their progenitor cells (OPCs) in this study. Orthogonal representations of confocal images for Cx32 staining and B) the OPC marker PDGFαR, C) the OPC marker NG2, and D) the neural progenitor cell marker nestin. No Cx32 immunoreactivity is seen in PDGFαR$^+$ cells (B, arrowhead) although immunoreactivity along other cell processes is observed (B, C, yellow arrows). Double labelling of Cx32 and NG2$^+$ cell fibers can be observed (C, arrows) while Cx32$^+$ processes are found in proximity to nestin$^+$ cells (D, asterisks). Scale bars - 10 μm. sg - granule cell layer, SGZ - subgranular zone.

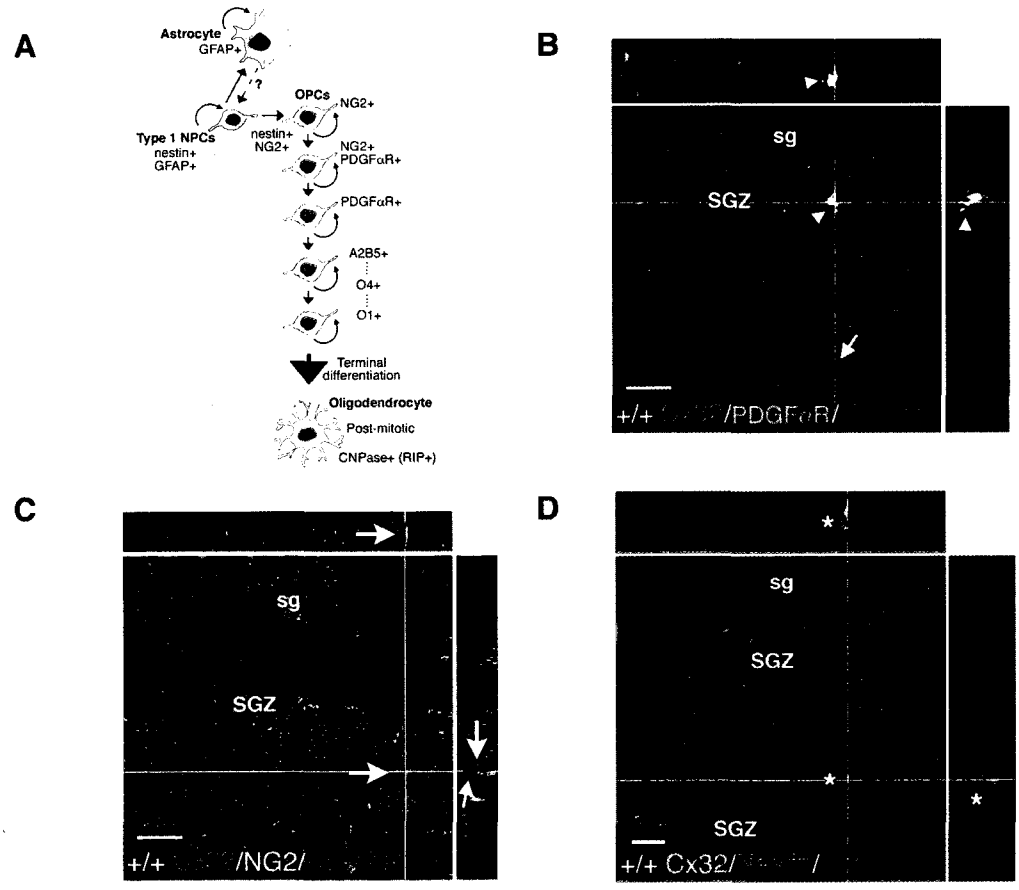
A
Astrocyte
GFAP+
?
OPCs
NG2+
Type 1 NPCs
nestin+
GFAP+
nestin+
NG2+
NG2+
PDGFαR+
PDGFαR+
A2B5+
O4+
O1+
Terminal
differentiation
Oligodendrocyte
Post-mitotic
CNPase+ (RIP+)
B
sg
SGZ
+/+ /PDGFαR/
C
sg
SGZ
+/+ /NG2/
D
sg
SGZ
SGZ
+/+ Cx32/

Figure 4.1

Figure 4.2 Cx29 is expressed by cells of the oligodendrocyte lineage within the dentate gyrus. Orthogonal representations of confocal images of immunostaining for Cx29 or the β-galactosidase reporter protein found in $Cx29^{-/-}$ mice and A, B) the oligodendrocyte marker RIP, C, D) the OPC marker PDGFαR, E, F) the OPC marker NG2, and G,H) the neural progenitor marker nestin, demonstrating expression of Cx29 (and Cx29 promoter activity) in oligodendrocytes and OPCs. Note the close proximity of $Cx29^{+}$ processes and $\beta\text{-gal}^{+}$ cells to nestin^{+} Type 1 neural progenitor cells. Arrows indicate double-positive cells while arrowheads denote single-positive cells. Asterisks highlight proximity between the examined cell types. Scale bars - 10 μm. sg - granule cell layer, SGZ - subgranular zone, po - polymorphic layer.

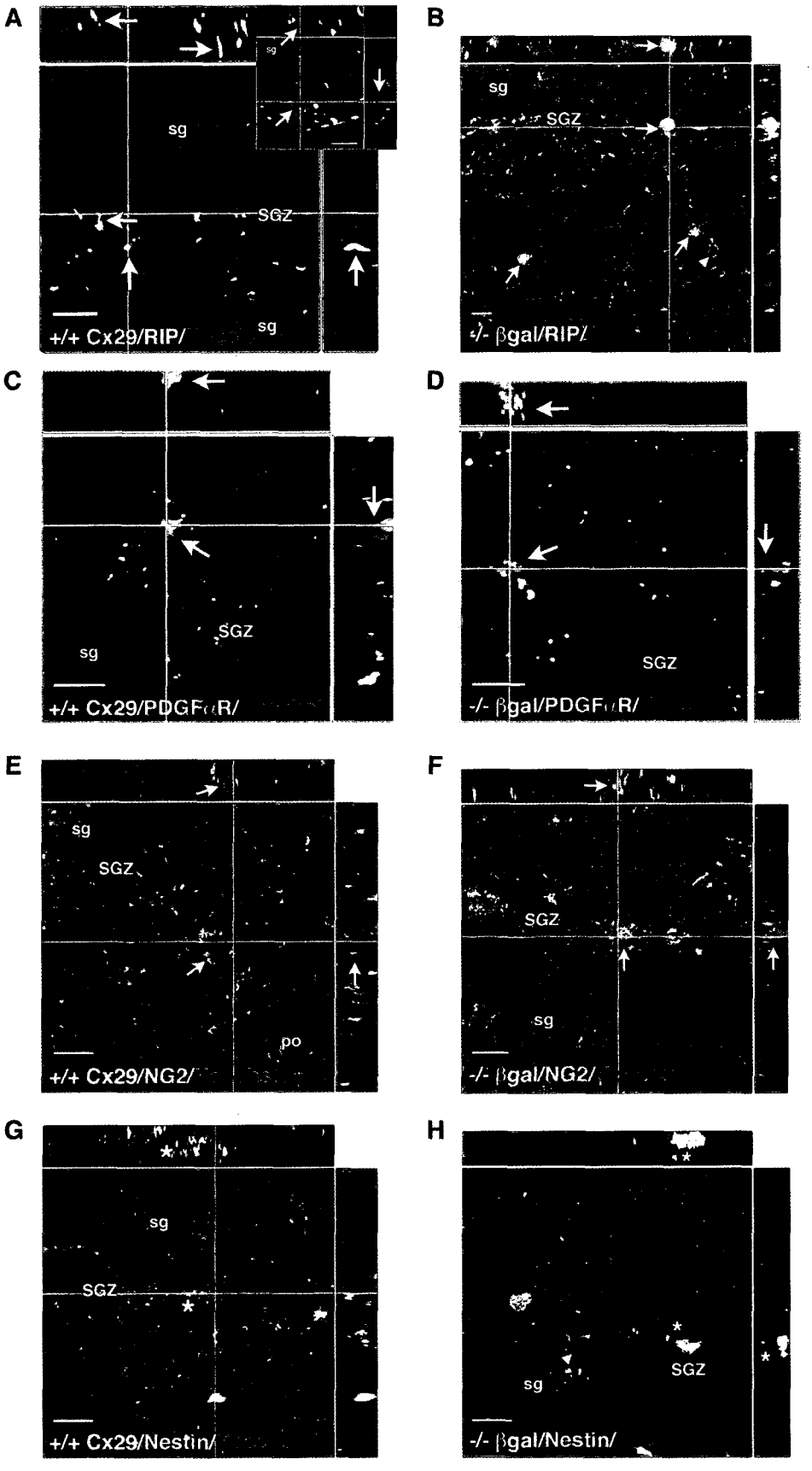
A
sg
sg
SGZ
sg
+/+ Cx29/RIP/
B
sg
SGZ
-/- βgal/RIP/
C
SGZ
sg
+/+ Cx29/PDGFαR/
D
SGZ
-/- βgal/PDGFαR/
E
sg
SGZ
po
+/+ Cx29/NG2/
F
SGZ
sg
-/- βgal/NG2/
G
sg
SGZ
+/+ Cx29/Nestin/
H
SGZ
sg
-/- βgal/Nestin/

Figure 4.2

punctate at the cell soma (Figure 4.2a, inset, arrows) but appeared more uniform along processes (compare Figure 4.2a with the inset). The morphology of $Cx29^+$ cells resembled that of cells immunoreactive for oligodendrocyte markers and double labelling of RIP^+ oligodendrocytes for Cx29 was clearly detected (Figure 4.2a, arrows). This observation was confirmed using Cx29 null-mutant mice (Figure 4.2b, arrows) wherein β-galactosidase (β-gal) engineered with a nuclear localization signal is expressed in place of Cx29 (13). Not all RIP^+ oligodendrocytes expressed Cx29 in wild-type animals (Figure 4.2a, green fibers) or β-gal in null-mutant animals (Figure 4.2b, arrowhead) suggesting Cx29 is expressed by only a subset of post-mitotic oligodendrocytes. In null-mutant animals, the $RIP^-/\beta\text{-}gal^+$ cells often exhibited less intense β-gal immunoreactivity than the double-labelled RIP^+ cells. Furthermore, these cells often possessed oblong nuclei as opposed to the small, condensed nuclei of RIP^+ oligodendrocytes (data not shown). Antigenic lineage assessment identified these cells as OPCs immunoreactive for either PDGFαR (Figure 4.2c, d) or NG2 (Figure 4.2e, f) but not NPCs immunoreactive for nestin (Figure 4.2g, h). As with $Cx32^+$ cells, $Cx29^+$ processes were consistently found in very close proximity to $nestin^+$ cells and/or $nestin^+$ processes (Figure 4.2g, asterisks), as were $\beta\text{-}gal^+$ cells (Figure 4.2h, asterisks).

By contrast, Cx47 immunoreactivity displayed very large puncta surrounding the soma and along proximal processes of RIP^+ oligodendrocytes of the SGZ and PO (Figure 4.3a, arrows) consistent with the immunostaining pattern of gap junction plaques (14). We did not observe Cx47 expression in progenitor cells of the oligodendrocyte lineage (Figure 4.3b-d, arrowheads), however, many $Cx47^+$ cells were found in extremely close apposition to $nestin^+$ or $NG2^+$ cells (Figure 4.3 c,d, asterisks). Furthermore, $Cx47^+$ cells, when in proximity to $NG2^+$ cells, were often found grouped within clusters of $NG2^+$ cells (data not shown). This pattern suggested to us expression following terminal differentiation within foci of OPCs actively undergoing oligodendrogenesis.

Figure 4.3 Cx47 is only expressed by oligodendrocytes of the dentate gyrus. Orthogonal representation of confocal imaging of immunostaining for Cx47 and A) the oligodendrocyte marker RIP, B) the OPC marker PDGFαR, C) the OPC marker NG2, and D) the neural progenitor marker nestin. RIP^+ oligodendrocytes express Cx47 (A, arrows) while OPCs and Type 1 neural progenitor cells do not (B-D, arrowheads). However, $Cx47^+$ cells and processes are observed in proximity to all these cells types, especially $NG2^+$ and $nestin^+$ cells (C and D, asterisks). Scale bars - 10 μm. sg - granule cell layer, SGZ - subgranular zone, po - polymorphic layer.

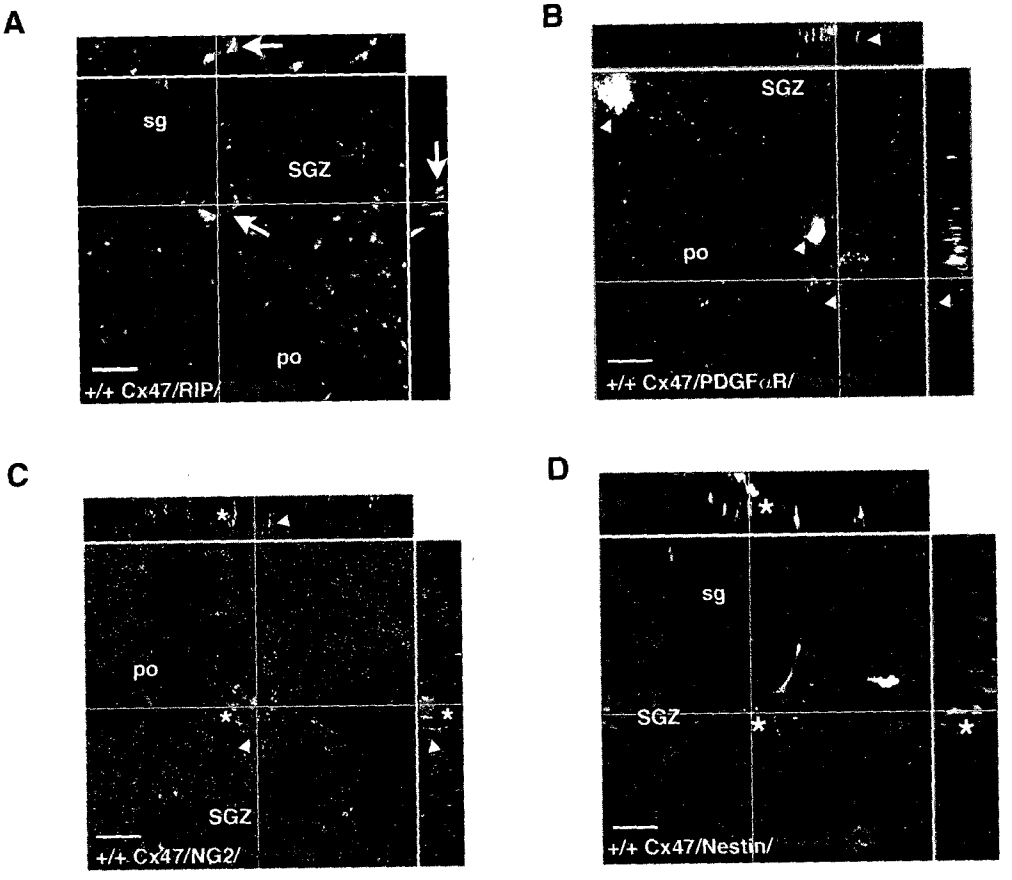
A
sg
SGZ
po
+/+ Cx47/RIP/
B
SGZ
po
+/+ Cx47/PDGFαR/
C
po
SGZ
+/+ Cx47/NG2/
D
sg
SGZ
+/+ Cx47/Nestin/

Figure 4.3

4.7.2 Loss of Cx32, Cx29 and Cx47 differentially affects progenitor cell proliferation

We used a null-mutant loss-of-function approach to assess the impact of Cx29 and Cx32 expression on OPC phenotype in the postnatal hippocampus. In agreement with unpublished data from the Paul laboratory (Dr. D.L. Paul personal communication), we observed Cx29$^{-/-}$Cx32$^{-/Y}$Cx47$^{-/-}$ triple null-mutant mice were phenotypically similar to Cx32$^{-/Y}$Cx47$^{-/-}$ double null-mutants and showed no overt increase in severity or in premature onset of the symptoms described by Menichella *et al.* (14) for Cx32$^{-/Y}$Cx47$^{-/-}$ null-mice (e.g., development of a coarse action tremor by the third postnatal week, followed by tonic seizures and death generally within six weeks following birth). As such, it is unlikely the loss of Cx29 affects survival of oligodendrocytes in the major fibre tracts, above and beyond the deficit conferred by the concomitant loss of Cx32 and Cx47.

Using BrdU to label proliferating cells, we found a significant increase in the number of BrdU$^+$ cells in the dentate gyrus of Cx29$^{-/-}$ single null-mutant mice compared to congenic wild-type mice (Figure 4.4, *$p<0.05$, ANOVA *post-hoc* Tukey). No significant changes in the number of BrdU$^+$ cells were seen in the other genotypes (Cx32$^{-/Y}$, Cx29$^{-/-}$Cx32$^{-/Y}$, Cx32$^{-/Y}$Cx47$^{-/-}$, nor Cx29$^{-/-}$Cx32$^{-/Y}$Cx47$^{-/-}$) compared to wild-type (Figure 4.4). To determine the identity of the proliferating populations we performed antigenic lineage analysis of the BrdU$^+$ cells for markers of the oligodendrocyte lineage (Figure 4.5a). A significant increase in the number of actively proliferating NG2$^+$ cells was apparent in Cx32$^{-/Y}$, Cx29$^{-/-}$, and Cx29$^{-/-}$Cx32$^{-/Y}$Cx47$^{-/-}$ mice compared to wild-type controls (Figure 4.5b). Interestingly, we also detected an increase in the number of proliferating astrocytes (BrdU$^+$/Nestin$^-$/GFAP$^+$) in Cx29$^{-/-}$ null-mutant mice consistent with our previous *in vitro* assessments (4). This phenotype was specific given no change was observed in the percentage of actively proliferating Type 1 neural progenitors (BrdU$^+$/Nestin$^+$/GFAP$^+$), Type 2 neural progenitors (BrdU$^+$/Nestin$^+$/GFAP$^-$), PDGFαR$^+$ OPCs, or BrdU$^+$/RIP$^+$ newborn oligodendrocytes, in any of the genotypes tested (Figure 4.5b). In contrast to our *in vitro* data, we did not observe increased astrogenesis at the expense of oligodendrogenesis in the absence of Cx29.

Figure 4.4 Cx29 $^{-/-}$ mice show increased BrdU^{+} proliferating cells within the subgranular zone of the dentate gyrus. Animals received 50 mg/kg BrdU twice daily (4-5 h apart) for two consecutive days (postnatal days 27 and 28), once on postnatal day 29 followed by sacrifice on postnatal day 30, 24 h after the last dose of BrdU. Representative immunostaining for BrdU within the dentate gyrus of the hippocampal formation of A) +/+, B) Cx32$^{-/Y}$, C) Cx29$^{-/-}$, D) Cx29$^{-/-}$Cx32$^{-/Y}$, E) Cx29 $^{-/-}$Cx32$^{-/Y}$Cx47$^{-/-}$, and F) Cx32$^{-/Y}$Cx47$^{-/-}$ animals are shown. G) Quantification of BrdU^{+} cells per 0.1mm^{2} of the dentate gyrus for the indicated genotypes where N represents the number of animals analyzed per group. Scale bar - 50 μm. * $p<0.05$, ANOVA and *post-hoc* Tukey.

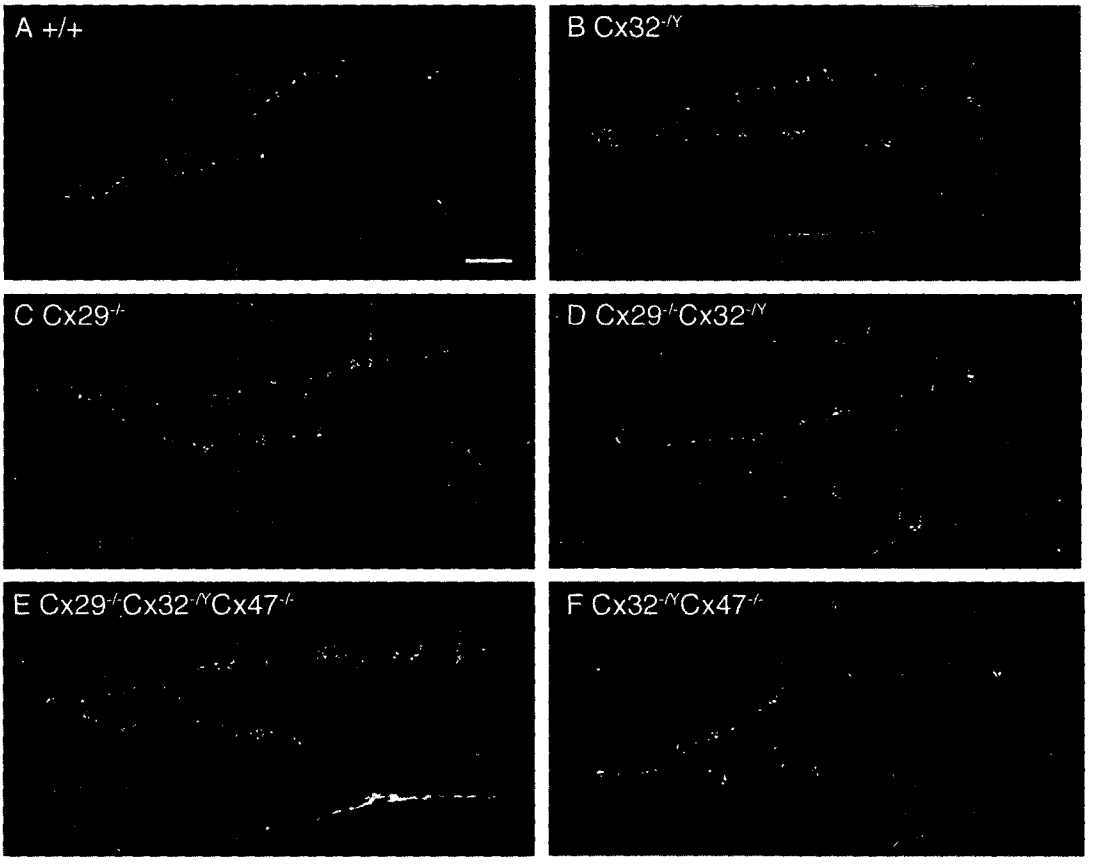
A +/+
B Cx32-/Y
C Cx29-/-
D Cx29-/-Cx32-/Y
E Cx29-/-Cx32-/YCx47-/-
F Cx32-/YCx47-/-

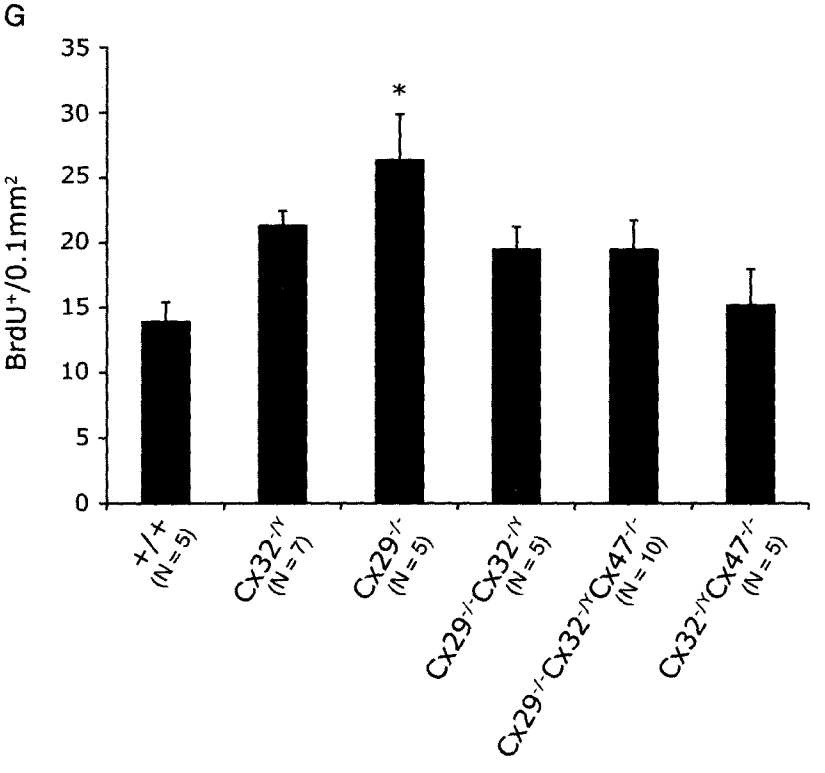
G
BrdU+/0.1mm2
35
30
25
20
15
10
5
0
*
+/+ (N=5)
Cx32-/Y (N=7)
Cx29-/- (N=5)
Cx29-/-Cx32-/Y (N=5)
Cx29-/-Cx32-/YCx47-/- (N=10)
Cx32-/YCx47-/- (N=5)

Figure 4.4

Figure 4.5 Increased proliferation of NG2$^+$ oligodendrocyte progenitor cells and/or GFAP$^+$ cells account for the majority of BrdU$^+$ cell numbers in Cx32$^{-/Y}$, Cx29$^{-/-}$, and Cx29$^{-/-}$ Cx32$^{-/Y}$ Cx47$^{-/-}$ null-mutant mice. A) Diagram of postnatal hippocampal gliogenesis arising from Type 1 nestin$^+$/GFAP$^+$ neural progenitor cells. B) Animals received 50 mg/kg BrdU twice daily (4-5 h apart) for two consecutive days and once on the third day followed by sacrifice on postnatal day 30, 24 h after the last dose. Immunostaining for BrdU and the indicated cell-type specific lineage markers was carried out on serial sections from the number of animals indicated. Shown is the quantification of the lineage analysis performed on BrdU$^+$ cells of all indicated genotypes. Note the increase in the BrdU$^+$/NG2$^+$ fraction of proliferating cells in Cx32$^{-/Y}$, Cx29$^{-/-}$, and Cx29$^{-/-}$Cx32 $^{-/Y}$Cx47$^{-/-}$ mice. There is also a significant increase in the number of BrdU$^+$/GFAP$^+$ astrocytes in Cx29$^{-/-}$ mice. * $p<0.05$, ** $p<0.01$, *** $p<0.001$, ANOVA *post-hoc* Tukey.

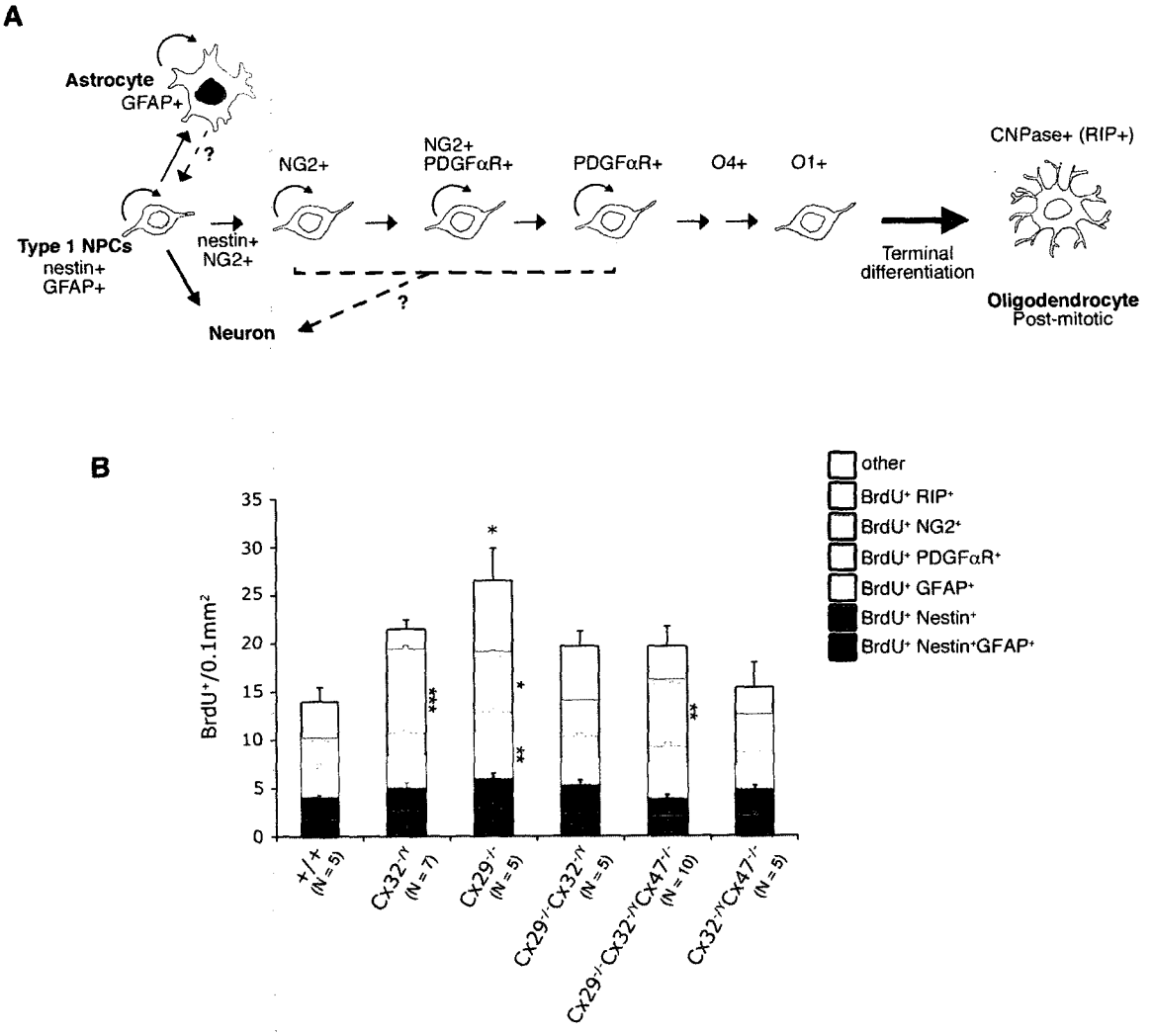
A
Astrocyte
GFAP+
?
Type 1 NPCs
nestin+
GFAP+
nestin+
NG2+
NG2+
NG2+
PDGFαR+
PDGFαR+
O4+
O1+
CNPase+ (RIP+)
Terminal
differentiation
Oligodendrocyte
Post-mitotic
?
Neuron
B
other
BrdU+ RIP+
BrdU+ NG2+
BrdU+ PDGFαR+
BrdU+ GFAP+
BrdU+ Nestin+
BrdU+ Nestin+GFAP+
BrdU+/0.1mm²
35
30
25
20
15
10
5
0
*
***
**
*
**
+/+ (N=5)
Cx32-/- (N=7)
Cx29-/- (N=5)
Cx29-/-Cx32-/- (N=5)
Cx29-/-Cx32-/-Cx47-/- (N=10)
Cx32-/-Cx47-/- (N=5)

Figure 4.5

Figure 4.6 RIP immunoreactivity is unaltered in all genotypes. A) Diagram of the region used to quantify RIP immunoreactivity within the dentate gyrus B) Representative immunostaining for RIP within this region. C) Quantification of RIP immunoreactivity across +/+, Cx32 $^{-/Y}$, Cx29 $^{-/-}$, Cx29 $^{-/-}$ Cx32 $^{-/Y}$, Cx29 $^{-/-}$ Cx32 $^{-/Y}$ Cx47 $^{-/-}$, and Cx32 $^{-/Y}$ Cx47 $^{-/-}$ mice where N is the number of animals analyzed per genotype. Scale bar - 50 μm. sg - granule cell layer, SGZ - subgranular zone, po - polymorphic layer.

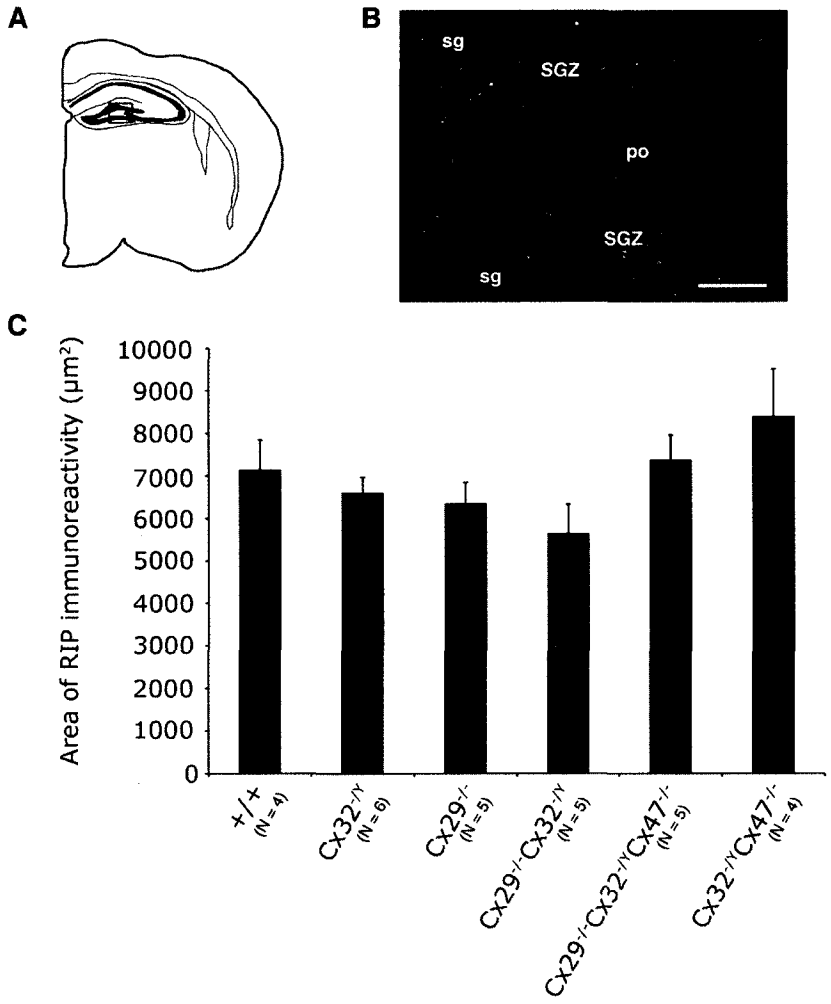
A
B
sg
SGZ
po
SGZ
sg
C
Area of RIP immunoreactivity (µm²)
10000
9000
8000
7000
6000
5000
4000
3000
2000
1000
0
+/+ (N=4)
Cx32-/- (N=6)
Cx29-/- (N=5)
Cx29-/-Cx32-/- (N=5)
Cx29-/-Cx32-/-Cx47-/- (N=5)
Cx32-/-Cx47-/- (N=4)

Figure 4.6

Furthermore, despite the increase in the $BrdU^+/NG2^+$ progenitor pool, we did not observe an increase in total oligodendrocyte number based on quantification of RIP immunoreactivity within the dentate gyrus (Figure 4.6).

4.8 Discussion

Here we extend our *in vitro* observations to *in vivo* studies whereby Cx29 and Cx32 are expressed not only by oligodendrocytes but also by OPCs in the P30 mouse dentate gyrus. We further show these connexins are likely expressed by discrete populations of OPCs given detection of Cx29 in both $NG2^+$ and $PDGF\alpha R^+$ OPCs but of Cx32 only in $NG2^+$ OPCs. We find Cx47 is restricted to oligodendrocytes and is not detected earlier in the OPC lineage. Using a genetic loss of function approach, we show Cx29 null-mutation results in increased proliferation of $NG2^+$ cells and astrocytes, whereas loss of Cx32 impacts only upon $NG2^+$ cell proliferation. When placed in context with our previous studies, this finding lends further support to the idea Cxs intrinsically regulate OPC potential within the dentate gyrus.

We have previously observed Cx32 immunoreactivity in $NG2^+$ cells of the adult dentate gyrus and shown loss of Cx32 impairs OPC specification in the uninjured adult hippocampus *in vivo*. In this case, a subset of hyperproliferating $NG2^+$ OPCs fails to progress towards an oligodendrocyte lineage and is deleted by an apoptotic-like mechanism (5). Here, we confirm Cx32 is expressed by $NG2^+$ cells at an earlier developmental time, P30. Interestingly, we did not detect Cx32 in $PDGF\alpha R^+$ OPCs as previously reported. This may be because Cx32 is only expressed in the processes of $PDGF\alpha R^+$ OPCs where immunoreactivities fall below the level of detection of our current methodologies and not in the perinuclear region of PDGFαR+ OPCs, which shows stronger antigenicity. However, it may also indicate Cx32 is not expressed in this cell type at this particular developmental age.

For the first time *in vivo*, we have demonstrated the expression of Cx29 by both $NG2^+$ and $PDGF\alpha R^+$ OPCs. This expression was confirmed using the Cx29 null-mutant mouse, which expresses a β-galactosidase reporter gene under the control of the Cx29 promoter (13). An increase in the number of total proliferating

(BrdU$^+$) cells within the dentate gyrus of Cx29$^{-/-}$ mice was detected, which was restricted to the NG2$^+$ OPC and GFAP$^+$ astrocyte populations. However, Cx29 does not intrinsically regulate cell proliferation as when, in the absence of Cx29, hippocampal progenitor cells are removed from their niche and cultured *in vitro,* no significant change in proliferative or apoptotic indices is observed. Conversely, loss of Cx29 is sufficient to impair NPC oligodendrogenesis in neurosphere culture and, in addition, to redirect their OPC-like progeny towards an astrocytic lineage (4, manuscript submitted). Here, we show *in vivo,* that in Cx29 null-mutant mice, an increase in proliferating astrocytes accompanies the increase in NG2$^+$ OPCs.

Our data also provide evidence of genetic crosstalk between Cx29 and Cx32 that may compensate for the loss of one or the other gene. Given the localization of Cx29 to NG2$^+$ and PDGFαR$^+$ OPCs found in this study, and the expression of Cx32 by NG2$^+$ cells, we hypothesize these may represent two different progenitor populations. Ergo, Cx32 is expressed by NG2$^+$ cells (polydendrocytes, (19)) and Cx29 is expressed by NG2$^+$/PDGFαR$^+$ OPCs of the dentate gyrus. This possibility would not be unprecedented as NG2$^+$ cells show heterogeneity, especially within the hippocampal formation (20). We suggest the failure of one population to specify to an oligodendrocyte lineage in single null-mutant animals likely triggers the compensatory proliferation of the other subset to overcome this block and maintain hippocampal oligodendrocyte number. Our current data support this hypothesis as the hyper-proliferation of these specific progenitor cell populations is abrogated in the Cx29$^{-/-}$Cx32$^{-/Y}$ double-null mutant. Note however, it is also possible NG2$^+$ cells express both Cx29 and Cx32. Certainly, this and the above hypothesis will require further validation, notably through examination of the expression levels of either connexin in the null-mutant animals to confirm compensatory activation of either Cx29$^+$ cells in Cx32 null-mutant mice or of Cx32$^+$ cells in Cx29$^{-/-}$ mice.

Here, we also determined Cx47 expression is restricted to oligodendrocytes although Cx47$^+$ cells/processes are found near NG2$^+$ and nestin$^+$ progenitor cells. Interestingly, Cx29$^+$ and Cx32$^+$ cells were also found in close proximity to nestin$^+$ neural progenitor cells. This leads us to speculate about possible instructive roles for

oligodendrocytes and Cx proteins in progenitor cell proliferation and/or specification in addition to any cell intrinsic role they might also possess.

Taken together, these data provide the first evidence that both Cx32 and Cx29 play a regulatory role in directing OPC fate and that both connexins may compensate for the other's loss by promoting the expansion of different subsets of OPCs within the uninjured hippocampus.

4.9 References

1. Geurts, J.J., L. Bo, S.D. Roosendaal, T. Hazes, R. Daniels, F. Barkhof, M.P. Witter, I. Huitinga, and P. van der Valk. 2007. Extensive hippocampal demyelination in multiple sclerosis. *J Neuropathol Exp Neurol* 66:819-827.

2. Jessberger, S., N. Toni, G.D. Clemenson, Jr., J. Ray, and F.H. Gage. 2008. Directed differentiation of hippocampal stem/progenitor cells in the adult brain. *Nat Neurosci* 11:888-893.

3. Imbeault, S., L.G. Gauvin, H.D. Toeg, A. Pettit, C.D. Sorbara, L. Migahed, R. DesRoches, A.S. Menzies, K. Nishii, D.L. Paul, A.M. Simon, and S.A. Bennett. 2009. The extracellular matrix controls gap junction protein expression and function in postnatal hippocampal neural progenitor cells. *BMC Neurosci* 10:13.

4. Imbeault, S., and S. Bennett. 2009. Reduction of platelet-derived growth factor receptor alpha expressing cells in hippocampal-derived neural progenitor cell cultures derived from connexin29 null-mutant mice. Program No. 706.20. *Neuroscience Meeting Planner*

5. Melanson-Drapeau, L., S. Beyko, S. Dave, A.L. Hebb, D.J. Franks, C. Sellitto, D.L. Paul, and S.A. Bennett. 2003. Oligodendrocyte progenitor enrichment in the connexin32 null-mutant mouse. *J Neurosci* 23:1759-1768.

6. Elias, L.A., D.D. Wang, and A.R. Kriegstein. 2007. Gap junction adhesion is necessary for radial migration in the neocortex. *Nature* 448:901-907.

7. Sohl, G., and K. Willecke. 2003. An update on connexin genes and their nomenclature in mouse and man. *Cell Commun Adhes* 10:173-180.

8. Vandecasteele, M., J. Glowinski, and L. Venance. 2006. Connexin mRNA expression in single dopaminergic neurons of substantia nigra pars compacta. *Neurosci Res* 56:419-426.

9. Dere, E., Q. Zheng-Fischhofer, D. Viggiano, U.A. Gironi Carnevale, L.A. Ruocco, A. Zlomuzica, M. Schnichels, K. Willecke, J.P. Huston, and A.G. Sadile. 2008. Connexin31.1 deficiency in the mouse impairs object memory and modulates open-field exploration, acetylcholine esterase levels in the striatum, and cAMP response element-binding protein levels in the striatum and piriform cortex. *Neuroscience* 153:396-405.

10. Kreuzberg, M.M., J. Deuchars, E. Weiss, A. Schober, S. Sonntag, K. Wellershaus, A. Draguhn, and K. Willecke. 2008. Expression of connexin30.2 in interneurons of the central nervous system in the mouse. *Mol Cell Neurosci* 37:119-134.

11. Rouach, N., E. Avignone, W. Meme, A. Koulakoff, L. Venance, F. Blomstrand, and C. Giaume. 2002. Gap junctions and connexin expression in the normal and pathological central nervous system. *Biol Cell* 94:457-475.

12. Nagy, J.I., F.E. Dudek, and J.E. Rash. 2004. Update on connexins and gap junctions in neurons and glia in the mammalian nervous system. *Brain Res Brain Res Rev* 47:191-215.

13. Altevogt, B.M., and D.L. Paul. 2004. Four classes of intercellular channels between glial cells in the CNS. *J Neurosci* 24:4313-4323.

14. Menichella, D.M., D.A. Goodenough, E. Sirkowski, S.S. Scherer, and D.L. Paul. 2003. Connexins are critical for normal myelination in the CNS. *J Neurosci* 23:5963-5973.

15. Nelles, E., C. Butzler, D. Jung, A. Temme, H.D. Gabriel, U. Dahl, O. Traub, F. Stumpel, K. Jungermann, J. Zielasek, K.V. Toyka, R. Dermietzel, and K. Willecke. 1996. Defective propagation of signals generated by sympathetic nerve stimulation in the liver of connexin32-deficient mice. *Proc Natl Acad Sci U S A* 93:9565-9570.

16. Kleopa, K.A., J.L. Orthmann, A. Enriquez, D.L. Paul, and S.S. Scherer. 2004. Unique distributions of the gap junction proteins connexin29, connexin32, and connexin47 in oligodendrocytes. *Glia* 47:346-357.

17. Nagy, J.I., A.V. Ionescu, B.D. Lynn, and J.E. Rash. 2003. Connexin29 and connexin32 at oligodendrocyte and astrocyte gap junctions and in myelin of the mouse central nervous system. *J Comp Neurol* 464:356-370.

18. Altevogt, B.M., K.A. Kleopa, F.R. Postma, S.S. Scherer, and D.L. Paul. 2002. Connexin29 is uniquely distributed within myelinating glial cells of the central and peripheral nervous systems. *J Neurosci* 22:6458-6470.

19. Nishiyama, A. 2007. Polydendrocytes: NG2 cells with many roles in development and repair of the CNS. *Neuroscientist* 13:62-76.

20. Karram, K., S. Goebbels, M. Schwab, K. Jennissen, G. Seifert, C. Steinhauser, K.A. Nave, and J. Trotter. 2008. NG2-expressing cells in the nervous system revealed by the NG2-EYFP-knockin mouse. *Genesis* 46:743-757.

Chapter 5: General Discussion

5.1. General Summary

In this thesis, I have presented data demonstrating multiple Cxs are expressed by hippocampal OPCs and their progeny both *in vivo* (Chapter 4) and when removed from their niche and cultured *in vitro* (Chapters 2 and 3); that the repertoire of Cx expression becomes increasingly restricted as NPCs adopt a given lineage (Chapter 2); and that this expression does not simply correlate with specification but plays a role in mediating both the expansion of intermediate progenitor populations and their ability to respond to extrinsic differentiation cues (Chapters 3 and 4). Furthermore, I show Cx expression can be specifically modulated by components present in the ECM resulting in functional changes in Cx-mediated communication (Chapter 2). Finally, focusing on one specific Cx-family member, Cx29, I have localized this protein to OPCs *in vitro* and *in vivo* (Chapters 2, 3, 4) and have shown the loss of Cx29 is sufficient to redirect OPCs away from an oligodendrocyte lineage and towards an astrocytic lineage *in vitro* (Chapter 3). I have found progeny are blocked at the $NG2^+$ OPC stage and fail to transition towards the $PDGF\alpha R^+$ OPC stage. This intrinsic impairment results in lower numbers of $PDGF\alpha R^+$ OPCs, thereby reducing the number of oligodendrocytes obtained (Chapter 3). Furthermore, $NG2^+$ cells apparently adopt an astrocytic fate as a result of this block (Chapter 3). Taken together, this is the first demonstration Cx29, a Cx with as yet unknown function, participates in the regulation of OPC specification and more specifically the NPC-derived OPCs generated in hippocampal neurosphere cultures.

I have found that, *in vivo,* the intrinsic control of Cx29 on OPC fate can be compensated for by the increased proliferation of $NG2^+$ OPCs. I hypothesize this compensation is mediated by activation of a separate subset of $NG2^+$ cells that express Cx32 (Chapter 4). It is interesting to note, as observed *in vitro*, that $Cx29^{-/-}$ mice exhibit an increase in the number of activated (i.e., proliferating) astrocytes *in vivo* possibly indicative of increased specification of $NG2^+$ cells to an astrocytic

lineage although we will need to directly fate map these cells to validate this interpretation. My data further confirm previous reports from our laboratory that loss of Cx32 results in a significant increase in the number of proliferating $NG2^+$ OPCs in the hippocampus, which, I argue, likely represents reciprocal compensation of the Cx29-responsive population in Cx32 null-mutant mice. Finally, in support of both hypotheses, I show null-mutation of both Cx29 and Cx32 in the same animal abrogates this compensatory proliferative response (Chapter 4). It should be noted the results of this genetic dissection must be interpreted cautiously given I did not observe any significant reduction in oligodendrocyte number *in vivo* in any of the genotypes tested (Chapter 4) as was seen *in vitro* (Chapter 3). It is likely the intrinsic regulation of OPC fate by Cx29 and Cx32 is further modulated by other extrinsic signalling mechanisms that compensate for Cx loss in null-mutant mice *in vivo* but not *in vitro*. Together, the work presented in this thesis demonstrates Cxs, and more specifically, Cx29 and Cx32, and Cx-mediated communication help regulate neural progenitor cell proliferation and specification in the postnatal hippocampus where they likely contribute to the maintenance of proper progenitor and mature cell numbers.

5.2 Niche cues - instructive cells and extracellular matrix modulation

Although the underlying signalling mechanisms mediating these effects remain unclear, in Chapter 2, we observed changes in Cx expression following laminin engagement by hippocampal-derived NPCs that translated into a functional loss of hemichannel activity. Hemichannel activity has been shown to be important in stimulation of proliferation of retinal progenitor cells by the retinal pigment epithelium (1). Similarly, hemichannel activity in our cultures may help maintain the "stemness" of the hippocampal-derived NPCs when grown without laminin. Interestingly, data from Chapter 2 also shows Cx32 expression can be induced by laminin. This is likely through laminin-integrin signalling, an important pathway in the direction of OPCs towards a mature lineage (2). This demonstrates the interdependency of Cx signalling and niche cues whereby the niche and the ECM

components present within can modulate Cxs in order to alter the signalling properties conferred to cells by the Cx proteins. Further underscoring the role of niche cues *in vivo* is the proximity of Cx29, Cx32, and Cx47$^+$ cells to nestin$^+$ NPCs and in the case of Cx47$^+$ cells to NG2$^+$ OPCs as demonstrated in Chapter 4. This might indicate an instructive role for these Cx-expressing cells in fate determination of NPC progeny as they respond to competing gliogenic and neurogenic stimuli. Although we cannot confirm whether some of these cells were OPCs, we can conclude the Cx47$^+$ cells were oligodendrocytes. Perhaps oligodendrocytes provide additional feedback to NG2 cells within the hilus of the dentate gyrus in addition to the feedback provided by neurons (3-5). Thus, NG2 cells may serve to monitor the global health and number of oligodendrocytes above and beyond their role in monitoring neuronal activity and modulating the oligodendrocyte response to these neuronal inputs.

5.3 Roles of Cx29

The function of Cx29 in the CNS has, so far, only been hypothesized. Localized across from axonal Kv1.2 channels, it is thought Cx29 helps buffer K^+ ions but this hypothesis has never been concretely tested (6, 7). The localization of Cx29 to OPCs in this thesis is a novel finding. Loss of Cx29 in hippocampal-derived NPCs results in a profound reduction in the specification of NPC-like progenitors to oligodendrocytes *in vitro,* indicating a possible function of Cx29 in this process. Future work using heterologous and endogenous expression systems will address the specific way in which Cx29 affects OPC specification. It is possible Cx29 has more than one function, depending on the cell type in which it is expressed. Perhaps Cx29 indeed removes K^+ from the periaxonal space into oligodendrocytes. The simplest explanation is Cx29 acts as a hemichannel allowing the passage of K^+ ions from the periaxonal space into the cytosol. Alternatively, it may form intercellular channels with the Kv1.2 channels present on the axonal membrane although such heterologous coupling of a connexon with another channel-forming protein has, to our knowledge, never been reported. It is more likely Cx29 possess "typical"

hemichannel activity, and, like other channels, can uptake and release small molecules such as ATP. Indeed, ATP had been shown to promote specification of OPCs (8, 9) therefore loss of this cue would result in smaller numbers of oligodendrocytes being generated.

Work performed in Chapters 3 and 4 demonstrate a novel role for Cx29 in specification of oligodendrocytes. As loss of Cx29 results in reduced oligodendrocyte numbers in free-floating neurospheres or in the presence of laminin but does not translate to an *in vivo* loss of function, it is possible the cues associated with Cx29 are overridden by extrinsic niche cues not present in our culture systems. It is also quite telling the effect on astrocytes is maintained between our *in vitro* and *in vivo* studies, pointing to an additional intrinsic effect of Cx29 on OPC plasticity. The origins, progeny, and plasticity (multipotency) of OPCs are the subject of much scrutiny in the field. Recently, it has been demonstrated the loss of Olig2 in NG2 cells allows these cells to become astrocytes (10). Expression of Olig2 thus restricts OPCs to an oligodendroglial fate. Perhaps Cx29 is part of a signalling pathway with Olig2 (or maintains Olig2 transcription) and loss of Cx29 results in partial "recommitment" of a subset of NG2 cells to the astrocyte lineage. Studies investigating this possibility are underway.

It is also interesting loss of Cx29 results in reduced numbers of PDGFαR expressing OPCs *in vitro*. Based on this effect and co-localization of Cx29 puncta with PDGFαR puncta in free-floating neurospheres, we are currently examining whether Cx29 and PDGFαR may interact as part of a signalling pathway. It is tempting to speculate the interaction of Cx29 with PDGFαR at the plasma membrane stabilizes receptor protein expression and thus enables ligand interactions that signal further population expansion (proliferation) and progression to an oligodendrocyte lineage. This hypothesis is also currently under investigation.

5.4 Interplay between Cx29 and Cx32 in OPCs

Because Cx29 is found in our *in vitro* system, while Cx32 seems to be expressed only upon exposure of NPCs to laminin, this suggests these Cxs are

differentially regulated and therefore may possess unique roles in the maintenance and specification of OPCs. Furthermore, *in vivo* localization implies Cx29 and Cx32 might not be expressed in the same subsets of OPCs as we were not able to find Cx32 expression in PDGFαR$^+$ cells. It is possible discrete Cx32 puncta may be found in PDGFαR$^+$ OPC processes, which we were unable to detect, however, the idea Cx29 and Cx32 are found in different subpopulations of OPCs is conceptually attractive. Heterogeneity of NG2 cells in the hippocampus has been reported - these cells possess different electrophysiological properties and heterogeneous growth factor responsiveness (11). Furthermore, a subset of hippocampal NG2$^+$ cells expresses glutamine synthetase (12) while another does not. It is not inconceivable these cells might show differential Cx expression.

There is an added layer of complexity to the interplay between "oligodendrocytic connexins" revealed by our genetic dissection approach. Loss of both connexins separately results in increased proliferation of NG2$^+$ cells while simultaneous loss of Cx29 and Cx32 in the double null-mutants reverses this phenotype. I hypothesize this reflects compensation by two different connexin-responsive NG2$^+$ cell populations. However, the combined loss of Cx29, Cx32, and Cx47 restores the increased proliferative NG2$^+$ cell phenotype not observed in Cx32$^{-/Y}$Cx47$^{-/-}$ double null-mutants. Certainly, Cx32 and Cx47 play a role in ensuring the survival of newly born oligodendrocytes that can be mutually compensated for in single but not double null-mutants (13, 14). Because the same demyelinating phenotype is observed in Cx29$^{-/-}$Cx32$^{-/Y}$Cx47$^{-/-}$ and Cx32$^{-/Y}$Cx47$^{-/-}$ null-mutant mice, we cannot argue the increased NG2$^+$ cell proliferation seen in the triple null-mutant is due to a higher demand for oligodendrocyte production as a result of the failure of mature cells to thrive. Without knowing the exact roles of Cx29 and Cx32 in OPCs it is harder to reconcile the proliferation defects seen in double and triple null-mutant mice. Further dissection of the 1) intrinsic, 2) extrinsic, 3) signalling, and, 4) instructive roles, of Cx29 and Cx32 using single-null mutants must be performed before data from the double and triple null-mutants can be concretely collated.

5.5 Conclusions

In summary, this thesis has shown the "oligodendrocytic" connexins play a bigger role than previously thought in maintenance of brain homeostasis, one that extends beyond their putative participation in K^+ homeostasis in the glial syncytium. The implication hemichannel activity in OPCs is modulated by connexin null-mutation rather points to a glial network formed of $Cx29^+$ and $Cx32^+$ OPCs and oligodendrocyte instructive cells that likely help regulate the proper number of progenitor and mature cell numbers in the postnatal brain (Figure 5.1). We thus conclude Cx29 and Cx32 likely restrict OPCs to the oligodendroglial lineage and that Cx29 helps to intrinsically regulate oligodendrocyte specification. It is also likely modulation of these connexins may be beneficial in modifying OPC proliferation and specification in the treatment of demyelinating disorders.

Figure 5.1. A glial connexin network regulates progenitor cell number and K+ homeostasis in the hippocampus. Schematic diagram of how oligodendrocytes, astrocytes and oligodendrocyte progenitor cells form a glial network which not only is responsible for buffering K+ following neuronal activity but is also responsible for monitoring and maintaining oligodendrocyte progenitor cells (OPC) cell number via hemichannel activity. Following neuronal activity, K+ is taken up by oligodendrocytes (OL) which transfers the K+ to astrocytes (A) via gap junctional intercellular communication mediated mainly by Cx47:Cx43 and Cx32:Cx30 channels. K+ then flows through the astrocytic network to be extruded into the blood stream or cerebral spinal fluid via astrocytic endfeet. Based on the repertoire of connexins expressed by OPCs, possible interactions between OPCs and astrocytes may exist. Hemichannel activity via Cx29 and Cx32 on the OPCs is also possible and may regulate, along with cues from the ECM and ECM components (shown in black) the proliferation of OPCs within the dentate gyrus of the hippocampus. BV - blood vessel, ECM - extracellular matrix.

Figure 5.1

5.6 References

1. Pearson, R.A., N. Dale, E. Llaudet, and P. Mobbs. 2005. ATP released via gap junction hemichannels from the pigment epithelium regulates neural retinal progenitor proliferation. *Neuron* 46:731-744.

2. ffrench-Constant, C., and H. Colognato. 2004. Integrins: versatile integrators of extracellular signals. *Trends Cell Biol* 14:678-686.

3. Bergles, D.E., J.D. Roberts, P. Somogyi, and C.E. Jahr. 2000. Glutamatergic synapses on oligodendrocyte precursor cells in the hippocampus. *Nature* 405:187-191.

4. Nishiyama, A., M. Komitova, R. Suzuki, and X. Zhu. 2009. Polydendrocytes (NG2 cells): multifunctional cells with lineage plasticity. *Nat Rev Neurosci* 10:9-22.

5. De Biase, L.M., A. Nishiyama, and D.E. Bergles. Excitability and Synaptic Communication within the Oligodendrocyte Lineage. *J Neurosci* 30:3600-3611.

6. Altevogt, B.M., K.A. Kleopa, F.R. Postma, S.S. Scherer, and D.L. Paul. 2002. Connexin29 is uniquely distributed within myelinating glial cells of the central and peripheral nervous systems. *J Neurosci* 22:6458-6470.

7. Rash, J.E. 2009. Molecular disruptions of the panglial syncytium block potassium siphoning and axonal saltatory conduction: pertinence to neuromyelitis optica and other demyelinating diseases of the central nervous system. *Neuroscience*

8. Agresti, C., M.E. Meomartini, S. Amadio, E. Ambrosini, B. Serafini, L. Franchini, C. Volonte, F. Aloisi, and S. Visentin. 2005. Metabotropic P2 receptor activation regulates oligodendrocyte progenitor migration and development. *Glia* 50:132-144.

9. Agresti, C., M.E. Meomartini, S. Amadio, E. Ambrosini, C. Volonte, F. Aloisi, and S. Visentin. 2005. ATP regulates oligodendrocyte progenitor migration, proliferation, and differentiation: involvement of metabotropic P2 receptors. *Brain Res Brain Res Rev* 48:157-165.

10. Zhu, X., Q.R. Lu, and A. Nishiyama. 2009. Olig2 regulates the oligodendrocyte-astrocyte fate choice of NG2 cells. Program no. 31.3. *Neuroscience Meeting Planner*

11. Mason, J.L., and J.E. Goldman. 2002. A2B5+ and O4+ Cycling progenitors in the adult forebrain white matter respond differentially to PDGF-AA, FGF-2, and IGF-1. *Mol Cell Neurosci* 20:30-42.

12. Karram, K., S. Goebbels, M. Schwab, K. Jennissen, G. Seifert, C. Steinhauser, K.A. Nave, and J. Trotter. 2008. NG2-expressing cells in the nervous system revealed by the NG2-EYFP-knockin mouse. *Genesis* 46:743-757.

13. Menichella, D.M., D.A. Goodenough, E. Sirkowski, S.S. Scherer, and D.L. Paul. 2003. Connexins are critical for normal myelination in the CNS. *J Neurosci* 23:5963-5973.

14. Odermatt, B., K. Wellershaus, A. Wallraff, G. Seifert, J. Degen, C. Euwens, B. Fuss, H. Bussow, K. Schilling, C. Steinhauser, and K. Willecke. 2003. Connexin 47 (Cx47)-deficient mice with enhanced green fluorescent protein reporter gene reveal predominant oligodendrocytic expression of Cx47 and display vacuolized myelin in the CNS. *J Neurosci* 23:4549-4559.

Appendix 1: Curriculum Vitae

Sophie Imbeault

Education

Present — **Ph.D. Candidate (Biochemistry)**
Department of Biochemistry, Microbiology and Immunology
University of Ottawa, Ottawa, ON, CA
Thesis: Connexin-mediated control of gliogenesis
Supervisor: Steffany A.L. Bennett

2002-2005 — **M.Sc. (Neuroscience)**
Department of Psychiatry
University of British Columbia, Vancouver, BC, CA
Thesis: Overexpression of NF-E2 related factor 2 via viral-mediated gene transfer in vivo
Supervisor: Timothy H. Murphy

1998-2002 — **B.Sc. (Honours Biochemistry)** *Summa Cum Laude*
University of Ottawa, Ottawa, ON, CA
Honours Thesis: Effect of ectopic expression of G-protein coupled receptor 4 on viability, proliferation and differentiation of PC12 cells – a role for sphingosylphosphocholine

Publications

Imbeault S, Gauvin LG and Bennett SAL. (2009) Connexin 29 regulates oligodendrogenesis in postnatal hippocampal culture. *submitted to the Journal of Neuroscience 02/2010.*

Imbeault S*, Gauvin LG*, Toeg HD, Pettit A, Sorbara CD, Migahed L, DesRoches R, Menzies AS, Nishii K, Paul DL, Simon AM and Bennett SAL. (2009) The extracellular matrix controls gap junction protein expression and function in postnatal hippocampal progenitor cells. *BMC Neuroscience.* **10**(1):13. ***Authors contributed equally to this work.**

Shih AY*, **Imbeault S***, Barakauskas V, Erb H, Lei J, Li P and Murphy TH. (2005) Induction of the Nrf2-driven antioxidant response confers neuroprotection during mitochondrial stress *in vivo. J Biol Chem.* **280**(24):22925-22936. ***Authors contributed equally to this work.**

Brewer C, Bonin F, Bullock P, Nault M-C, Morin J, **Imbeault S**, Shen TY, Franks DJ and Bennett SAL. (2002) Platelet activating factor-induced apoptosis is inhibited by ectopic expression of the platelet activating factor receptor. *J Neurochem.* **82**(6):1502-1511.

Abstracts

Imbeault S and Bennett SAL (2009) Reduction of platelet-derived growth factor receptor alpha expressing cells in hippocampal-derived neural progenitor cell cultures derived from conexin 29 null-mutant mice. Poster. Society for Neuroscience 39th Annual Meeting. Chicago, IL, USA. October 17-21 2009.

Imbeault S and Bennett SAL. (2009) A glial connexin network regulates oligodendrocyte progenitor cell fate in the postnatal hippocampus: Lessons learned from single, double and triple-null mutations in Cx29, Cx32, and Cx47. ***Selected for Oral Presentation***. International Gap Junction Conference 2009. Sedona, AZ, USA, July 25-30 2009.

Imbeault S and Bennett S. (2009) Loss of connexin 29 in hippocampal-derived neural progenitor cells reduces total number of platelet-derived growth factor receptor alpha expressing cells. *Poster.* 3rd Annual Canadian Association for Neuroscience Meeting. Vancouver, BC, Canada, May 24-27 2009.

Imbeault S, Peshdary V, Toeg H and Bennett SAL. (2008) Localization of connexin 29 to oligodendrocyte progenitor cells and role in progenitor proliferation. *Poster.* Society for Neuroscience 38th Annual Meeting. Washington, D.C., USA, November 15-19 2008.

Peshdary V, **Imbeault S**, Wurts K, Gauvin LG, Bennett SAL and Fai S. (2008) 3D modelling of connexin expression in postnatal neural progenitor cells. *Poster.* Society for Neuroscience 38th Annual Meeting. Washington, D.C., USA, November 15-19 2008.

Imbeault S, Gauvin LG, McLean AC, Menzies AS, Paul DL, Simon A and Bennett SAL. (2007) Connexin expression by postnatal hippocampal progenitor cells is dependent upon cell-cell and cell-extracellular matrix interactions. *Poster.* International 2007 Gap Junction Conference, Copenhagen, Denmark, August 4-9 2007.

Imbeault S and Bennett SAL. Localization of connexin 29 to oligodendrocyte progenitor cells (OPCs) in the adult mouse brain. *Oral presentation.* Department of Biochemistry, Microbiolgy and Imunology Research Symposium – University of Ottawa, Ottawa, ON, Canada. February 21st 2007.

Imbeault S, Gauvin L and Bennett SAL. Determination of neural progenitor cell survival and specification in Cx29 null-mutant mice. *Poster.* Department of Biochemistry, Microbiology and Immunology Graduate Poster Presentations – University of Ottawa. Ottawa, ON, Canada. May 18tth 2006.
Note: This poster was awarded 2nd place in the Ph.D. category.

Shih AY, **Imbeault S,** Barakauskas V, Erb H, Lei J, Li P and Murphy TH. Induction of the Nrf2-driven antioxidant response confers neuroprotection during mitochondrial stress *in vivo*. *Poster.* Society for Neuroscience 35th Annual Meeting. Washington, D.C., USA, November 12-16 2005.

Imbeault S, Lallier J, Hebb ALO, Haykal S, Davé S, Morin MY, Hill J, Melanson-Drapeau J and Bennett SAL. Hormonally induced hyperproliferation in Cx32 null mutant females exhausts progenitor self-renewal *in vivo*. *Poster.* International 2005 Gap Junction Conference. Whistler, BC, Canada. August 13-18 2005.

Imbeault S, Shih AY and Murphy TH. Role of coordinated anti-oxidant enzyme induction mediated by Nrf2 overexpression in protection against a mitochondrial complex II inhibitor *in vivo*. *Poster.* Society for Neuroscience 34th Annual Meeting. San Diego, CA, USA. October 23-27 2004.

Sun X, Johannssen H, **Imbeault S**, and Murphy TH. *In vivo* and *in vitro* 2-photon imaging of glutathione indicates that meningeal and ependymal cells are the major antioxidant buffer in mammalian brain. *Poster.* Society for Neuroscience 34th Annual Meeting. San Diego, CA, USA. October 23-27 2004.

Shih AY, Li P, Earl N, **Imbeault S**, Cheng MN, Gilbert R, Robertson GS and Murphy TH. A coordinated Nrf2-mediated antioxidant response promotes neuronal survival following cerebral ischemia *in vivo*. *Poster.* Society for Neuroscience 34th Annual Meeting. San Diego, CA, USA. October 23-27 2004.

Imbeault S. *In vivo* overexpression of NF-E2 related factor 2 promotes cell survival after challenge with a mitochondrial complex II inhibitor. *Oral presentation*. Department of Psychiatry 19th Annual Research Day. Detwiller Pavillion, University of British Columbia, Vancouver, BC, Canada. April 1, 2004.

Imbeault S, Shih AY, Erb HE, Jiang L, Toda S, Kalivas P and Murphy TH. Ectopic expression of the cystine/glutamate antiporter xCT confers protection against oxidative glutamate toxicity. *Poster.* Society for Neuroscience 33rd Annual Meeting. New Orleans, LA, USA. November 8-13 2003.

Shih AY, Li P, Erb H, **Imbeault S** and Murphy TH. Nrf2 activation protects neurons from experimental stroke by inducing a multi-faceted antioxidant defense. *Poster.* Society for Neuroscience 33rd Annual Meeting. New Orleans, LA, USA. November 8-13 2003.

Imbeault S and Bennett SAL. Effect of G-protein coupled receptor 4 expression on proliferation, differentiation, and viability of PC12 cells. *Poster.* Biochemistry Research Presentations. Roger-Guidon Hall, University of Ottawa, Ottawa, ON, Canada. April 12, 2002.

Awards and Achievements

Postgraduate (Doctoral)

2009	Fisher Scientific/Faculty of Medicine Doctoral Excellence Award - $555
2009-2010	Ontario Graduate Scholarship in Science and Technology (OGSST) - $4 000/term with support from the *Parkinson Research Consortium (PRC)*
2009-2010	University of Ottawa Excellence Scholarship – value of tuition
2007-2009	OGSST – $5 000/term with support from the PRC and the *Centre for Stroke Recovery*
2007-2009	University of Ottawa Admission Scholarship – value of tuition
2005-2007	NSERC Postgraduate scholarship (Doctoral) - $21 000/yr
2005-2007	University of Ottawa Excellence Scholarship – value of tuition
2005-2006	University of Ottawa Strategic Areas of Development Award - $6 000
2005-2006	*Ontario Graduate Scholarship - $5 000/term (declined)*

Postgraduate (Master's)

2004-2005	*Ontario Graduate Scholarship – $5 000/term (declined)*
2004-2005	NSERC Postgraduate Scholarship Master's - $17 300/yr
2003-2005	Michael Smith Foundation for Health Research - Masters Trainee Award 9 700$/ yr **top up** award, $2 500/yr Research & Travel
2003-2004	Canada Graduate Scholarship for Master's studies $17 500/yr
2003-2004	*Ontario Graduate Scholarship - $5 000/term (declined)*
2002	University of British Columbia/Faculty of Graduate Studies Graduate Entrance Scholarship - $3 000

Undergraduate

2002	*NSERC Undergraduate Student Research Award (USRA) – (declined)*
2001	NSERC USRA - $5 000
1998-2002	University of Ottawa Admission Scholarship - $10 000
1998-2002	NavCanada Scholarship - $6 000
1998-2002	Dean's Honour List, Faculty of Science, University of Ottawa

Teaching & Work Experience

2010 **Brain Awareness Week Lecturer**
Nepean High School (March 9, 2010)
topic: A general introduction to the nervous system with emphasis on the effects of drugs on the brain

2009 **Teaching Assistant:** BPS4900 B – Seminar
Department of Biochemistry, Faculty of Science, University of Ottawa
Tasks were to attend student presentations on assigned journal articles and to provide questions, feedback and an evaluation of the students' presentation skills

2008 **Laboratory Demonstrator:** BCH2333 and BCH2733 – Laboratoire de Biochimie I
Department of Biochemistry, Faculty of Science, University of Ottawa
Tasks were to supervise students during the lab sessions, answer questions during and following the session and to correct lab reports.
experiment: *Bligh and Dyer lipid extraction and visualization using 2D thin layer chromatography*

2007 **Laboratory Demonstrator:** BCH2733 – Laboratoire de Biochimie I
Department of Biochemistry, Faculty of Science, University of Ottawa

2006 **Laboratory Demonstrator:** BCH3356 – Molecular Biology Laboratory
Department of Biochemistry, Faculty of Science, University of Ottawa
Tasks were to supervise students during the lab sessions, answer questions during and following the session and to correct lab reports.
experiments: *isolation of total RNA using Tri-Reagent, isolation of poly(A)+ RNA via oligo-d(T) column, RT-PCR, T/A cloning into pBluescript vector, miniprep bacterial plasmid isolation, in vitro transcription/translation, site-directed mutagenesis, endonuclease restriction digest & agarose gel electrophoresis, Northern, Southern, and Western blotting.*

2004 **Tutorial Lecturer**: Summer Science 101 Program
Faculty of Science, University of British Columbia (August 4th, 2004)
topic: Human Physiology

2002 **Laboratory Demonstrator:** BCH 2736 – Laboratoire de Biochimie I
Department of Biochemistry, Faculty of Science, University of Ottawa

Judging and Conference Experience

2009 **Session Chair/Présidente de session** : Neuroscience, santé mentale et toxicomanie
77e Congrès de l'ACFAS, Université d'Ottawa (12 mai, 2009)

2008 **Project Judge**(Senior Health Sciences/Environmental Special Awards): Canada Wide Science Fair
University of Ottawa (May 12 &13, 2008)

2007 **Project Judge** (Junior Health Science Division): Ottawa Regional Science Fair
Carleton University (March 31, 2007)

2004 **Poster Judge**: 2nd Annual Multidisciplinary Undergraduate Research Conference
University of British Columbia (March 6th, 2004)

Professional Affiliations

Society for Neuroscience
Canadian Association for Neuroscience
ACFAS

Languages

English (spoken and written)
French (spoken and written)